

29. PALEOMAGNETISM OF DEEP SEA DRILLING PROJECT LEG 85 SEDIMENTS: NEogene MAGNETOSTRATIGRAPHY AND TECTONIC HISTORY OF THE CENTRAL EQUATORIAL PACIFIC¹

Norbert Weinreich, Institut für Geophysik, Ruhr-Universität Bochum
and
Fritz Theyer, Hawaii Institute of Geophysics, University of Hawaii²

ABSTRACT

On Leg 85, 16 holes were cored at five sites. Thirteen of the holes were cored with the hydraulic piston corer (HPC) or the variable-length hydraulic piston corer (VLHPC) or both; the remainder were rotary drilled. Partially duplicating stratigraphic sections were successfully recovered by hydraulic piston coring at Sites 572 to 575. Sub-bottom penetration was deepest (about 210 m) at HPC Hole 575A, which bottomed in lower Miocene sediments. Penetration by hydraulic piston coring was limited at all sites not by the failure of the corer to stroke out but by the excessive force (overpull) necessary to retrieve the core barrel from the hole. The sediments recovered are relatively uniform siliceous-calcareous oozes to calcareous ooze-chalks. Paleomagnetic measurements were made at all stratigraphic levels, but magnetostratigraphic sequences could be resolved only for the Pleistocene-Pliocene and for brief upper, middle, and lower Miocene sections.

In the younger and less consolidated sediments, the declination often shows large-scale azimuthal rotations down-core. These smooth trends vary from core to core, indicating either rotation between the sediment and the core liner or the rotation of the core barrel during the coring or retrieval process. Thus, azimuthal orientation of the samples was impossible even though a Kuster azimuthal orientation tool was used during the hydraulic piston coring.

At all sites, the downhole shift from mainly siliceous to mainly calcareous ooze-chalk coincided with a decrease in NRM intensity of at least one order of magnitude, to 1.0×10^{-8} G. Diagenesis is the probable reason for this behavior, although the dilution of magnetic carriers as the result of higher accumulation rates may also be a factor. A tectonic analysis using data from samples with stable remanence indicates a northward plate motion of about $0.3^\circ/\text{m.y.}$ during the last 18 m.y., a rate that agrees with most previous reconstructions of Pacific Plate motion.

INTRODUCTION

The primary objective of Leg 85 of the Deep Sea Drilling Project was to analyze sediments from holes that formed a transect of the central equatorial Pacific high-productivity belt. The study was undertaken because it was hoped that the use of a tool then relatively new, the variable-length hydraulic piston corer (VLHPC), would permit the recovery of largely undisturbed sediment from as deep as 300 m sub-bottom; undisturbed sediment was desired because it would permit the highest possible stratigraphic resolution of the cored material. The study of paleomagnetism was considered central to the studies to be undertaken, especially those using the pre-Pliocene sequences, for which correlation between calcareous nanofossil datums and magnetic reversals is incomplete.

The VLHPC had been used for paleomagnetic research in the Atlantic (Kent and Spariosu, 1982a, b; Tauxe et al., 1983), but it had never been used before in this part of the Pacific, although successful paleomagnetic work has been done in the central equatorial Pacific with conventional piston cores (Hays et al., 1969; Opdyke, 1972; Hammond et al., 1974; Opdyke et al., 1974; Theyer and Hammond, 1974; Theyer et al., 1978). The rotary-drilled cores acquired during four previous DSDP cruises to the

central Pacific have yielded meager paleomagnetic results. It has generally been thought that drilling disturbance has been responsible for the poor results, although workers also observed that the older, highly calcareous oozes yielded very weak intensities. By using the VLHPC we hoped to establish magnetostratigraphic reference profiles for the entire section, including the Neogene, for this region. Unfortunately, our aims were thwarted, not by drilling disturbance or operational difficulties but by the nature of the magnetic remanence of the older sediments.

MATERIALS AND METHODS

Square, plastic boxes with a capacity of approximately 7 cm^3 were used to sample the working half of each core. We wanted to achieve a stratigraphic resolution of about 0.05 to 0.1 m.y. at all levels. Therefore, except where the sediment was disturbed, we acquired samples at roughly equal time intervals, using shipboard-derived rates of sedimentation to adjust the sampling intervals. Where possible we also preferentially sampled horizons that showed horizontal bedding in order to avoid parts of the section that might be affected by subtle coring-induced disturbance. The directions and intensities of NRM_0 (untreated natural remanent magnetization) were measured on board on selected samples by using a Digi-co spinner magnetometer; the results of this preliminary work are reported in the site chapters (this volume). For the present study, samples from about upper Miocene to Recent were analyzed at the Ruhr-Universität Bochum

¹ Mayer, L., Theyer, F., et al., *Init. Repts. DSDP*, 85: Washington (U.S. Govt. Printing Office), Contribution No. 1463 of the Hawaii Institute of Geophysics.

² Addresses: (Weinreich) Institut für Geophysik, Ruhr-Universität Bochum, 4630 Bochum, Federal Republic of Germany; (Theyer, present address) Department of Geological Sciences, University of Southern California, Los Angeles, CA 90089.

(RUB), and samples older than about upper Miocene were analyzed at the Hawaii Institute of Geophysics (HIG). All except a few measurements were made by using cryogenic magnetometers (Goree and Fuller, 1976). Alternating-field (AF) demagnetization studies were performed at RUB by using a Schonstedt GSD-1 single-axis demagnetizer and at HIG by using a three-axis sample tumbler, which was also driven by a GSD-1. For the sediments measured at RUB (upper Miocene and younger), systematic stepwise AF demagnetization series were carried out on each sample in addition to the NRM_0 measurement. All these series were taken to the median destructive field (MDF), and most were taken to the 500-Oe level. The direction of the stable remanent magnetization (RM) was then determined for each sample by analyzing its demagnetization behavior. For this purpose plots of the normalized intensity of magnetization (J/J_{NRM}) versus the applied demagnetization field, vector diagrams (Zijderveld, 1967), and stereographic projections of total vector and of difference vectors of magnetization (Hoffman and Day, 1978) were studied. The stable RM direction for each sample was then determined by finding the mean of at least three consecutive demagnetization steps which showed the least directional dispersion during Fisherian (Fisher, 1953) analysis (Appendix A). We interpret this stable RM direction as the magnetic component that carries the Earth's paleofield information.

Because the samples from the older sediments (those studied at HIG) were generally characterized by uniformity and extremely low intensities, they were treated in a different way. NRM_0 was measured for only some of the holes and for only some depth intervals, and progressive AF demagnetization was performed solely on selected samples. After we reviewed the demagnetization series, we demagnetized all the HIG samples by applying an alternating field of 50 Oe, a level we hoped would leave measurable magnetization yet remove some viscous components. The resulting data are listed in Appendix B.

All the Leg 85 sites lie near the equator. Therefore, most of the inclination data scattered within a few degrees of zero, and 180° variations in the declination data were used to define polarity changes. This made the determination of the true polarity of the samples difficult, especially since the azimuthal orientation was unknown. At first we hoped that the Kuster single-shot orientation device, which we used during VLHPC operation, would provide azimuthal orientation. This device takes a photograph, just before the VLHPC barrel strokes out, of the position with respect to a compass needle of a double line marked on the core liner. The camera is triggered as the corer falls through a nonmagnetic collar in the drill string, an arrangement that makes the exact chronological relationship between the coring and the orientation photograph uncertain. Many mechanical, photographic, and handling difficulties were encountered with the Kuster tool, but about 57% of the slides recorded data. Unfortunately, onshore paleomagnetic analysis made it obvious that there are systematic rotations in the declination data that wholly negate the device's usefulness for azimuthal orientation purposes. For ex-

ample, the downhole declination data for Cores 4 and 5 of Hole 573 show continuous clockwise and anticlockwise rotations of different magnitudes in addition to the 180° polarity offsets (Fig. 1). In Core 4 there is an anticlockwise rotation of approximately 120° ; in Core 5 there is a clockwise rotation of about 200° ; and neither rotation is constant. These variations are due to relative motion between the sediment, core liner, and possibly even the VLHPC barrel itself. Therefore, only the uppermost part of a VLHPC core may be oriented as shown by the Kuster photo, and even that is open to question, because neither the vertical position of the camera nor the exact time at which the camera takes the photo is known (motion between sediment, core liner,

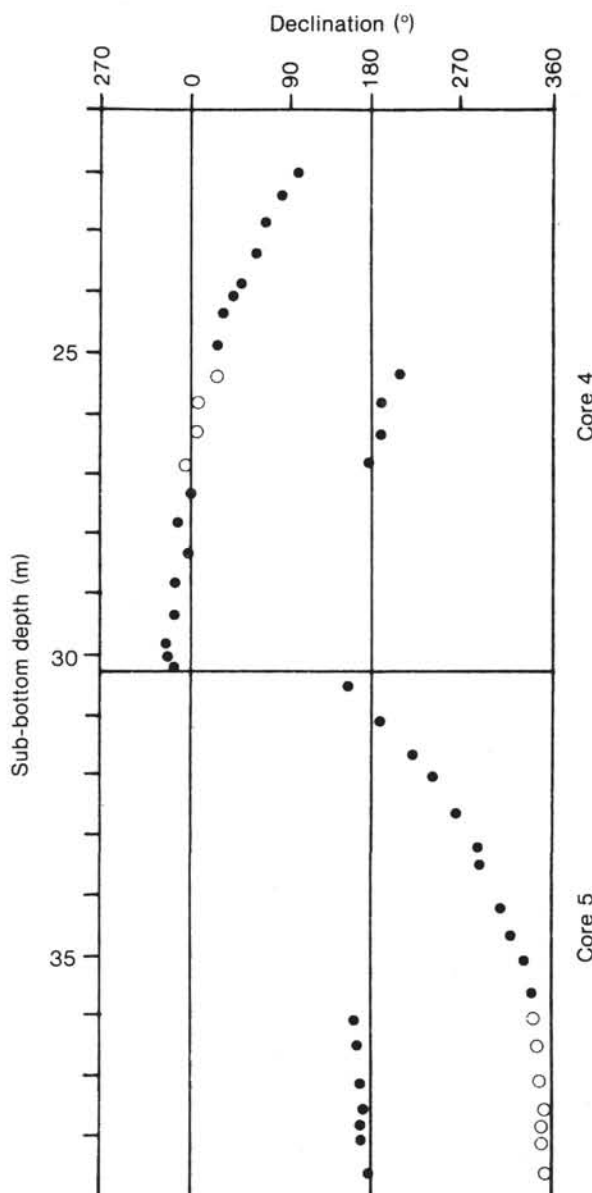


Figure 1. Downcore variation of the uncorrected declination data for Cores 4 and 5 of Hole 573, showing rotation produced during VLHPC coring. See text for details. Solid circles indicate actual data; open circles are 180° projections made to provide visual continuity in the trends.

and barrel, may occur between the time when the photograph is exposed and the actual coring process). In other words, the photo shows the azimuthal orientation of the core liner at a certain instant, but the azimuthal orientation may change before or as the coring actually takes place. In this report, therefore, only relative declination directions are used (those found by referring to the position of the line marked on the core liner).

The younger cores (those measured at RUB) yielded acceptable magnetic data, and the declination data are mostly well grouped azimuthally (180° shifts indicate polarity changes). Thus, average declinations were calculated for these cores as described by Kent and Spariosu (1982a). We did not do this for the sediments analyzed at HIG, because these older sediments displayed weak NRM intensities and were consequently nearly useless for magnetostratigraphy. Arbitrary declinations are shown from core to core for these sediments. All data, corrected and uncorrected, are listed in Appendixes A and B.

The data in Appendixes A and B provide the basis for our magnetostratigraphic and tectonic interpretations. The polarity sequences were constructed by assuming that the topmost interval of continuous polarity is the Brunhes Normal Chron and that the first 180° shift of declination is the Brunhes/Matuyama boundary at 0.72 Ma (Ness et al., 1980). The underlying cores were interpreted by assuming that 180° changes between two cores resulted not from changes in polarity but rather from the rotation of the cores themselves. The azimuthal average of the uppermost (Brunhes) declination sequence was then arbitrarily set at 0° , which resulted in an azimuthal average of 180° for the reversed Matuyama sequence that followed below. Subsequent downcore 180° swings of declination were then used to define the magnetostratigraphy. In some intervals this method failed, and the interpretation of polarity was guided by inclination behavior and biostratigraphy. Finally, a few intervals were so difficult to interpret that the sequence of polarities can only be considered an estimate.

RESULTS AND DISCUSSION

Magnetic Behavior of Sediments

The direction of the stable RM may be overprinted by weaker magnetic components of low coercivity (Kent and Lowrie, 1974). Figure 2 illustrates a sample from a cyclic siliceous–calcareous lithologic unit in Hole 573A (Core 2) that carries multiple components of magnetization with almost antiparallel directions. The components are revealed by the increase in the normalized magnetization from an NRM_0 level of 5.8×10^{-6} G (Fig. 2A) and by the wide scatter in the total vector of magnetization in the stereographic projection (Fig. 2C). After about 200 Oe these weaker components are removed, and the very high MDF of 652 Oe indicates the high stability of the stable RM (Fig. 2A). The vector diagram (Fig. 2B) and the difference-vector projection (Fig. 2D) show the multiple components of the system in more detail. One weaker component is removed at about 50 Oe and another at 200 Oe. This behavior is reflected in both the xy- and the yz-planes (Fig. 2B). The ensuing monotonous de-

crease of the orthogonal components toward zero suggests that there are no other components. The weak component of the sample of Figure 2 can be identified as a viscous magnetization acquired during the Brunhes Chron, whereas the stable component reflects the reversed direction of the Matuyama Chron.

Figure 3 shows the response of Sample 574C-34-2, 109–111 cm, which is from a metalliferous sediment layer overlying basalt. The sample is characterized by a relatively high NRM_0 intensity (7.4×10^{-6} G). The increase in the normalized intensity curve (Fig. 3A) and the vector diagram (Fig. 3B) suggest that it too may contain separate components of magnetization. The weaker component persists to about 100 Oe, and the MDF of the components with higher stability lies at 310 Oe. Even though the stereographic projection of the total vector of magnetization shows only one direction (Fig. 3C), the difference-vector diagram (Fig. 3D) allows a qualitative and quantitative definition of the two antiparallel directions of the sample. The inclination data define the polarity of the low-coercivity component (0 to 100 Oe) as reversed and that of the stable component as normal (Fig. 3D).

Sample 573A-1-3, 90–92 cm, which is from a siliceous–calcareous lithologic unit of Brunhes age, carries an NRM_0 intensity of 2.5×10^{-6} G. Its behavior (Fig. 4) suggests a single component. The normalized intensity shows a continuous decrease during stepwise AF cleaning (Fig. 4A). The vector diagram (Fig. 4B) and the stereographic projections (Figs. 4C, D) show a single pattern, and the MDF of 270 Oe reflects the inherent stability of the component.

Finally, Figure 5 gives an example of useless data obtained on a weakly magnetized sample. This material (Sample 575A-18-1, 144–146 cm) is from highly calcareous ooze and had an NRM_0 intensity of 6.7×10^{-7} G. Although the stereographic projection in Figure 5C suggests stability, the other diagrams (Figs. 5A, B, D) reveal its erratic behavior upon AF treatment. This sample was typical of the highly calcareous (older than uppermost Miocene) sediments recovered during Leg 85.

Leg 85 Magnetostratigraphy

A satisfactory magnetostratigraphy was derived for the Pliocene and Pleistocene sediments, which had intensities that were in a reasonable range ($> 10^{-8}$ G) for measurement on the cryogenic magnetometer, even after AF demagnetization. In contrast, the calcareous oozes from the Miocene and below allowed the determination of magnetostratigraphic sequences at only a few intervals. The boundary between usable and unusable data coincided with the boundary between cyclic siliceous–calcareous ooze and calcareous ooze. Within the lower, highly calcareous sediments, the weakness of the NRM_0 intensities made AF demagnetization impossible, and the NRM_0 data alone did not contain coherent stratigraphies.

Polarity boundaries had to be inferred from 180° shifts of declination because of the shallowness of the inclinations. However, some of the sites crossed the equator, and in the absence of azimuthal orientation neither declination nor inclination was an unequivocal guide to po-

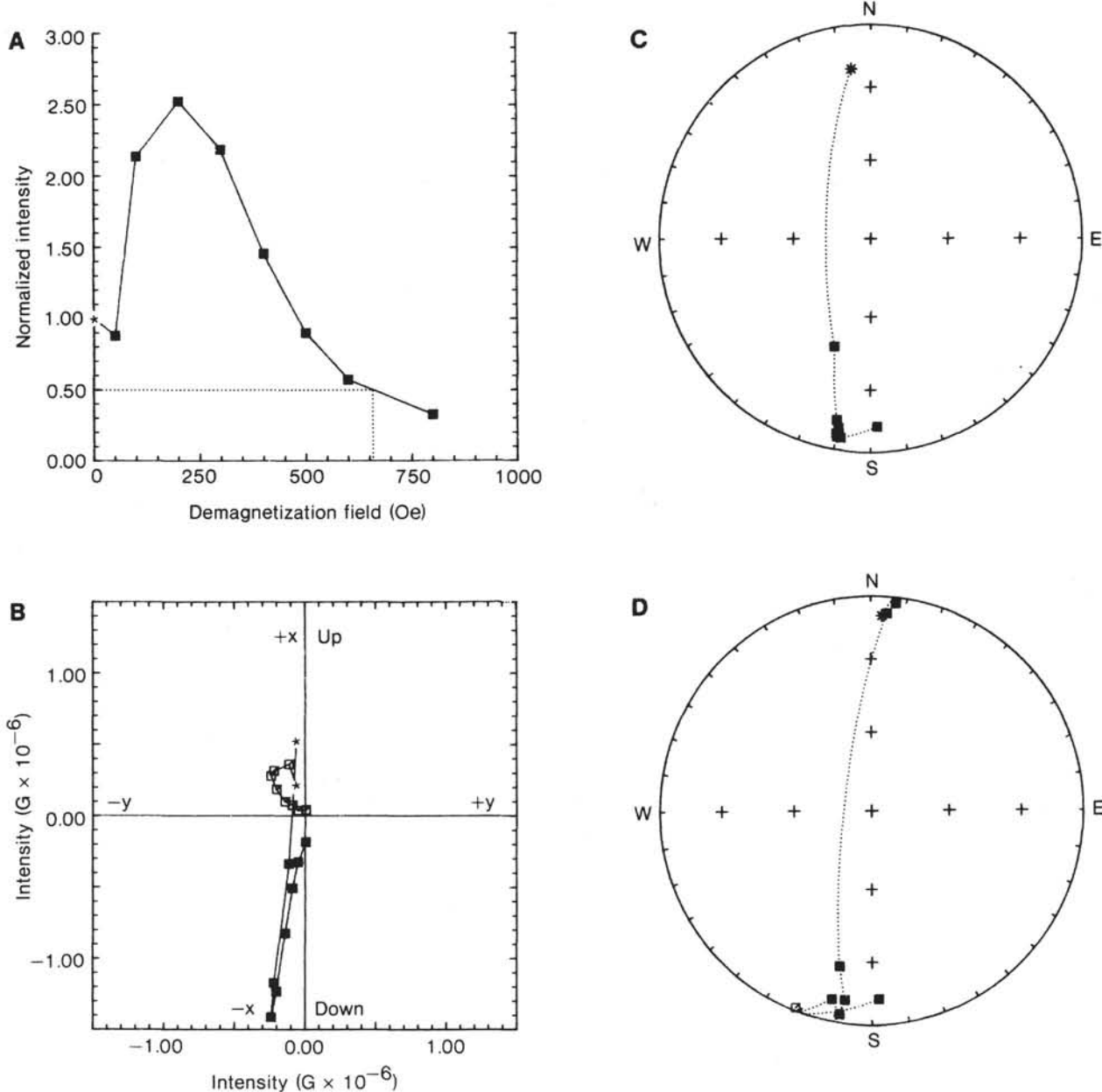


Figure 2. Behavior of the magnetization of Sample 573A-2-3, 67-69 cm, taken from a cyclic siliceous-calcareous lithologic unit, during successive AF demagnetization. A. Normalized intensity of magnetization plotted against the applied demagnetization field. Dotted line indicates the MDF. Asterisk indicates NRM₀. B. Vector diagram of the orthogonal components (x, y, z) of magnetization. Closed symbols represent the horizontal (x, y) plane, open symbols the vertical (z, y) plane. Asterisk indicates NRM₀ components. C. Stereographic projection of the total vector of magnetization. Closed symbols indicate normal, open reversed polarity. Asterisk indicates NRM₀ direction. All directions are connected by great-circles. D. Stereographic projection of the difference vectors. Closed symbols indicate normal, open symbols reversed polarity. The starting point is marked by an asterisk.

larity. We developed our magnetostratigraphy for these sites by (1) comparing the relative lengths of the polarity intervals with the known polarity sequence and (2) referring to biostratigraphy. In the metalliferous sediment layer at Site 574 (which contains the Eocene/Oligocene boundary), intensities increased to about 10^{-5} G, but despite the apparent stability of most of the samples from this layer (see the AF demagnetization series in Fig. 3), the directions (especially the inclinations) fail to indicate a coherent stratigraphic pattern.

Site 571

Only one core (7.10 m) was recovered at Site 571. Shipboard paleomagnetic analysis of NRM₀ indicates that the polarity pattern is coherent throughout this core. Biostratigraphic dating defined the core as Quaternary, from Recent to about 0.46 Ma. Thus, it correlates with the Brunhes Chron. NRM₀ intensities vary from 2.4×10^{-6} G to 7.4×10^{-6} G, with a geometric mean of 4.7×10^{-6} G. The AF-cleaned data, especially the inclina-

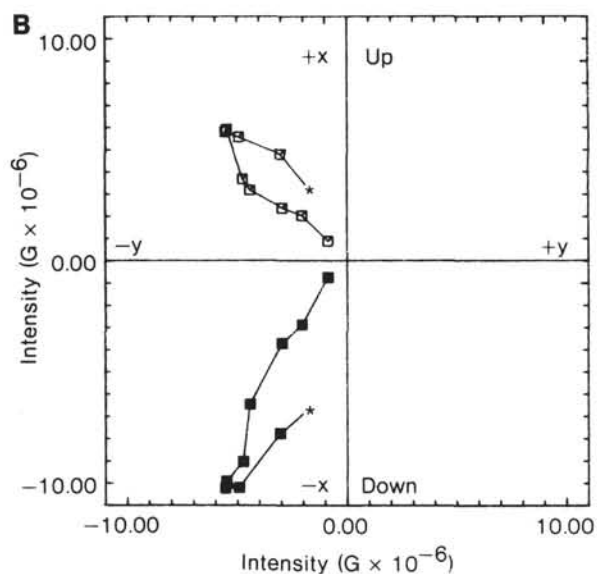
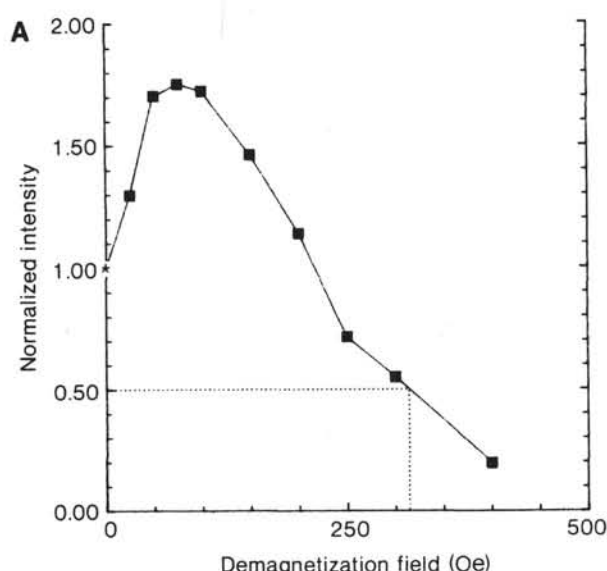
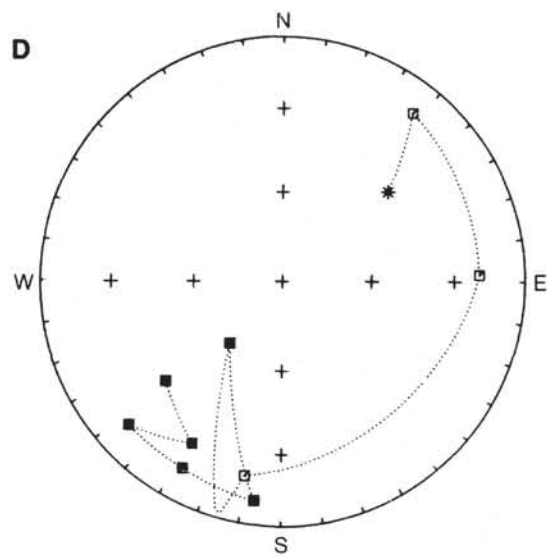
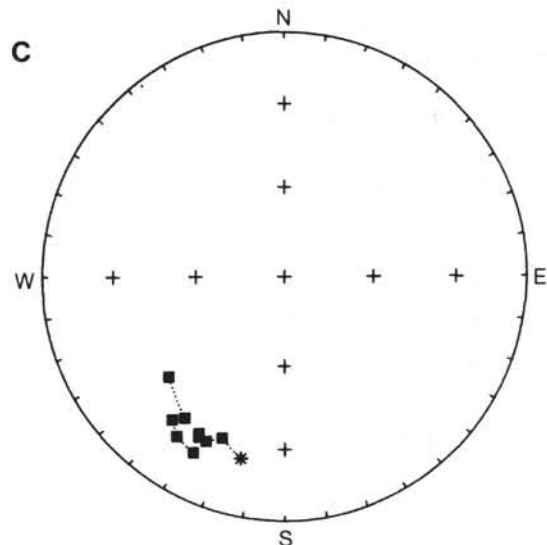


Figure 3. Behavior of Sample 574C-34-2, 109–111 cm. This sample was rotary drilled from the metalliferous sediments overlying basement at Site 574. See Figure 2 caption for details.

tions, show very stable behavior; we were able to derive a mean stable inclination of 7.6° , which gives a dipole paleolatitude of 3.8°N . This is in good agreement with the present site latitude of 4.0°N .

Site 572

No magnetostratigraphy could be established for Site 572. Most of the NRM_0 intensities of the sediments recovered with the HPC were at the noise level of the cryogenic magnetometer, so that demagnetization studies were pointless. In addition, the NRM_0 directional data show almost random scatter. Although some intervals in the older, rotary-drilled sediments show high intensities, their inclinations are scattered about zero, and AF cleaning



did not improve the results. The data are therefore presented in tabular form only (Appendix B).

Site 573

Site 573 is the southernmost site in a three-site north-south transect along about 133°W . The transect cuts across the north-central region of the equatorial high-productivity zone. Two holes were cored with the VLHPC at Site 573, and one was rotary drilled to basement (which was at a sub-bottom depth of 529 m; Table 1). Both the sediment (which ranged in age from Quaternary to upper Eocene) and the basalt were sampled for paleomagnetic analysis. A drastic decrease in intensity occurs at about 45 m sub-bottom in both Holes 573 and 573A

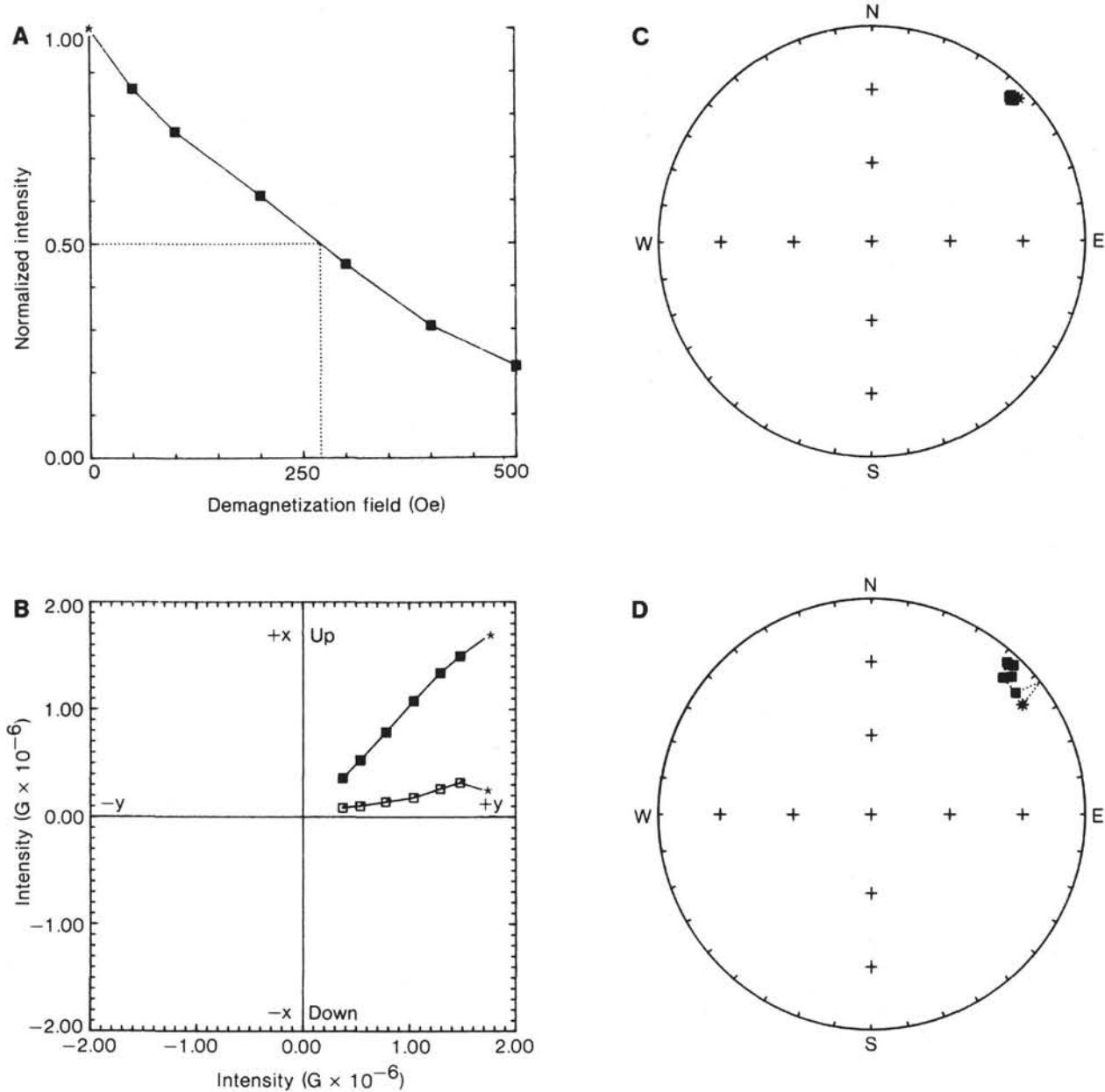


Figure 4. Behavior of Sample 573A-1-3, 90–92 cm. This sample was taken from Brunhes-age siliceous–calcareous sediments. See Figure 2 caption for details.

(Fig. 6); it defines the lower limit of the interpretable data and coincides with a change in lithology from cyclic siliceous–calcareous ooze (Unit I) to calcareous ooze (Unit II). The decrease in intensity exceeds one order of magnitude. The intensities throughout lithologic Unit I show a variation about a mean of $2.31 \pm 1.74 \times 10^{-6}$ G, a mean similar to that at Site 571. The intensities exhibited by other Neogene siliceous–calcareous pelagic sediments are comparable (Kent and Spariosu, 1982a, b; Tauxe et al., 1983). Throughout the underlying lithostratigraphic Unit II (from 45.1 m to 520.0 m sub-bottom), there are intervals of remarkably constant intensities that average about 10^{-7} G, but these intervals do not provide interpretable data. Within the metalliferous chalk to claystone unit (lithologic Unit III, from 520.0 m

to 526.6 m sub-bottom) and the short upper Eocene sequence of pelagic limestone (lithologic Unit IV, 526.6 m to 529.0 m sub-bottom), the intensities increase to a maximum of about 10^{-3} G, but the data are useless for magnetostratigraphic work because of their almost random scatter. The inclinations, which during the latest Eocene and early Oligocene are expected to reflect a southerly latitude of some 7 to 10°, do not allow the identification of polarity sequences. The NRM_0 intensities of the six basalt samples measured have a mean of $3.7 \pm 2.7 \times 10^{-4}$ G, which is typical of such material (Petersen and Roggenthen, 1980).

The magnetostratigraphies developed for the uppermost parts of Holes 573 and 573A are shown in Figure 6. Core-to-core interpretation was straightforward because

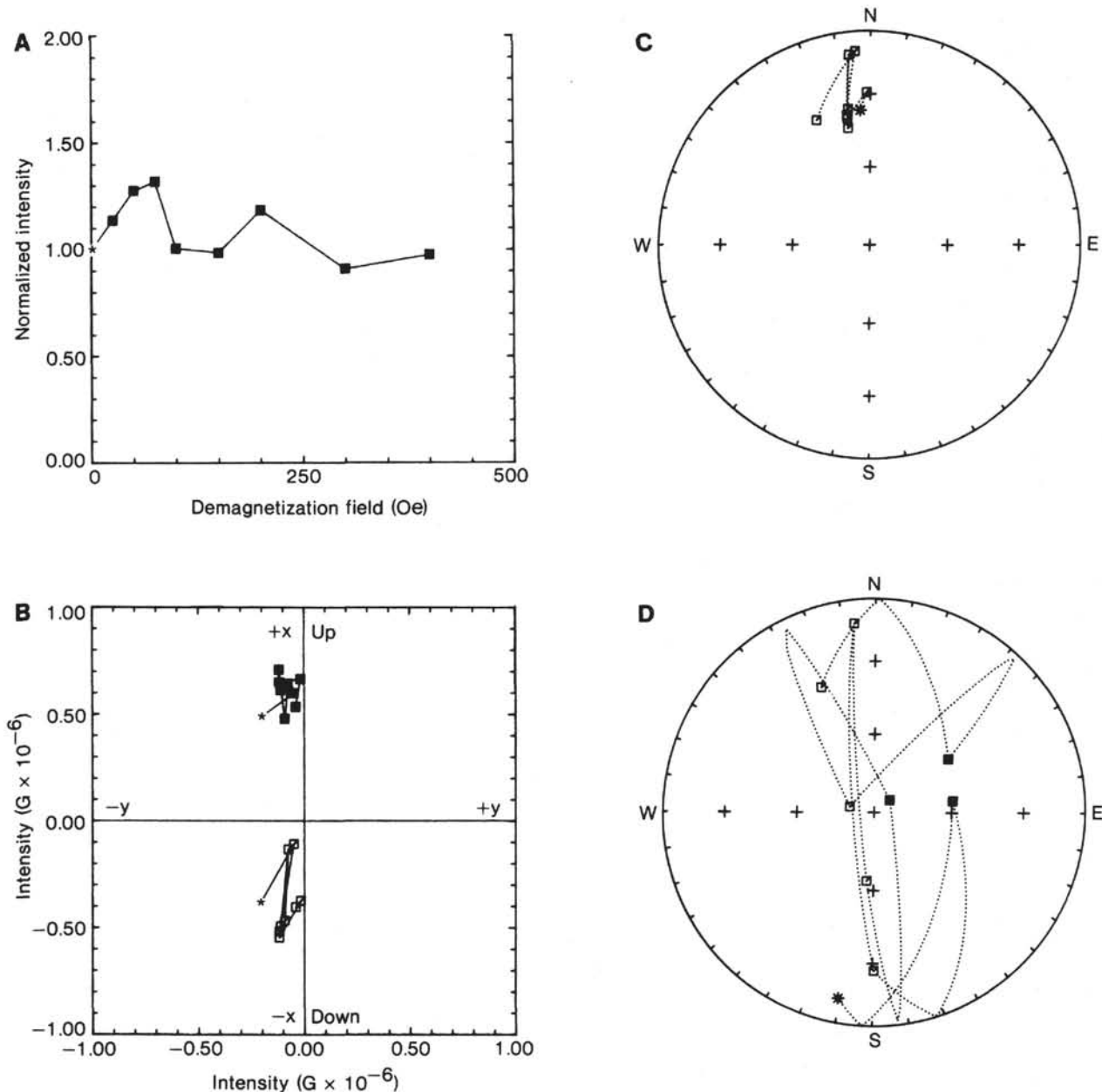


Figure 5. Behavior of Sample 575A-18-1, 144–146 cm. This sample represents the majority of sediments encountered on Leg 85. It comes from a highly calcareous unit and is very weakly magnetized, its NRM intensity being 6.7×10^{-7} G. See Figure 2 caption for details.

of the 180° declination shifts in Hole 573. In both holes the record spans from the lower Mammoth transition at 3.19 Ma (Ness et al., 1980) to the Brunhes/Matuyama boundary. Table 2 lists the depths of polarity changes found in both holes; it also gives the position of the last sample of the upper polarity sequence and the first sample of the lower sequence, thus defining the depth-uncertainty range for each polarity change (Fig. 7, dotted intervals). As shown in Table 2 and Figure 7, the stratigraphically equivalent 180° shifts in declination occur at different depths in the holes. In Figure 7, the points that define the same polarity transition in the holes plot along three 45° line segments, and the top segment is offset from zero. Within the depth intervals indicated by each 45° line segment, the drilling-related displacement of

material is absent and the net sedimentation rate is constant. The breaks between the line segments may be explained in three ways: (1) net sedimentation rates may have changed from hole to hole, although such variation is unlikely, given the general uniformity of the region's seismic properties and sedimentation rates; (2) coring procedures may have introduced disturbances in the form of missing material and partial core recovery; and (3) shifts in the magnetic boundaries may have been introduced by reworking, direct disturbance, or postdepositional effects (Lövlie, 1976).

The top line segment may be offset from zero because the top of the section in Hole 573A is missing. However, we believe that solution or erosion caused the sediment sequence from the Brunhes Chron in Hole 573A to be

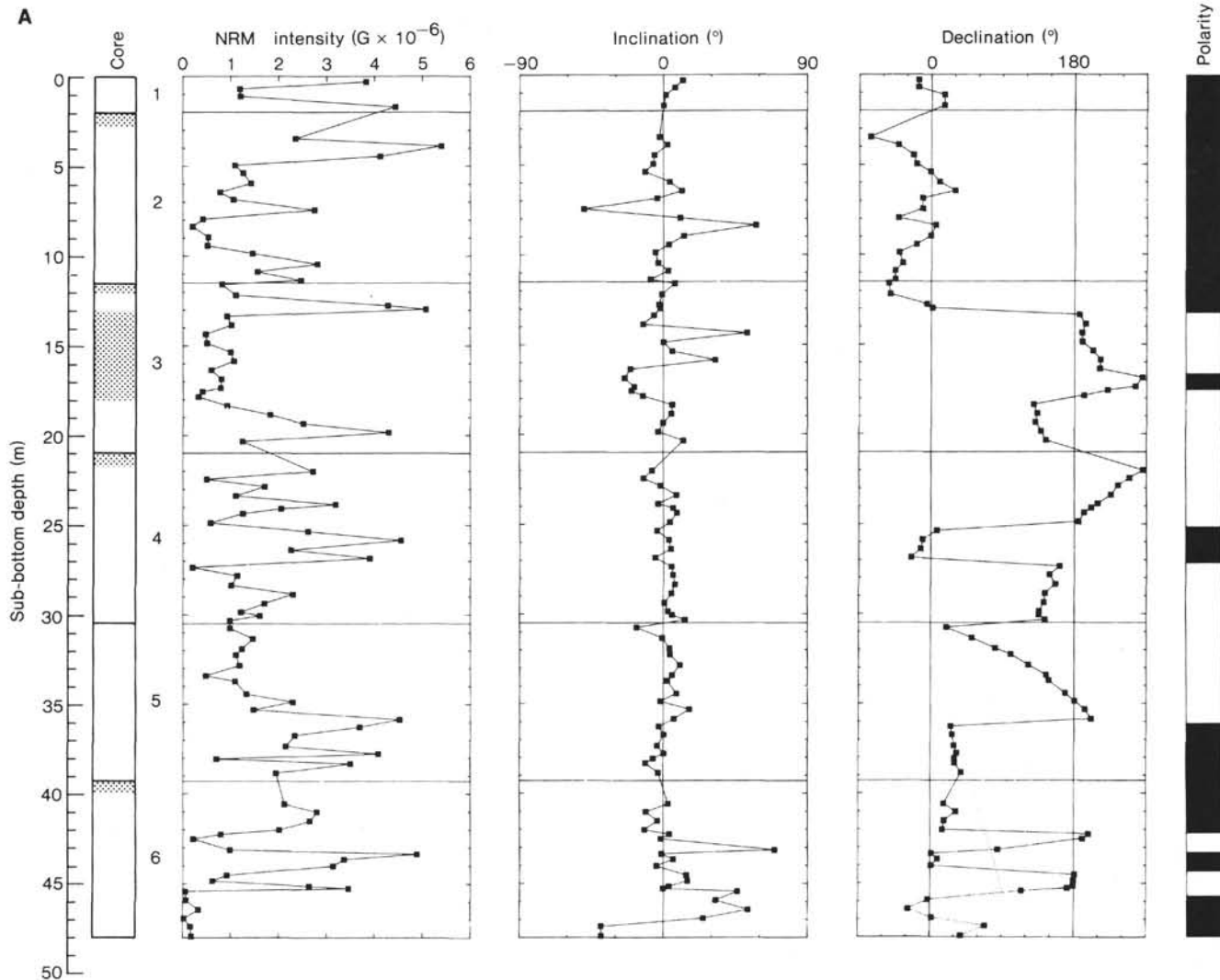


Figure 6. NRM intensity and paleomagnetic polarity for (A) Hole 573 and (B) Hole 573A. In the column showing the depths of the cores, dotted intervals are those identified on the barrel sheets as disturbed by drilling. The remaining columns show the downhole variation of NRM intensity; stable inclination and corrected declination (see text for details); and paleomagnetic polarity (derived from 180° shifts in the declination data). Black indicates intervals of normal polarity, white intervals of reversed polarity, and striping intervals that could not be interpreted.

Table 1. Summary of Leg 85 coring.

Site	Location	Maximum depth of penetration (m)	Hole	Interval cored (m sub-bottom)	Estimated age of oldest sediment (Ma)	Nature of basement
571	114°08.53'W, 3°59.84'N	7.1	571	0-7.1	0.46	Not reached
572	113°50.52'W, 1°26.09'N	486.0	572	0-19.0	14-15	Basalt
			572A	0-154.0		
			572B	154.0-172.1		
			572C	0-169.5		
573	133°18.57'W, 0°29.91'N	529.0	573D ^a	151.0-486.0	38-39	Basalt
			573	0-158.6		
			573A	0-53.2		
574	133°19.81'W, 4°12.52'N	532.5	573B ^a	138.5-529.0	38-39	Basalt
			574	0-206.5		
			574A	0-180.2		
			574B ^a	185.0-204.0		
			574C ^a	194.5-532.5		
575	135°02.16'W, 5°51.00'N	208.3	575	0-98.6	22	Not reached
			575A	0-208.3		
			575B	3.3-119.0		
			575C	0-15.8		

^a Rotary drilled.

more compressed than in Hole 573, an interpretation consistent with the shortness of both the first reversed interval of the Matuyama Chron and the Jaramillo subchron in Hole 573A. On the other hand, both the Jaramillo subchron and the Brunhes/Matuyama boundary in Hole 573 fall within an interval disturbed by coring (Fig. 6A).

The first break in the 45° line (Fig. 7) occurs in the early part of the Matuyama Chron. It too can be interpreted as a compaction effect, because again there is some shortening in Hole 573A, but in this case it is more likely to be due to the coring process. The Jaramillo, Olduvai, and all the polarity changes in the Gauss Chron follow the predicted sequence. Between the Matuyama/Gauss boundary and the beginning of the Olduvai subchron, there is a second break in the 45° line (Fig. 7); it occurs at the boundary between Cores 4 and 5 in Hole 573 and between Cores 3 and 4 in Hole 573A. It is likely that sediments were lost between those cores:

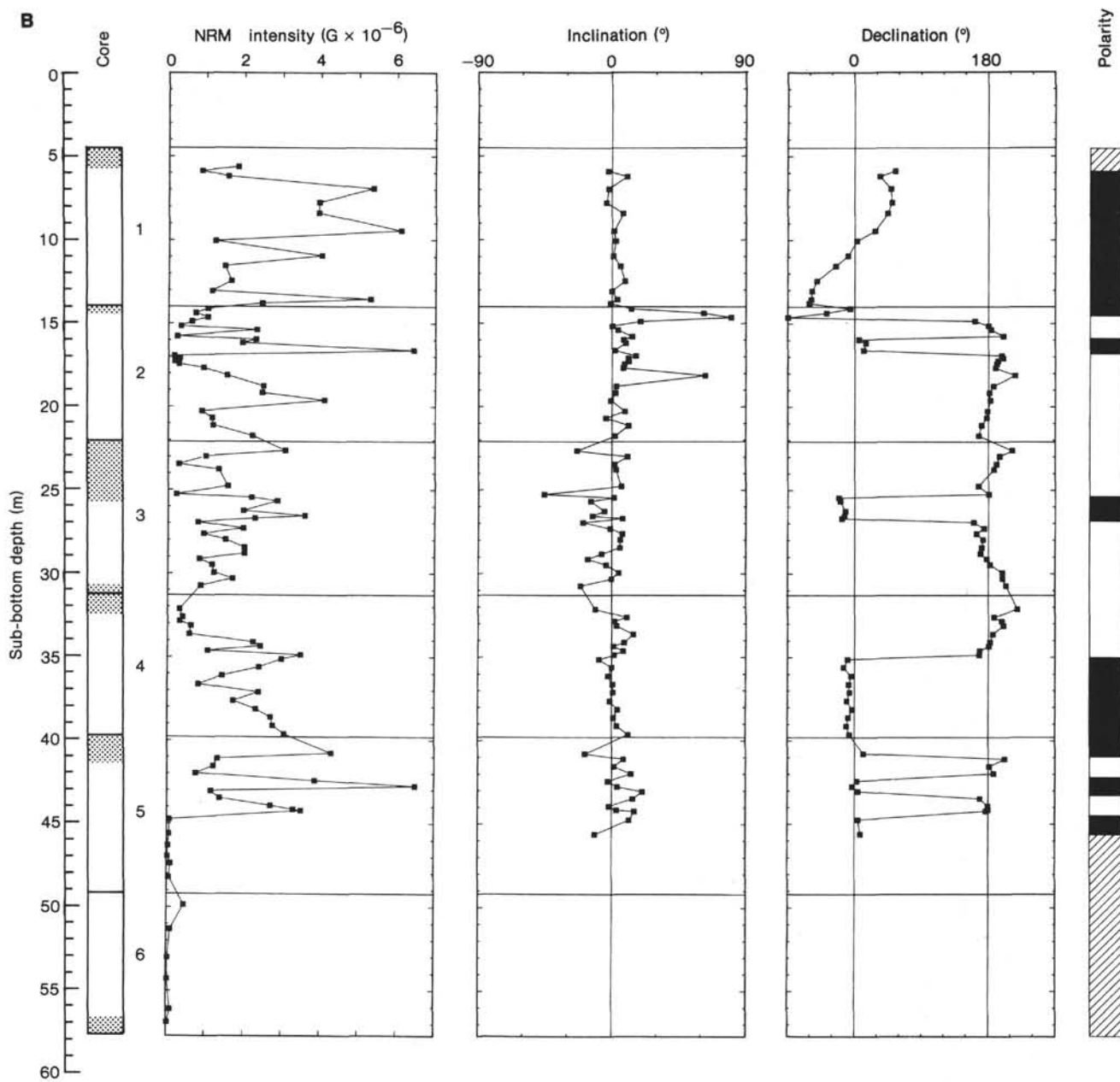


Figure 6. (Continued).

adding about 1 m of sediment between Cores 4 and 5 in Hole 573 and between Cores 3 and 4 in Hole 573A would produce a straight line from the Gauss/Gilbert boundary to the Jaramillo subchron.

Site 574

Site 574, at $4^{\circ}12.52'N$ and $133^{\circ}19.81'W$, was near the northern edge of the high-productivity belt. A sediment sequence from upper Eocene to Quaternary was recovered, as well as a few pieces of basalt drilled from basement. All cores were sampled (Appendices A and B), although only the samples from the uppermost 10 cores of Holes 574 and 574A are discussed here because of the low intensities lower in the section. The intensities are characteristic of lithologic Unit I (cyclic siliceous-

calcareous ooze) down to about 84 m sub-bottom; they show significant variations that are in accord with the lithostratigraphic subunits (site chapters, this volume). For Subunit IA (Hole 574), a mean intensity of $3.93 \pm 2.94 \times 10^{-6}$ G was obtained. In both holes there is a very sharp decrease in intensity of more than one order of magnitude at the transition from Subunit IA to Subunit IB. The intensities of the sediments in Subunit IC are slightly lower than in Subunit IA ($2.12 \pm 1.14 \times 10^{-6}$ G in Hole 574 and $1.56 \pm 1.16 \times 10^{-6}$ G in Hole 574A). Throughout lithologic Unit II (calcareous ooze-chalk), the intensities are in the range of 10^{-7} G (Fig. 8), and the resulting data are not usable for magnetostratigraphy. With few exceptions, the magnetic directions and the intensities to 520 m sub-bottom are either randomly

Table 2. Magnetostratigraphy for Holes 573 and 573A.

Boundary	Age (Ma) ^a	Hole 573		Hole 573A	
		Depth of boundary (m sub-bottom) ^b	Uncertainty range (Core-Section, level in cm) ^c	Depth of boundary (m sub-bottom) ^b	Uncertainty range (Core-Section, level in cm) ^c
Brunhes/Matuyama	0.72	13.17	3-1, 147/3-2, 36	14.63	2-1, 38/2-1, 88
upper Jaramillo	0.91	16.61	3-4, 36/3-4, 86	15.98	2-2, 28/2-2, 68
lower Jaramillo	0.97	17.47	3-4, 136/3-5, 7	16.96	2-2, 113/2-3, 28
upper Olduvai	1.66	25.12	4-3, 88/4-3, 136	25.48	3-3, 173/3-3, 58
lower Olduvai	1.87	27.11	4-4, 136/4-5, 36	26.77	3-3, 147/3-4, 36
Matuyama/Gauss	2.47	35.97	5-4, 86/5-4, 128	35.19	4-3, 33/4-3, 84
upper Kaena	2.91	42.05	6-2, 123/6-2, 147	41.25	5-1, 99/5-1, 131
lower Kaena	2.98	43.15	6-3, 84/6-3, 106	42.52	5-2, 69/5-2, 114
upper Mammoth	3.07	44.19	6-24, 23/6-4, 74	43.58	5-3, 26/5-3, 69
lower Mammoth	3.17	45.58	6-5, 13/6-5, 62	44.80	5-3, 144/5-4, 46

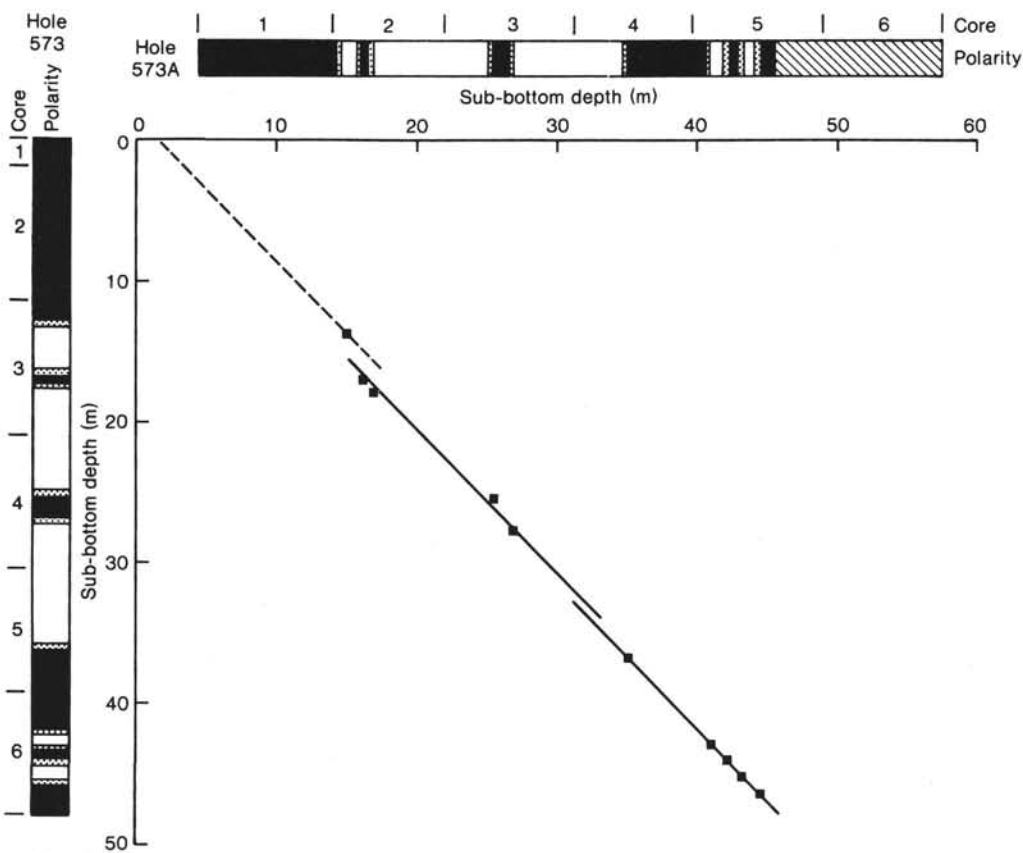
^a Ness et al. (1980).^b Interpolated from coring summary (site chapter).^c Last sample of upper polarity sequence/first sample of lower polarity sequence.

Figure 7. Comparison of paleomagnetic polarity logs for Holes 573 and 573A. Correlative polarity transitions are plotted. The dotted intervals above and below the transitions indicate lack of samples and thus the uncertainty in the depth of a boundary. Black indicates intervals of normal polarity, white intervals of reversed polarity, and striped intervals that were not interpreted.

scattered or remain virtually constant for considerable depth intervals, and both of these patterns preclude coherent interpretation. Typically, both the declinations and the intensities follow this pattern, possibly indicating remagnetization or chemical alteration of the magnetic carriers (Henshaw and Merrill, 1980). In the upper Eocene metalliferous chalk unit (Unit III), we measured stronger intensities (in the range of some 10^{-5} G), but

the inclination data did not allow the establishment of a meaningful stratigraphic pattern.

Hole 574

The magnetostratigraphy for the upper 10 cores of Site 574 (Figs. 8A and B) is coherent, although it contains a gap as the result of the very low intensities of Cores 6 to 8 in lithologic Subunit IB. The polarity se-

quence in Hole 574 starts with the Brunhes Chron in Core 1 (Fig. 8A). Core 2 contains Matuyama sediments (as defined by inclination data), and the next interval of normal polarity indicates the Olduvai subchron; the Brunhes/Matuyama boundary and the Jaramillo subchron are missing in this hole. The normal section at the bottom of Core 2 marks the top of the Gauss Chron. Throughout the upper part of Core 3, coring disturbance prohibits interpretation; the Gauss/Gilbert boundary alone is well defined. The first normal subchron within the Gilbert Chron, the Cochiti subchron, is poorly expressed in Core 4, but the lower three Gilbert subchrons can easily be identified (Fig. 8A). The transition (reversed to normal) in Core 5 defines the Gilbert/Chron 5 boundary, and the Chron 5/Chron 6 boundary can be distinguished in Core 6. Farther below, a brief normal subchron may occur, but it is not clearly indicated because of the low intensity and the noise in the inclination data. From Section 574-6-4 to Section 574-9-4 no stratigraphy is discernible. The polarity sequence in Cores 9 and 10 indicates the presence of the youngest normal subchron in Chron 8 and the transition from Chron 8 to Chron 9. This interpretation disagrees, however, with the biostratigraphic dating of this depth interval and may well be erroneous: the polarity sequence is discontinuous with that above Core 9, and the inclination data give no indication of polarity. Our interpretation is based on a linear extrapolation and on a comparison to the length of the polarity intervals of the actual time scale (Ness et al., 1980).

Hole 574A

Hole 574A (Fig. 8B) is similar to Hole 574 (Fig. 8A). No paleomagnetic data are available from Core 1 because of poor recovery, but Core 2 correlates with the Matuyama Chron, and the first interval of normal polarity is interpreted as the Olduvai subchron. The next, poorly defined transition from reversed to normal may be the Matuyama/Gauss boundary at 2.47 Ma (Ness et al., 1980). The initial polarity of Core 3 is interpreted as reversed only because of its length. If this interpretation is accurate, Core 3 is of Gilbert age and the older part of the Gauss Chron (between Cores 2 and 3) is missing. Consequently, the transition at the lower part of Core 3 may be the younger boundary of the Cochiti subchron at 3.86 Ma, and Core 4 may contain the four normal subchrons of the Gilbert Chron. The Gilbert/Chron 5 boundary can be identified in Core 5, and the Chron 5/Chron 6 boundary can be identified in Core 6. Because the older normal polarity interval of Chron 5 is very short, however, material might have been lost between Cores 5 and 6. From the lower part of Core 6 down to Core 9 (lithologic Subunit IB), the low intensity precludes the determination of any polarity change from either the inclination or declination data, as in Hole 574 (Fig. 8B). Cores 9 and 10 are interpreted as containing the Chron 8/Chron 9 transition and parts of Chron 9. The data from the lower part of Core 10 are poor and must be interpreted by extrapolation, as for Hole 574. Table 3 shows the polarity changes in Holes 574 and 574A by depth and age (Ness et al., 1980). The possible

reasons for the differences in depth of some polarity transitions are discussed above.

Site 575

Site 575, at $5^{\circ}51.00'N$, $135^{\circ}02.16'W$, constitutes the northernmost of three sites drilled in a north-south transect across the equatorial high-productivity belt. Miocene to Quaternary sediments were recovered at this site; basement was not reached. The entire set of cores was sampled for paleomagnetic analysis, and a magnetostratigraphy into the lower Miocene was established, although unfortunately it has some gaps due to weak magnetization in the lower to middle Miocene (Fig. 9). The intensities throughout lithologic Unit I at Holes 575, 575B, and 575C show large-scale variations ranging from 10^{-7} G to about 10^{-6} G, with constant averages. The magnetization properties of the Site 575 sediments are similar to those at the other sites. The lower Miocene sequence, which is characterized by a pale brown ooze (lithologic Subunit IIA), provided intensities with a mean of $8.97 \pm 7.81 \times 10^{-6}$ G.

Hole 575

If we assume that no polarity boundaries occur between cores, the magnetostratigraphic interpretation of the data for Hole 575 is straightforward. We correlate the uppermost polarity sequence with the Brunhes Normal Chron (Table 4A; Fig. 9A), a correlation supported by the inclination data. Lower we distinguish the Matuyama and Gauss Chrons, as documented by the declination data and, at 10.27 m sub-bottom, the Gilbert/Chron 5 transition (5.41 Ma; Ness et al., 1980), in agreement with the biostratigraphic results (Barron et al., this volume). Thus, the entire sequence of the Gilbert normal subchrons appears to be missing as the result of a hiatus. The normal polarity interval ranging from 10.27 to 13.17 m sub-bottom is interpreted as Chron 5. The magnetic record of the underlying normal polarity sequence (that from 16.15 to 22.77 m sub-bottom) is poor because of the disturbance of the sediments. The transition at 22.77 m appears to be the Chron 7/Chron 8 boundary (at 8.18 Ma; Ness et al., 1980). We assume that most of Chron 9 is missing as the result of a prominent hiatus (see Barron et al., this volume), but otherwise the polarity record down to the upper part of Chron 12 (Core 4) is reasonably well developed (Fig. 9A, Table 4A).

Hole 575C

The two cores that constitute Hole 575C provide an excellent record of the upper Miocene to Quaternary polarity sequence (Fig. 9C, Table 4C). As clearly indicated by the inclination data, the uppermost sequence of uniform declination can be interpreted as the Brunhes Chron. The Brunhes/Matuyama boundary occurs at 2.61 m sub-bottom in Core 1 and is followed by the Jaramillo and Olduvai subchrons (Table 4C). Between the termination and the onset of the Gauss Chron, both the Kaena and Mammoth subchrons are present (Fig. 9C; Table 4C). As in Hole 575 (see above), the polarity transition following the Gauss/Gilbert boundary (Core 575C-2; 9.91 m)

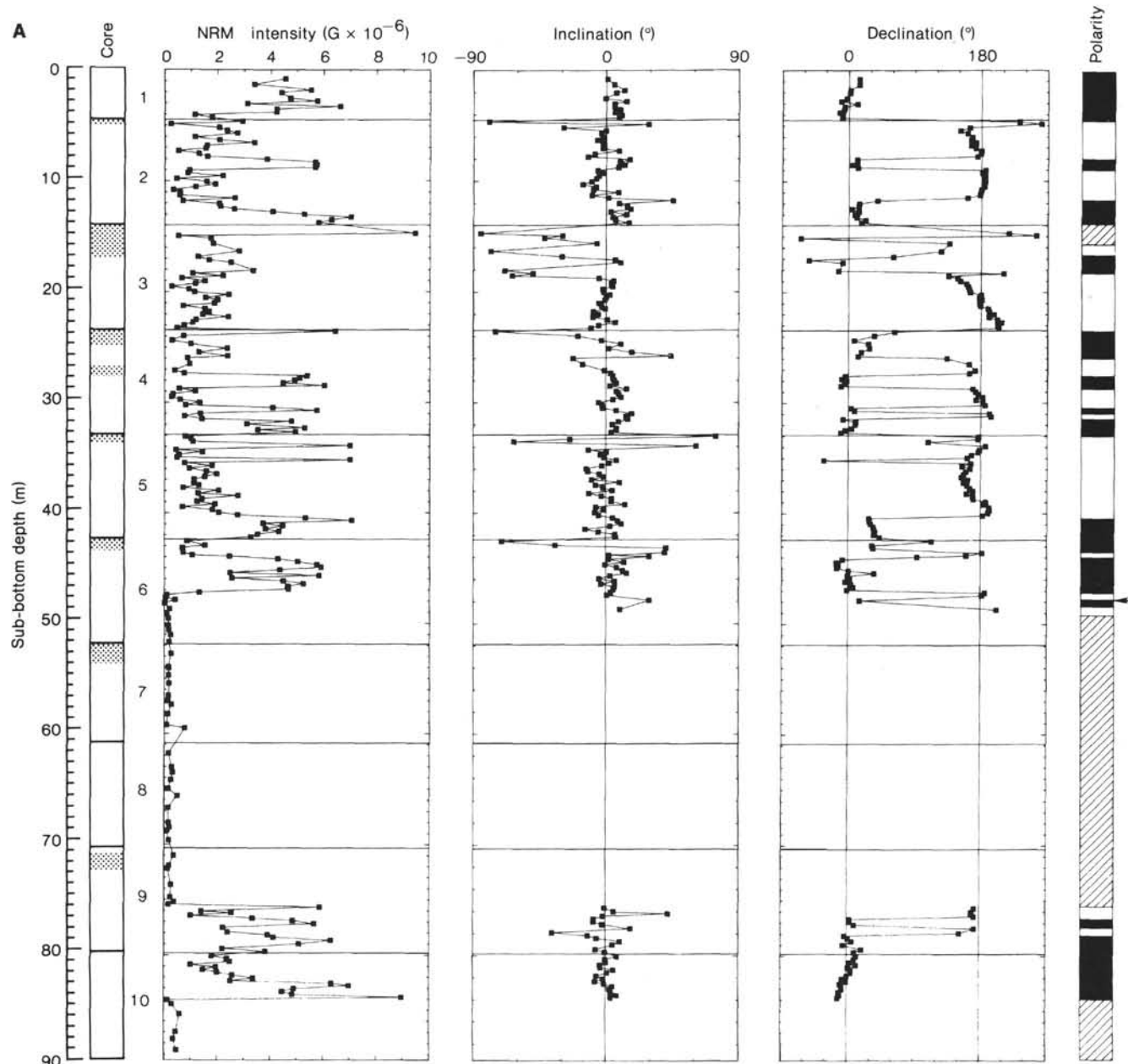


Figure 8. NRM intensity and paleomagnetic polarity logs for (A) Hole 574 and (B) Hole 574A. In the column showing the depths of the cores, dotted intervals are those identified on the barrel sheets as disturbed by drilling. The remaining columns show the downhole variation of NRM intensity; stable inclination and corrected declination (see text for details); and paleomagnetic polarity (derived from 180° shifts in the declination data). Black indicates intervals of normal polarity and white intervals of reversed polarity. Striping shows intervals where only erratic and NRM_0 data were available; these intervals were not interpreted. Arrows indicate polarity changes documented by one data point only.

is correlative to the Gilbert/Chron 5 boundary, a correlation that requires there to be a hiatus during the Gilbert Chron. All the polarity transitions in Chron 5 can be identified (Fig. 9C). The erratic 180° shifts in the declination data that occur in the lower normal interval of Chron 5 are caused by volcanic detritus (see site chapters, this volume). The polarity change at 15.57 m sub-bottom (Core 575C-2) agrees well with the N-R transition dated at 6.42 Ma (Ness et al., 1980).

Hole 575B

In contrast, the record of late Miocene to Quaternary magnetostratigraphy in Hole 575B is poor (Fig. 9B).

Core 575B-1 begins in the Brunhes Chron. The Brunhes/Matuyama boundary at 4.96 m sub-bottom is followed by the Jaramillo subchron (Fig. 9B). At 6.41 m the sampling of the first core was discontinued because of the severe disturbance of the sediments. Sampling was resumed at 12.81 m, at the top of Core 2, within an interval of normal polarity as indicated by the inclination data. The uppermost polarity change in Core 2, at 13.06 m, is correlated to the Gauss/Gilbert boundary (3.40 Ma). Since we assumed that there is a hiatus centered on the Gilbert Chron (see discussion above), the two intervals of normal polarity that follow are interpreted as Chron 5. Its upper boundary (5.41 Ma) occurs

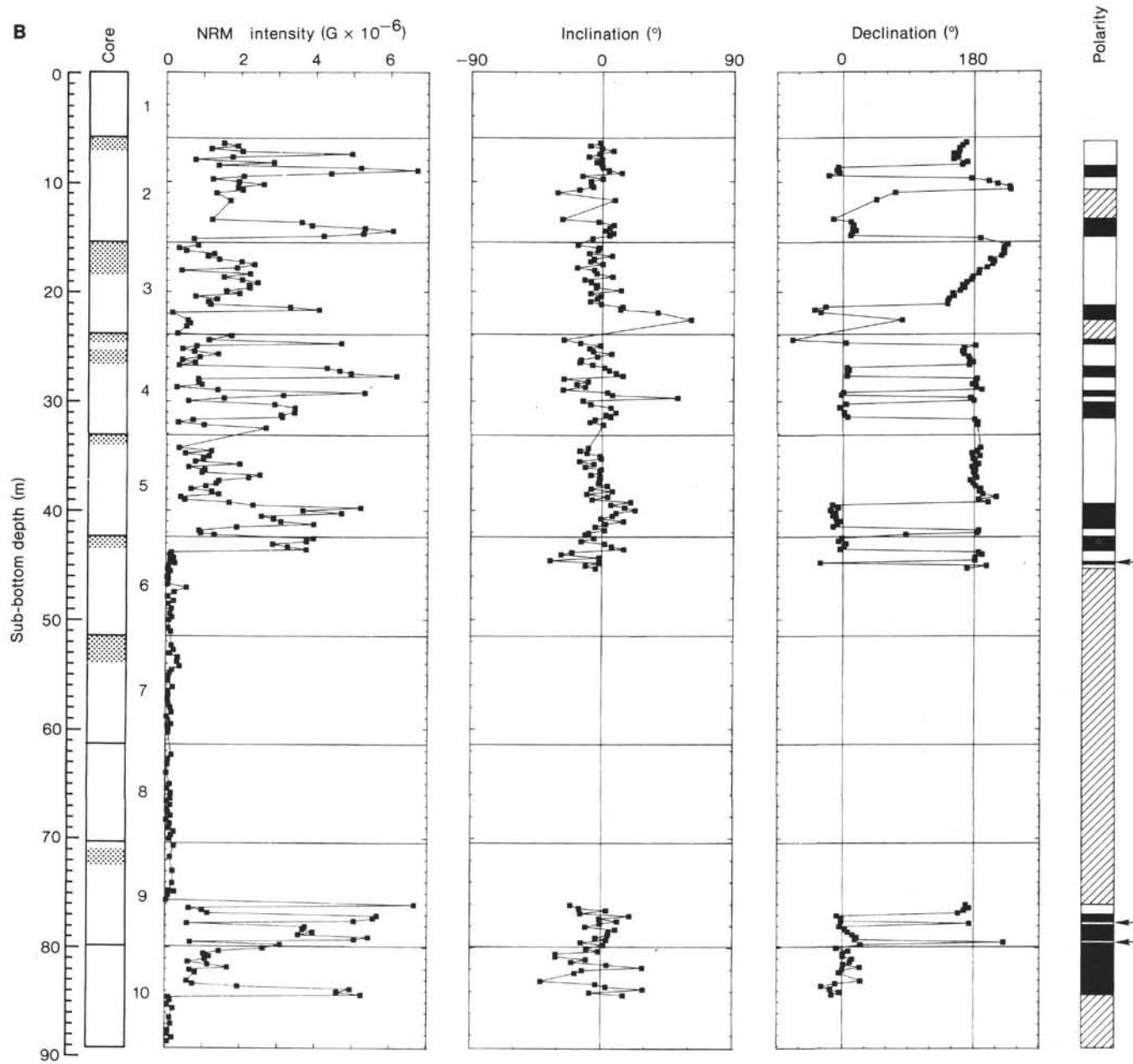


Figure 8. (Continued).

at 14.68 m, and its lower boundary occurs at 18.18 m sub-bottom. Erratic declinations occur in the lower interval of normal polarity of Chron 5, in a position stratigraphically correlative with those that occur in Core 575C-2 and for the same reason (volcanic detritus). The polarity change at 21.03 m sub-bottom in Core 575B-2 correlates with the N-R transition in Hole 575C that is dated at 6.42 Ma (Ness et al., 1980). The first 180° shift of declination identified in Core 575B-3 at 22.70 m, therefore, appears to be the transition at 6.55 Ma. Unfortunately, further magnetostratigraphic interpretation is impossible because of the weak intensities and erratic inclination and declination data that characterize the underlying sediments.

A comparison of the depths of polarity transitions in Holes 575C and 575B indicates a depth displacement.

Stratigraphically correlative intervals bounded by 180° shifts in declination (those from the Brunhes/Matuyama boundary down to the Chron 5/Chron 6 boundary and those in the intervals of volcanic detritus) were used to calculate a regression with a correlation coefficient, r^2 , of 0.997. This displacement between the holes amounts to 1.63 m, instead of the 3.30 m suggested by the coring logs (which show an offset of that amount between the mudline and the top of Core 575B-1). The determination of the depth of the top of each core was made difficult by the presence of both this within-hole displacement and the overcoring technique used in Holes 575B and 575A (see Site 575 chapter). For this study the length of the interval that was overcored (which is called washdown in the barrel sheets) was subtracted from the length of each core. The good correlation between the polarity

Table 3. Magnetostratigraphy for Holes 574 and 574A.

Boundary	Age (Ma) ^a	Hole 574		Hole 574A	
		Depth of boundary (m sub-bottom) ^b	Uncertainty range (Core-Section, level in cm) ^c	Depth of boundary (m sub-bottom) ^b	Uncertainty range (Core-Section, level in cm) ^c
Brunhes/Matuyama	0.72				
upper Jaramillo	0.91				
lower Jaramillo	0.97				
upper Olduvai	1.66	7.92	2-3, 30/2-3, 55	8.58	2-2, 66/2-2, 9
lower Olduvai	1.87	8.92	2-3, 130/2-4, 5	9.59	2-3, 16/2-3, 42
Matuyama/Gauss	2.47	11.67	2-5, 105/2-5, 130	12.10	2-3, 142/2-5, 110
upper Kaena	2.91			15.02	2-6, 110/2-6, 135
lower Kaena	2.98				
upper Mammoth	3.07				
lower Mammoth	3.17	16.89	3-2, 88/3-3, 40		
Gauss/Gilbert	3.40	18.46	3-3, 113/3-4, 30		
upper Cochiti	3.86	23.86	3-7, 30/4-1, 92	21.28	3-4, 115/3-4, 141
lower Cochiti	3.98	26.32	4-2, 49/4-3, 65	24.83	4-1, 81/4-1, 104
upper Nunivak	4.12	27.52	4-3, 90/4-3, 115	26.82	4-2, 130/4-3, 5
lower Nunivak	4.26	28.67	4-4, 55/4-4, 80	27.83	4-3, 81/4-3, 105
upper Sidufjall	4.41	30.42	4-5, 80/4-5, 105	29.08	4-4, 55/4-4, 81
lower Sidufjall	4.49	30.92	4-5, 130/4-6, 5	29.57	4-4, 105/4-4, 130
upper Thvera	4.59	31.47	4-6, 30/4-6, 55	30.12	4-5, 5/4-5, 38
lower Thvera	4.79	33.57	4-7, 28/5-1, 135	31.57	4-6, 6/4-6, 28
Gilbert/Chron 5	5.41	40.42	5-5, 130/5-6, 5	39.38	5-5, 15/5-5, 41
Chron 5/Chron 6	6.07	47.17	6-4, 5/6-4, 30	43.69	6-1, 116/6-1, 142
Core 6 to Core 9 data did not allow identification of specific reversals					
Chron 8/Chron 9	8.98	78.22	9-6, 10/9-6, 35	76.94	9-5, 42/9-5, 67

^a Ness et al. (1980).^b Interpolated from coring summary (site chapter).^c Last sample of upper polarity sequence/first sample of lower polarity sequence.

boundaries in Holes 575C and 575B (if the offset of Hole 575B is disregarded) supports this procedure.

Hole 575A

We could develop a reasonable magnetostratigraphy for only the uppermost 10 cores of Hole 575A. Overcorening was also used in this hole, so the actual core lengths were recalculated as described above. The stratigraphy was derived by defining the mean declination for each core. This mean was then used to arbitrarily align each core's declination with either 0° (normal polarity) or 180°. Figure 9D shows the resulting polarity pattern. We emphasize, however, that without usable inclination data it is impossible to define the polarity of the sequence on paleomagnetic grounds alone. The interpretation shown in Figure 9D was guided by the general biostratigraphic age of the sediments. Because of the age range of the interval (about 16 to 18 Ma), this interpretation of polarity also fits the anomaly pattern much better than would the opposite polarity solution. The uppermost sequence with uniform declination data, which starts at 93.80 m sub-bottom (the top of Core 1) was arbitrarily set at 0° or normal polarity. The three intervals of normal polarity that can be identified in Cores 1 to 3 are interpreted as Anomaly 5C (Mankinen and Dalrymple, 1979; Ness et al., 1980), which begins at 102.64 m sub-bottom (16.71 Ma). At the bottom of Core 5 (113.54 m) there is a 180° shift to 0°, and at the top of Core 6 (114.59 m) the declination shifts back to 180°. This normal polarity interval cannot be correlated to the geomagnetic time scale (Ness et al., 1980). The transition at 118.09 m sub-bottom is interpreted as the younger limit of Anomaly 5D (17.28 Ma), and the polarity change at 125.59 m (17.60 Ma; Ness et al., 1980) is interpreted as

its older limit. This interpretation agrees well with the accepted time scales and the biostratigraphy (Barron et al., this volume); and it also yields reasonable sedimentation rates for the lower Miocene.

Discussion of Magnetostratigraphy

The magnetostratigraphy of the Leg 85 sites is summarized in Figure 10. It was derived from the polarity boundaries of each hole by using the time scale of Ness et al. (1980) as a reference. Alternative geomagnetic time scales (McDougall, 1977; Mankinen and Dalrymple, 1979) would produce no significant differences in age for the late Neogene. The sedimentation rates defined by this magnetostratigraphy decrease from the south (Site 573) to the north (Site 575). The northward motion of the Pacific Plate and the migration of the sites into the high-productivity belt of the equatorial region (Winterer, 1973; van Andel et al., 1975) is generally confirmed by the increase in sedimentation rate that occurs as depth in Sites 574 and 575 increases.

The sedimentation rates at Site 573 are surprisingly constant at about 18.2 m/m.y. At Site 574, the rates change significantly at approximately 3 Ma (during the Gauss Chron), from about 5.5 m/m.y. above to about 12.2 m/m.y. below. Below the Chron 5/Chron 6 boundary, the sedimentation rates are poorly documented, however, because we lack reliable data. There should be a significant hiatus at about 9 to 10 Ma (Moore et al., 1978; Barron and Keller, 1972). The oldest polarity change determined at this site (at about 80 m sub-bottom) is interpreted here as the Chron 8/Chron 9 boundary. This interpretation disagrees with the biostratigraphic dating, which places the Chron 10/Chron 11 boundary at this level (Barron et al., this volume). Site 575 shows a more

Table 4A. Magnetostratigraphy for Hole 575.

Boundary	Age (Ma) ^a	Depth of boundary (m sub-bottom) ^b	Uncertainty range (Core-Section, level in cm) ^c
Brunhes/Matuyama	0.72	2.70	1-2, 115/1-2, 125
upper Jaramillo	0.91	3.10	1-3, 5/1-3, 15
lower Jaramillo	0.97	3.20	1-3, 15/1-3, 25
upper Olduvai	1.66	4.10	1-3, 105/1-3, 115
lower Olduvai	1.87	4.30	1-3, 125/1-3, 135
Matuyama/Gauss	2.47	5.40	1-4, 85/1-4, 95
upper Kaena	2.91	6.60	1-5, 55/1-5, 65
lower Kaena	2.98	6.90	1-5, 85/1-5, 95
upper Mammoth	3.07	7.19	1-5, 115/1-5, 123
lower Mammoth	3.17	7.31	1-5, 128/2-1, 4
Gauss/Gilbert	3.40	7.65	2-1, 30/2-1, 40
Gilbert/Chron 5	5.41	10.27	2-2, 140/2-3, 4
Chron 5/Chron 6	6.07	13.17	2-4, 128/2-4, 145
	6.42	16.15	2-6, 130/2-6, 140
Chron 7/Chron 8	8.18	22.77	3-4, 139/3-5, 5
	8.40	25.80	3-6, 140/3-7, 10
	8.49	26.05	3-7, 10/3-7, 20
	10.42	26.85	4-1, 50/4-1, 60
	10.47	27.11	4-1, 70/4-1, 91
	10.89	28.00	4-2, 7/4-2, 3
	10.96	28.42	4-2, 33/4-2, 90
Chron 10/Chron 11	11.42	29.32	4-2, 134/4-3, 20
	11.58	29.75	4-3, 40/4-3, 50
	11.71	30.65	4-3, 130/4-3, 140
Chron 11/Chron 12	11.98	31.50	4-4, 65/4-4, 75
	12.28	32.10	4-4, 125/4-4, 135
	12.32	32.67	4-5, 9/4-5, 65
	12.40	33.43	4-5, 91/4-5, 134
	12.45	34.24	4-6, 39/4-6, 48

^a Ness et al. (1980).^b Interpolated from coring summary (site chapter).^c Last sample of upper polarity sequence/first sample of lower polarity sequence.

Table 4B. Magnetostratigraphy for Hole 575B.

Boundary	Age (Ma) ^a	Depth of boundary (m sub-bottom) ^b	Uncertainty range (Core-Section, level in cm) ^c
Brunhes/Matuyama	0.72	4.96	1-2, 11/1-2, 21
upper Jaramillo	0.91	5.46	1-2, 61/1-2, 71
lower Jaramillo	0.97	5.72	1-2, 71/1-2, 113
Gauss/Gilbert	3.40	13.06	2-1, 101/1-1, 111
Gilbert/Chron 5	5.41	14.68	2-2, 113/2-2, 123
	5.70	15.75	2-3, 73/2-3, 83
	5.78	16.58	2-4, 3/2-4, 13
Chron 5/Chron 6	6.07	18.18	2-5, 13/2-5, 23
	6.42	21.03	2-6, 143/2-7, 13
	6.55	22.70	3-2, 9/3-2, 31 ^d

^a Ness et al. (1980).^b Interpolated from coring summary (site chapter) and corrected with regard to each core's washdown.^c Last sample of upper polarity sequence/first sample of lower polarity sequence.^d Correlation with the known polarity sequence was not possible in the rest of Core 3 or in Core 4.

complex pattern of accumulation rates. The rates are very low at the top (less than 3 m/m.y.), and there are two possible hiatuses. The youngest prominent hiatus seems to occur between about 3.6 and 5.3 Ma (Barron et al., this volume), so almost the entire Gilbert Chron may be missing at this site. The magnetic data from about 16 to 23 m sub-bottom (\approx 6.4 Ma) are uncertain because of coring disturbance. Shipboard biostratigraphy suggests that a second hiatus affects the record of Chron 9. If so, the polarity pattern of Chrons 10 to 12

Table 4C. Magnetostratigraphy for Hole 575C.

Boundary	Age (Ma) ^a	Depth of boundary (m sub-bottom) ^b	Uncertainty range (Core-Section, level in cm) ^c
Brunhes/Matuyama	0.72	2.61	1-2, 106/1-2, 116
upper Jaramillo	0.91	3.11	1-3, 6/1-3, 16
lower Jaramillo	0.97	3.21	1-3, 16/1-3, 26
upper Olduvai	1.66	4.11	1-3, 106/1-3, 116
lower Olduvai	1.87	4.21	1-3, 116/1-3, 126
Matuyama/Gauss	2.47	5.31	1-4, 76/1-4, 86
upper Kaena	2.91	6.66	2-1, 26/2-1, 46
lower Kaena	2.98	6.91	2-1, 56/2-1, 66
upper Mammoth	3.07	7.11	2-1, 76/2-1, 86
lower Mammoth	3.17	7.41	2-1, 106/2-1, 116
Gauss/Gilbert	3.40	8.01	2-2, 16/2-2, 26
Gilbert/Chron 5	5.41	9.91	2-3, 56/2-3, 66
	5.70	10.91	2-4, 6/2-4, 16
	5.78	11.51	2-4, 66/2-4, 76
Chron 5/Chron 6	6.07	12.71	2-5, 36/2-5, 46
	6.42	15.51	2-7, 16/2-7, 26

^a Ness et al. (1980).^b Interpolated from coring summary (site chapter).^c Last sample of upper polarity sequence/first sample of lower polarity sequence.

Table 4D. Magnetostratigraphy for Hole 575A.

Boundary	Age (Ma) ^a	Depth of boundary (m sub-bottom) ^b	Uncertainty range (Core-Section, level in cm) ^c
	16.25	95.79	1-1, 29/1-1, 69
	16.29	97.29	1-3, 29/1-3, 69
	16.46	99.69	2-1, 49/2-1, 109
	16.53	101.74	2-2, 109/2-3, 9
Anomaly 5C onset	16.71	102.64	3-1, 9/3-1, 59
	?	113.59	5-3, 39/5-3, 97
	?	114.59	6-1, 29/6-1, 69
Anomaly 5D termination	17.28	118.09	6-3, 69/6-3, 129
Anomaly 5D onset	17.60	125.59	8-2, 49/8-2, 109
	17.81	128.44	10-1, 1/10-1, 46
	17.83	129.83	10-1, 134/10-2, 41

^a Ness et al. (1980).^b Interpolated from coring summary (site chapter) and corrected with regard to each core's washdown.^c Last sample of upper polarity sequence/first sample of lower polarity sequence.

correlates with the measured magnetostratigraphy. From about 34.5 m to 93.8 m sub-bottom, very weak intensities again precluded the development of a coherent magnetostratigraphy. The polarity pattern established throughout the upper 10 cores of Hole 575A (Fig. 9D) is interpreted here as being correlated with Anomalies 5C and 5D (about 16 to 18 Ma; Ness et al., 1980), an interpretation that is generally compatible with biostratigraphic results (Barron et al., this volume). Despite the poor control, an increase in sedimentation rates up to 21.5 m/m.y. can be detected in the older sediments.

The transition at all Leg 85 sites from cyclic siliceous-calcareous oozes to highly calcareous oozes is accompanied by a remarkable decrease in NRM intensities that may be caused by a significant reduction in the proportion of magnetic grains in the Miocene and older sediments. It is more likely, however, that the magnetic carriers have been altered (Kent and Lowrie, 1974; Henshaw and Merrill, 1980). The alteration may be related to the change from mainly calcareous (foram-nanno)

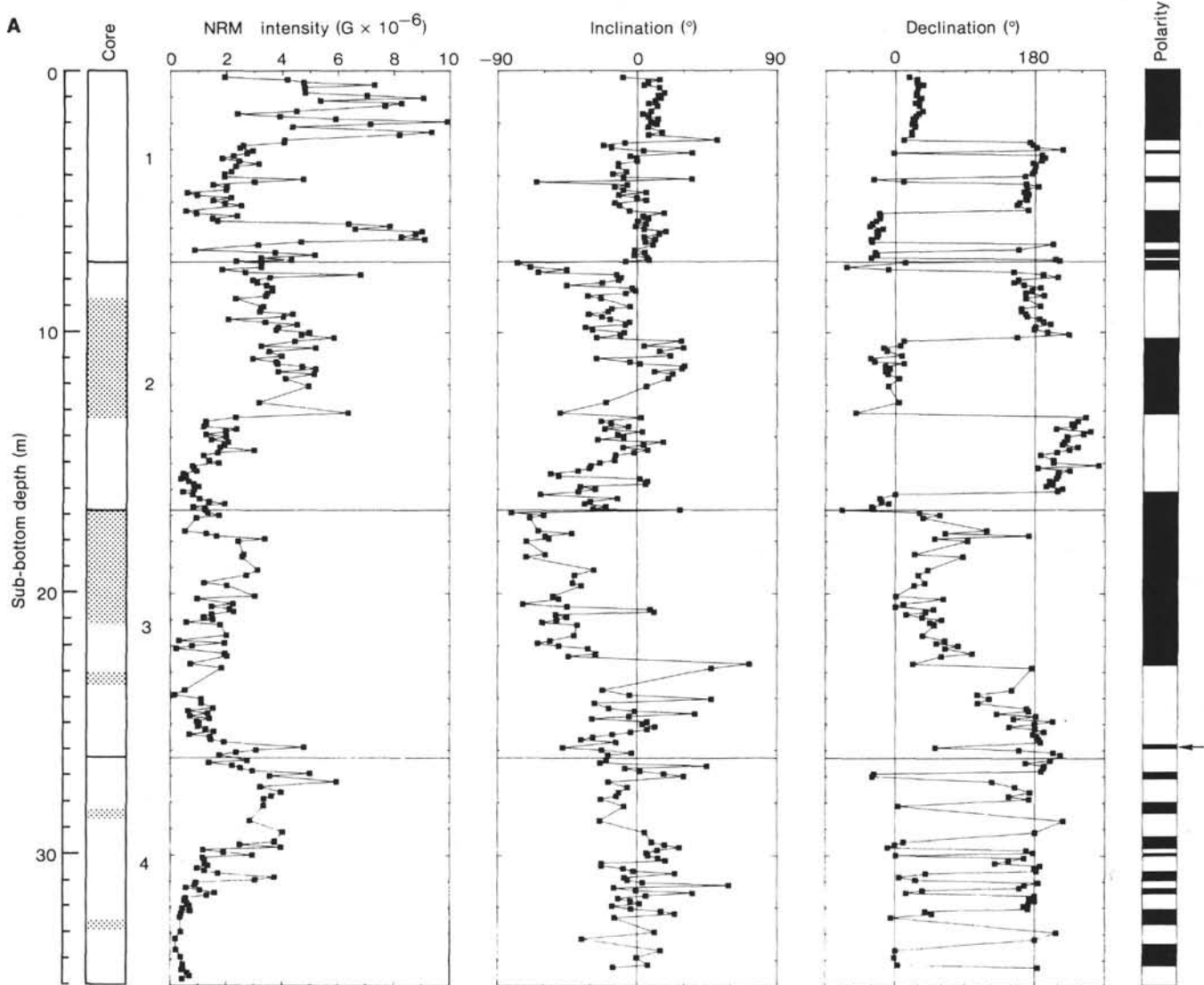


Figure 9. Polarity and NRM intensity logs for (A) Hole 575, (B) 575B, (C) Hole 575C, and (D) Hole 575A. See Figure 8 caption for further explanation.

oozes below to more siliceous sediments above or to diagenetic changes that begin at some 40 to 80 m sub-bottom at these sites. It is possible, of course, that all three of the conditions mentioned above are at work simultaneously. We performed no rock-magnetic analyses, so none of these ideas is supported by experimental evidence. However, Kent (1982) has shown that there is a correlation between low biogenic carbonate and high silica content and high NRM intensity. We noted an empirical relation between large-scale carbonate content variations and NRM intensity changes in the cyclic units of the Leg 85 sites, although no direct correlation was attempted. This relation may reflect a climatically driven, complex interaction between these parameters (Kent, 1982). No prominent changes in sedimentation rate or porosity were noted in these cyclic intervals (site chapters), so the amounts or properties of the magnetic materials (Hamano, 1980) are unlikely to be strongly affected by these factors. In contrast, the poor quality of the data in the metalliferous sediment layers overlying basement at Sites 573 and 574 is in all probability caused

by erratic chemical and thermal magnetic overprints due to hydrothermal alteration.

Tectonic Analysis

The Pacific Plate has moved northwest at the rate of a little less than $1^\circ/\text{m.y.}$ during the Mesozoic and Cenozoic. Different authors have used various methods to infer this motion. The methods include the study of the thickness of equatorial pelagic facies (Hays et al., 1969; Winterer, 1973; van Andel et al., 1975), basement age comparisons (Hays et al., 1972), hotspot traces (Minster et al., 1974; Epp, 1978; Gordon and Cape, 1981), the study of seamount magnetization (Sager, 1983), the study of magnetic anomaly patterns (Atwater and Menard, 1970; Herron, 1972), and the analysis of the paleomagnetism of central Pacific sedimentary cores (Hammond et al., 1974, 1975, 1979). Although our data are limited, we have attempted to study the northward component of plate motion by using Leg 85 paleomagnetic results. We divided the usable data from Sites 573, 574, and 575 into the time intervals or ranges listed in Table 5. These

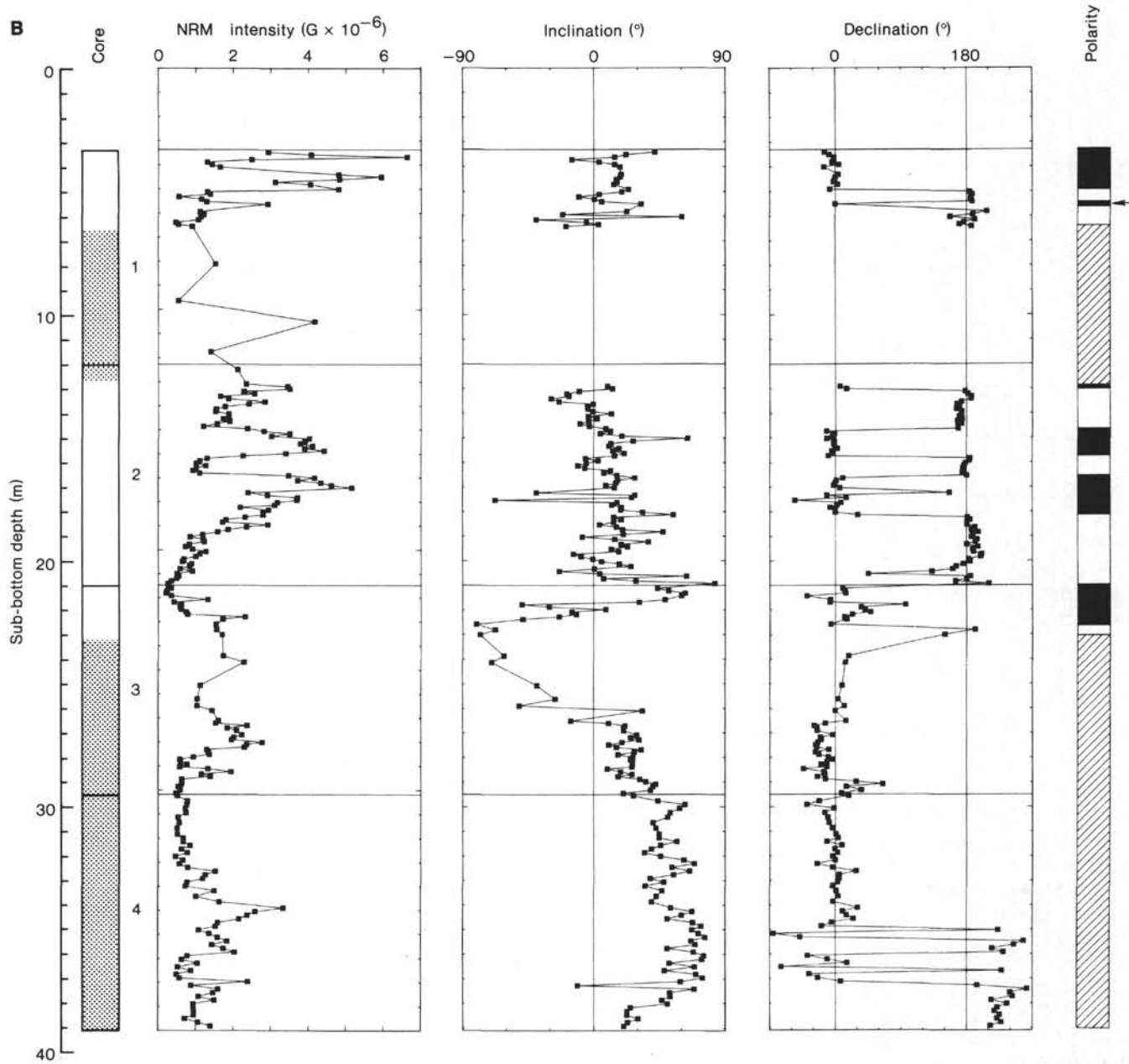


Figure 9. (Continued).

particular intervals were chosen because the resolution of our data varies (resolution is highest in the youngest intervals and lowest in the oldest sediments). Hiatuses, or inferred gaps, also influenced the choices. Thus, the Plio-Pleistocene data for Site 574, for example, were divided at the Gauss/Gilbert boundary into two intervals; an upper Miocene interval was also used. In the data for Site 575 a Pliocene hiatus was used as a boundary between two data sets; and a third interval between about 16 and 18 Ma was also analyzed (see previous discussion of Hole 575A). Using inclination data only, we averaged data from correlative intervals of parallel holes at each site (Fig. 10). We then calculated mean dipole paleolatitudes for each time interval by using statistics developed by Kono (1980), which provide 95% confidence limits. The mean paleolatitude for each time interval was then

normalized for present site latitudes, and a latitude differential, or δ latitude, was derived. The latter was plotted (Table 5, Fig. 11) against the mean age of the interval as shown in Bleil (1981). The regression coefficient of 0.99 indicates a good linear fit (Fig. 11), and the slope of the curve expresses a northward motion of $0.29^{\circ}/\text{m.y.}$, which agrees in general with previous approaches. (Figure 11 also supports our interpretation of the upper Miocene polarity sequence at Site 574. If that interval were as old as suggested by the biostratigraphy [Chron 8], the curve's fit would deteriorate.)

Paleolatitudes for Leg 85 sites were also calculated by using the rotation poles derived from a hotspot analysis (Epp, 1978). The backtracked positions of Sites 573 to 575 are shown in 1-m.y. steps in Figure 12. The hotspot paleolatitudes corresponding to the mean ages of the

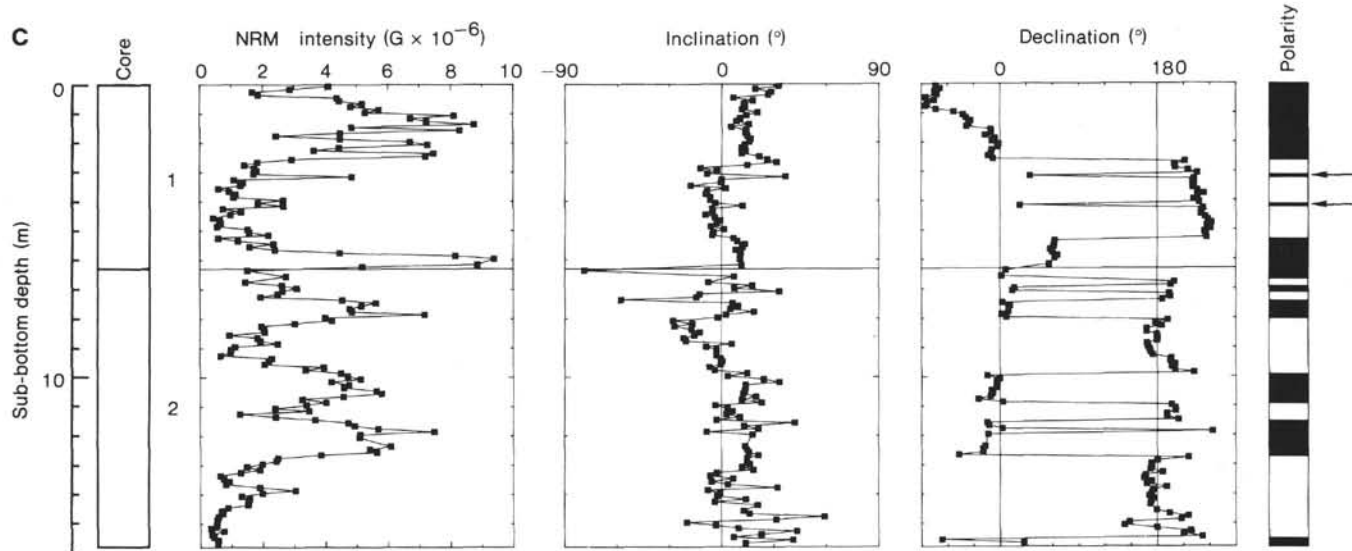


Figure 9. (Continued).

time intervals chosen here are listed in Table 5 together with present site latitude minus dipole paleolatitude and present site latitude minus hotspot paleolatitude. Table 5 shows that the hotspot-based differences are always smaller than those based on paleomagnetic data. If we assume that the hotspot data carry only tectonic information, this difference can be interpreted as an expression of oscillatory far-sided effects of the Earth's magnetic field (Epp et al., 1983). The regression ($r^2 = 0.99$) calculated from hotspot data shows a shallower slope ($0.23^\circ/\text{m.y.}$, indicating a slower northward motion for the Pacific Plate) than the slope resulting from a hotspot reference system, a conclusion that Epp et al. (1983) arrived at on the basis of central Pacific piston cores. As the authors pointed out, the differences could also be explained by assuming that the hotspot is not fixed with respect to the Earth's spin axis.

In addition to the above paleolatitude analysis, we also calculated paleo-pole positions for some time intervals. Gordon and Cox developed a technique (1980) that calculates a mean pole from a given model pole by using an iterative least-squares method. With this procedure it is possible to use heterogeneous (unoriented as well as azimuthally oriented) magnetic and paleomagnetic data to define paleo-pole positions. Because the Leg 85 data are confined to virtually one point on the Pacific and thus result in large uncertainties, paleomagnetic data from several HIG conventional piston cores (CPCs) were added. The CPCs, which were acquired 30 to 40° west of Leg 85's sites (at similar latitudes), span the same time interval as the Leg 85 data. Most of the CPC data have the advantage of being azimuthally oriented (Seyb et al., 1977), which improves the resolution of the Gordon and Cox (1980) method. We arbitrarily divided the entire data set into three age groups: Recent to about 6 Ma, 8 to approximately 11 Ma, and 15 to about 18 Ma (Table 6). Paleo-pole positions were then calculated (with Gordon and Cox's procedure) together with their semi-axes of the 95% oval of confidence (Table 6). These geograph-

ically well separated and internally coherent data sets produced relatively small and discrete 95% confidence ovals, although for the early Miocene pole the data are less numerous and the constraints are correspondingly broader. An apparent polar wander path (APWP) could thus be derived for the interval from 0 to 18 Ma (Fig. 13) that substantiates the overall northwest motion of the Pacific Plate. Our APWP shows a larger longitudinal and latitudinal displacement than the data published by Gordon and Cox (1981) for the Pacific Plate, although the trends are similar. Our paleo-pole latitudes indicate a northward component of motion for the Pacific Plate of about $0.59 \pm 0.08^\circ/\text{m.y.}$ during the last 18 m.y. This migration exceeds our earlier calculations, which are based on the Leg 85 inclination data alone. One can interpret this difference as reflecting the longitudinal separation (on the same plate) between the Leg 85 sites and the HIG CPCs. Hammond et al. (1979) gave an average northward motion calculated on the basis of inclination data from CPCs (which included the cores used in this paper) of about $0.59^\circ/\text{m.y.}$ Our tectonic analysis also shows that low-latitude inclination data, previously often considered to be useless, can be employed with significant success for tectonic work. Finally, the study confirms the results of previous work that had pointed out that Tertiary paleomagnetic data may contain appreciable components of long- and short-term paleofield variations in addition to tectonic information (Epp et al., 1983; Theyer et al., 1983).

ACKNOWLEDGMENTS

We thank all persons responsible for the success of DSDP Leg 85, especially the JOIDES Ocean Paleoenvironmental Panel, who were the original "movers" behind it all. Special appreciation is given to U. Bleil and V. Spiess for discussions and valuable comments. D. Wilson, S. Hammond, D. Epp, and W. Sager, all formerly at HIG, stimulated and helped with the paleomagnetic-tectonic phase. J. Barron and C. Nigrini assisted with stratigraphic data and discussions. N. Shackleton suggested changes in an early version of the manuscript, and two anonymous reviewers offered many suggestions for improvements. R.

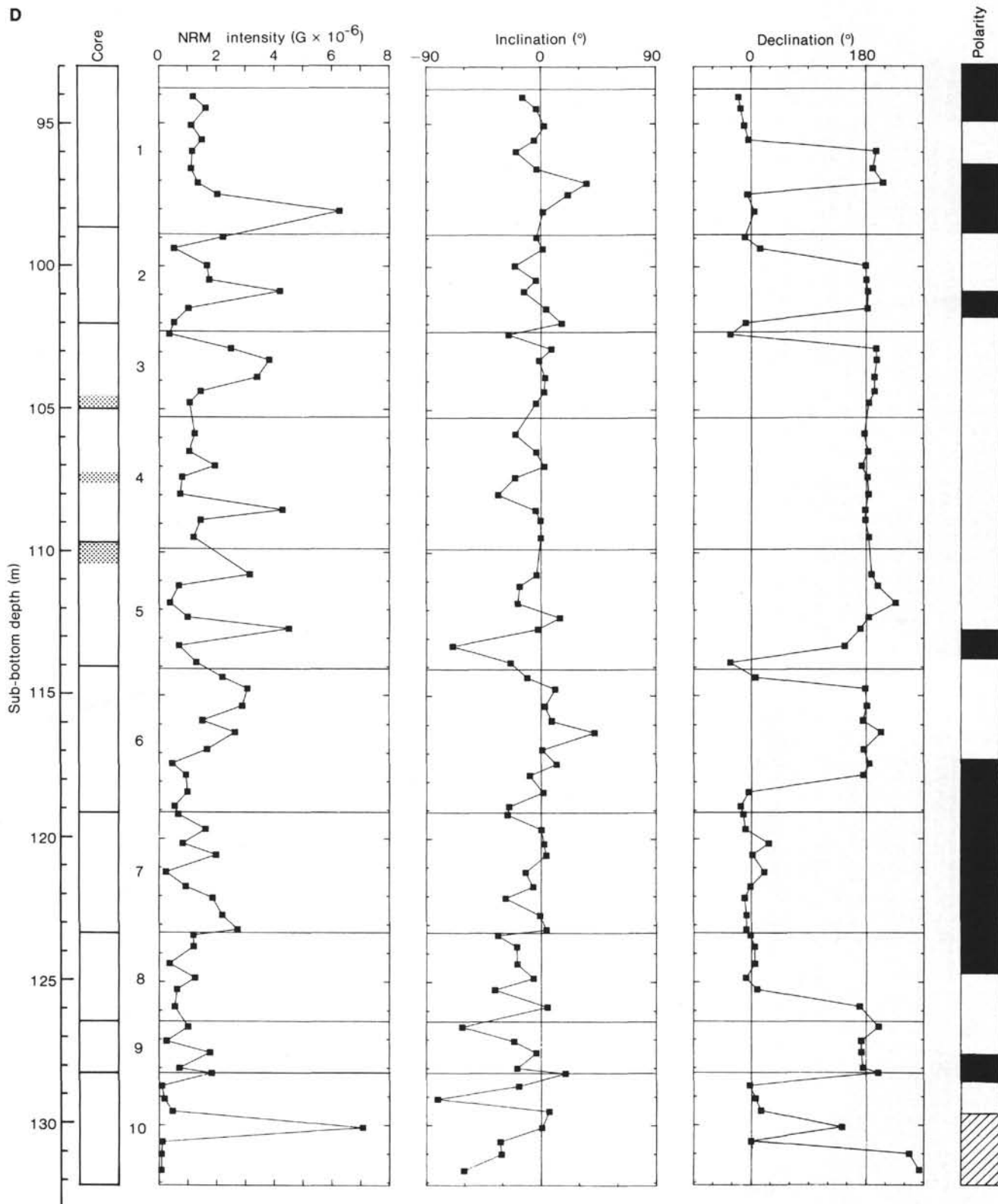


Figure 9. (Continued).

Pujalet also assisted with editorial advice. J. Tuthill helped develop tectonic software. We are also grateful to the members of the HIG Core Analysis Laboratory for their support.

N.W. thanks the Deutsche Forschungsgemeinschaft for support. F.T.'s research was in part supported under National Science Foundation Grant OCE81-17997. The HIG Core Analysis Laboratory is sup-

ported under NSF Grant OCE82-0196. This paper is HIG Contribution No. 1463.

REFERENCES

- Atwater, T., and Menard, H. W., 1970. Magnetic lineations in the northwest Pacific. *Earth Planet. Sci. Lett.*, 7:445-450.

- Barron, J. A., and Keller, G., 1982. Widespread Miocene deep-sea hiatuses: coincidence with periods of global cooling. *Geology*, 10: 577-581.
- Bleil, U., 1981. Paleomagnetism of Deep Sea Drilling Project Leg 60 sediments and igneous rocks from the Mariana region. In Husong, D. M., Uyeda, S., et al., *Init. Repts. DSDP*, 60: Washington (U.S. Govt. Printing Office), 855-873.
- Epp, D., 1978. Age and tectonic relationships among volcanic chains on the Pacific plate [Ph.D. Dissert.]. University of Hawaii, Honolulu.
- Epp, D., Sager, W., Theyer, F., and Hammond, S., 1983. Hotspot spin axis motion or far-sided effects? *Nature*, 303:318-320.
- Fisher, R. A., 1953. Dispersion on a sphere. *Proc. R. Soc. London*, 217:295-305.
- Gordon, G. G., and Cape, C. D., 1981. Cenozoic latitudinal shift of the Hawaiian hotspot and its implications for true polar wander. *Earth Planet. Sci. Lett.*, 55:37-47.
- Gordon, G. G., and Cox, A., 1980. Calculating paleomagnetic poles for oceanic plates. *Geophys. J. R. Astron. Soc.*, 63:619-640.
- Goree, W. S., and Fuller, M., 1976. Magnetometers using RF-driven SQUIDS and their applications in rock magnetism and paleomagnetism. *Rev. Geophys. Space Phys.*, 14:591-608.
- Hamano, Y., 1980. An experiment on the post-depositional remanent magnetization in artificial and natural sediments. *Earth Planet. Sci. Lett.*, 51:221-232.
- Hammond, S. R., Epp, D., and Theyer, F., 1979. Neogene relative motion between the Pacific plate, the mantle, and the Earth spin axis. *Nature*, 278:309-312.
- Hammond, S. R., Kroenke, L. W., and Theyer, F., 1975. Northward motion of the Ontong-Java plateau between -110 and -30 my: a paleomagnetic investigation of Site 289. In Andrews, J. E., Packham, G., et al., *Init. Repts. DSDP*, 30: Washington (U.S. Govt. Printing Office), 415-418.
- Hammond, S. R., Theyer, F., and Sutton, G. H., 1974. Paleomagnetic evidence of northward movement of the Pacific Plate in deep-sea cores from the central Pacific basin. *Earth Planet. Sci. Lett.*, 22: 22-28.
- Hays, J. D., et al., 1972. *Init. Repts. DSDP*, 9: Washington (U.S. Govt. Printing Office).
- Hays, J. D., Saito, T., Opdyke, N. D., and Burckle, L. H., 1969. Pliocene-Pleistocene sediments of the equatorial Pacific: their paleomagnetic, biostratigraphic, and climatic record. *Geol. Soc. Am. Bull.*, 80:1481-1514.
- Henshaw, P. C., and Merrill, R. T., 1980. Magnetic and chemical changes in marine sediments. *Rev. Geophys. Space Phys.*, 18: 483-504.
- Herron, E. M., 1972. Sea-floor spreading and the Cenozoic history of the east central Pacific. *Geol. Soc. Am. Bull.*, 83:1671-1692.
- Hoffman, K. A., and Day, R., 1978. Separation of multi-component NRM, a general method. *Earth Planet. Sci. Lett.*, 40:433-438.
- Kent, D. V., 1982. Apparent correlation of paleomagnetic intensity and climatic records in deep-sea sediments. *Nature*, 299:538-539.
- Kent, D. V., and Lowrie, W., 1974. Origin of magnetic instability in sediment cores from the central North Pacific. *J. Geophys. Res.*, 79:2987-3000.
- Kent, D. V., and Spariosu, D. J., 1982a. Magnetostratigraphy of equatorial Pacific Site 503 hydraulic piston cores. In Prell, W. L., Gardner, J. V., et al., *Init. Repts. DSDP*, 68: Washington (U.S. Govt. Printing Office), 435-440.
- _____, 1982b. Magnetostratigraphy of Caribbean Site 502 hydraulic piston cores. In Prell, W. L., Gardner, J. V., et al., *Init. Repts. DSDP*, 68: Washington (U.S. Govt. Printing Office), 419-433.
- Kono, M., 1980. Statistics of paleomagnetic inclination data. *J. Geophys. Res.*, 85:3878-3882.
- Løvlie, R., 1976. The intensity pattern of post-depositional remanence acquired in some marine sediments deposited during a reversal of the external magnetic field. *Earth Planet. Sci. Lett.*, 30:209-214.
- McDougall, I., 1977. *The Present Status of the Geomagnetic Polarity Time Scale*: Austr. Nat. Univ., Res. School Earth Sci. (Canberra), Publ. No. 1288.
- Mankinen, E. A., and Dalrymple, G. B., 1979. Revised geomagnetic polarity time scale for the interval 0-5 my B.P. *J. Geophys. Res.*, 84:615-626.
- Minster, J. B., Jordan, T. H., Molnar, P., and Haines, E., 1974. Numerical modeling of instantaneous plate tectonics. *Geophys. J. R. Astron. Soc.*, 36:541-576.
- Moore, T. C., van Andel, T. H., Sancetta, C., and Pisias, N., 1978. Cenozoic hiatuses in pelagic sediments. *Micropaleontology*, 24: 113-138.
- Ness, G., Levi, S., and Couch, R., 1980. Marine magnetic anomaly timescales for the Cenozoic and Late Cretaceous: a precis, critique, and synthesis. *Rev. Geophys. Space Phys.*, 18:753-770.
- Opdyke, N. D., 1972. Paleomagnetism of deep-sea cores. *Rev. Geophys. Space Phys.*, 10:213-249.
- Opdyke, N. D., Burckle, L. H., and Todd, A., 1974. The extension of the magnetic time scale in sediments of the central Pacific ocean. *Earth Planet. Sci. Lett.*, 22:300-306.
- Petersen, N., and Roggenthen, W. M., 1980. Rock- and paleomagnetism of Deep Sea Drilling Project Leg 54 basalts—East Pacific Rise and Galapagos Rift. In Rosendahl, B. R., Hekinian, R., et al., *Init. Repts. DSDP*, 54: Washington (U.S. Govt. Printing Office), 865-877.
- Sager, W. W., 1983. A late Eocene paleomagnetic pole for the Pacific plate. *Earth Planet. Sci. Lett.*, 63:408-422.
- Seyb, S. M., Hammond, S. R., and Gilliard, T., 1977. A new device for recording the behavior of a piston corer. *Deep Sea Res.*, 24: 943-950.
- Tauxe, L., Tucker, P., Petersen, N., and LaBrecque, J., 1983. The magnetostratigraphy of Leg 73 sediments. *Palaeogeogr. Palaeoclimatol., Palaeoecol.*, 42:65-90.
- Theyer, F., and Hammond, S. R., 1974. Cenozoic magnetic time scale in deep-sea sediments: completion of the Neogene. *Geology*, 2: 487-492.
- Theyer, F., Mato, C. Y., and Hammond, S. R., 1978. Paleomagnetic and geochronologic calibration of latest Oligocene to Pliocene radiolarian events, equatorial Pacific. *Mar. Micropaleontol.*, 3: 377-395.
- Theyer, F., Weinreich, N., and Bleil, U., 1983. Neogene polar wander path for the Pacific: plate motion and field behavior. Internat. Union Geol. Geophys. Gral. Assembly, Hamburg. (Abstract)
- van Andel, T. H., Heath, G. R., and Moore, T. C., 1975. Cenozoic history and paleoceanography of the central equatorial Pacific Ocean. *Mem. Geol. Soc. Am.*, 143:1-134.
- Winterer, E. L., 1973. Sedimentary facies and plate tectonics of equatorial Pacific. *Am. Assoc. Pet. Geol. Bull.*, 57:265-282.
- Zijderveld, J. D. A., 1967. AC demagnetization of rocks: analysis of results. In Collison, D. W., Creer, K. M., and Runcorn, S. K. (Eds.), *Methods in Paleomagnetism*: Elsevier (N.Y.), pp. 254-286.

Date of Initial Receipt: 18 August 1983

Date of Acceptance: 4 April 1984

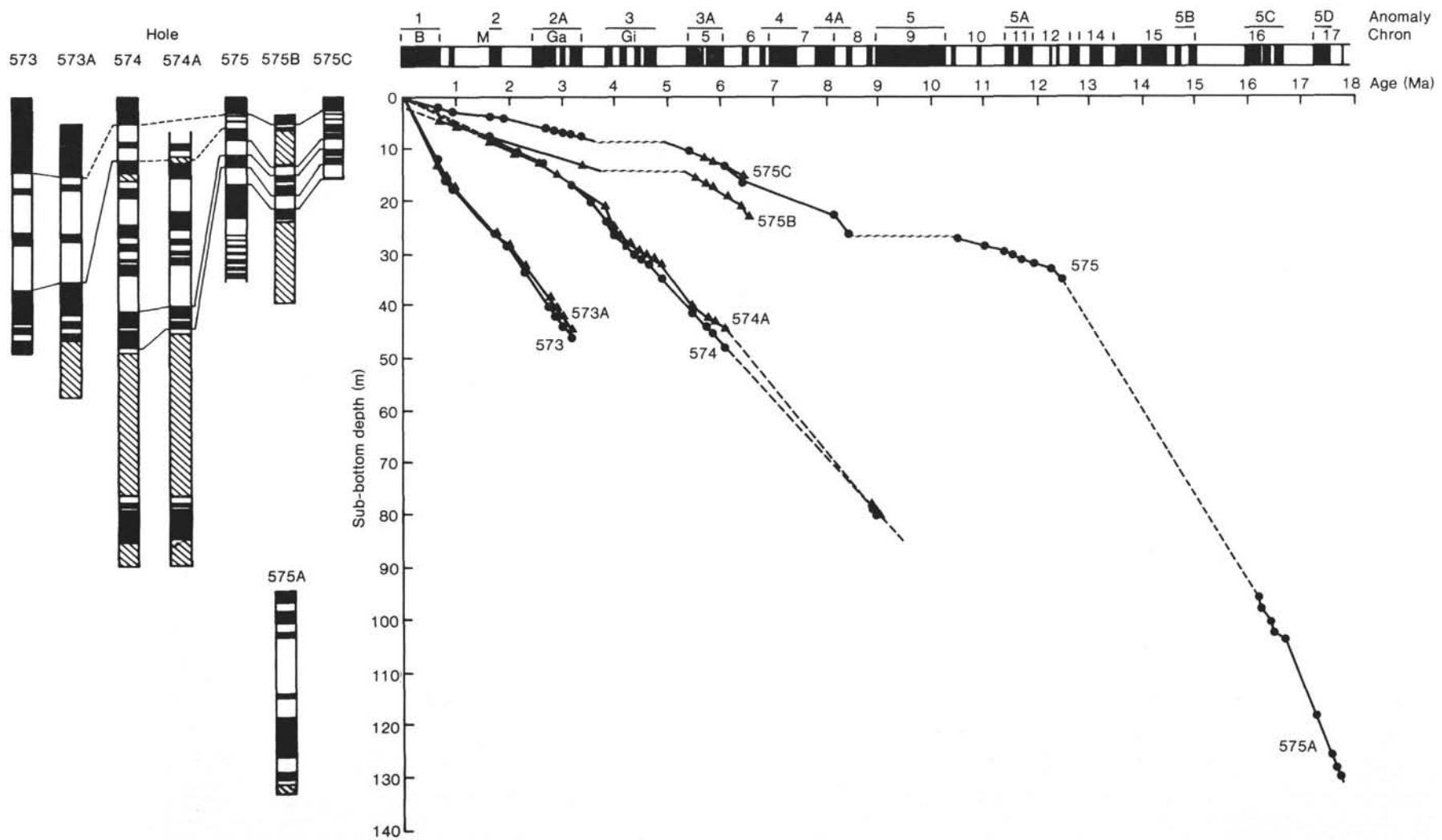


Figure 10. Summary of magnetostratigraphy and sedimentation rates for the sections at Sites 573, 574, and 575. Sediment depth and polarity are plotted against the geomagnetic time scale of Ness et al. (1980). The major marine magnetic anomalies are also shown (Mankinen and Dalrymple, 1979). The circles and triangles in the sedimentation curves distinguish data from different holes. Wavy lines indicate hiatuses. The dashed lines (Sites 574 and 575) indicate lack of data. Black indicates intervals of normal polarity, white intervals of reversed polarity, and striping intervals that could not be interpreted. B = Brunhes, M = Matuyama, Ga = Gauss, Gi = Gilbert Chron.

Table 5. Summary of tectonic parameters.

Site	Location	Age range (Ma) ^a	Arithmetic mean of age range (Ma)	Number of data used to calculate paleolatitude	Dipole paleolatitude ^b	95% confidence limit (°) ^c	Hotspot paleolatitude ^d	Difference (°) between present site and	
								Dipole paleolatitude	Hotspot paleolatitude
573	0.5°N, 133.3°W	0–3.3	1.7	162	0.81°S	±0.78	0.36°S	1.31	0.86
574	4.2°N, 133.3°W	0–3.4	1.7	74	2.95°N	±0.86	3.43°N	1.25	0.77
		3.4–6.2	4.8	182	1.91°N	±0.66	2.63°N	2.29	1.57
		8.7–10	9.4	58	0.30°N	±1.39	1.15°N	3.90	3.03
575	5.9°N, 135.0°W	0–3.4	1.7	125	4.13°N	±0.68	5.05°N	1.72	0.80
		5–6.4	5.7	102	3.21°N	±1.25	4.04°N	2.64	1.81
		16–18	17.0	50	0.06°N	±1.67	1.70°N	5.79	4.15

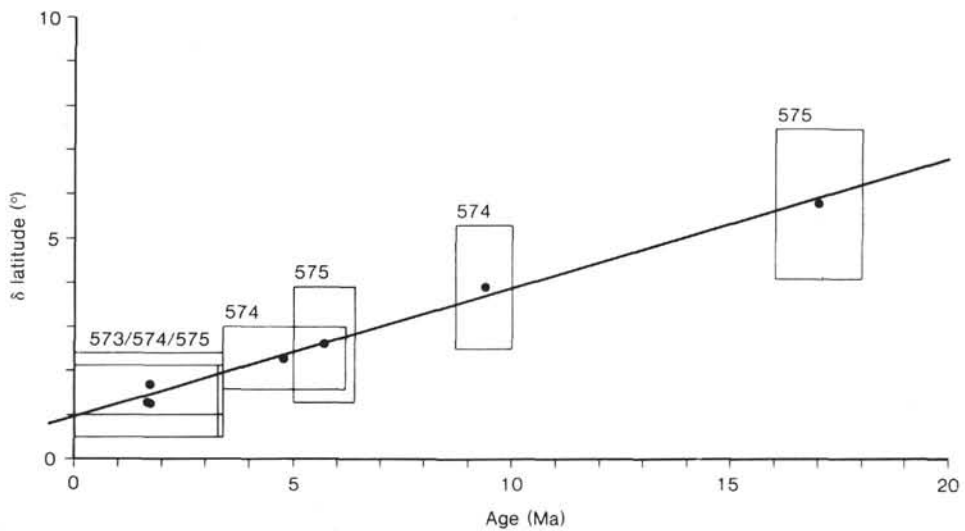
^a Age range used for tectonic calculations.^b Calculated by using the dipole formula and Kono's (1980) statistics.^c Calculated by using Kono's (1980) method.^d Calculated by using Epp's (1978) rotation poles for the Pacific Plate.

Figure 11. Delta latitude (site's present latitude minus its paleolatitude) versus age (Ma). Boxes represent the size of the error in latitude (which is based on Kono's [1980] statistics [Table 5]) and range of the error in age. The solid line is the regression curve (Table 5).

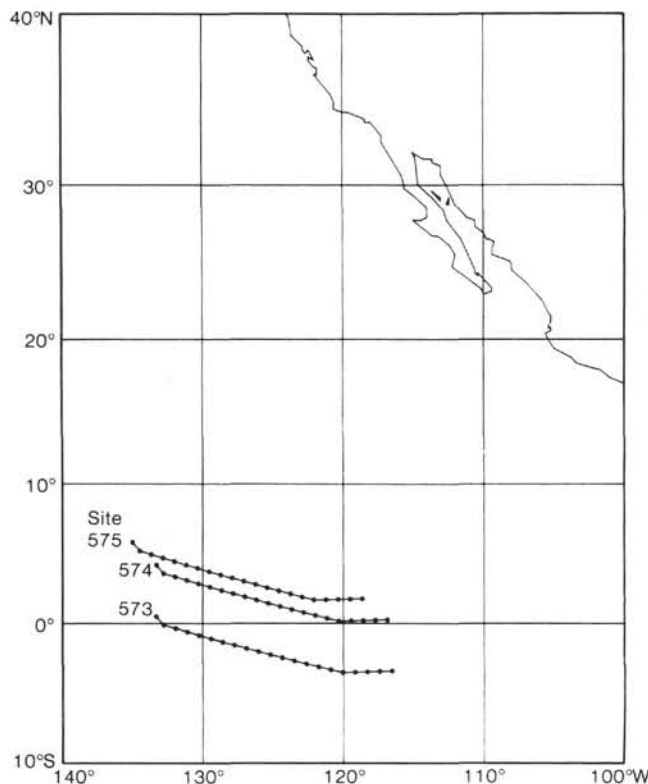


Figure 12. Stereographic projection of the migration of Sites 573, 574 and 575. Site positions (in 1-m.y. steps) were calculated by using the rotation poles for the Pacific Plate that Epp (1978) derived from the movement of Pacific island chains.

Table 6. Pliocene to early Miocene paleo-pole positions for the Pacific Plate derived from Leg 85 sites and HIG piston cores, using the method of Gordon and Cox (1980).

Number of DSDP site or HIG piston core	Present longitude, latitude	Age range used to calculate pole position (Ma)	Paleo-pole position	dp^a	dm^a	Number of samples
573	0.5°N, 133.3°W	0-3.3				
574	4.2°N, 133.3°W	0-6.2				
575	5.9°N, 135.0°W	0-6.4				
K78-5-11	7.5°N, 169.7°W	1.7-5.3	87.9°N, 59.6°E	0.9°	3.3°	106
K76-1-07	2.8°S, 177.9°E	3-4.8				
574	4.2°N, 133.3°W	8.7-10				
K76-1-11	0.9°N, 178.6°W	8-11	85.1°N, 4.7°E	2.3°	4.2°	71
K76-1-17	4.6°N, 176.6°W	8-11.5				
575	5.9°N, 135.0°W	16-18				
K78-5-18	8.7°N, 166.9°W	15-18	79.5°N, 31.7°W	2.9°	7.0°	35
K72-36	2.4°S, 177.8°W	16-19				

^a Semi-axes of the 95% oval for the calculated pole position.



Figure 13. Apparent polar wander path determined on the basis of Leg 85 and HIG piston core paleomagnetic data. Poles and their 95% ovals are calculated for three time intervals (0 to 6 Ma, 8 to 11 Ma, 16 to 18 Ma) using the method of Gordon and Cox (1980). Crosses show HIG locations (Table 6), and triangles indicate Sites 573 to 575.

APPENDIX A
Paleomagnetic Data Derived from Late Miocene to Recent Leg 85 Samples (samples were measured at RUB)

Core-Section (interval in cm)	Sub-bottom depth (m)	J_{NRM} (G)	I_{NRM}	D_{NRM}	I_{stable}	D_{stable}	Polarity	MDF (Oe)
Hole 573								
1-1, 30-32	0.31	3.83 E-6	+ 12.0	343.1	+ 12.1	343.7	N	498
1-1, 70-72	0.71	1.19 E-6	+ 8.8	343.2	+ 7.2	343.4	N	388
1-1, 111-113	1.12	1.20 E-6	+ 0.0	17.3	+ 1.5	16.2	N	350
1-2, 20-22	1.71	4.43 E-6	+ 0.7	15.8	+ 0.1	16.0	N	281
2-1, 145-147	3.46	2.35 E-6	+ 0.3	282.2	- 2.3	283.8	N	382
2-2, 38-40	3.89	5.40 E-6	+ 0.3	319.0	+ 2.6	318.8	N	347
2-2, 95-97	4.46	4.12 E-6	- 7.3	338.7	- 5.6	337.7	N	275
2-2, 145-147	4.96	1.09 E-6	- 4.5	343.3	- 6.4	341.7	N	411
2-3, 38-40	5.39	1.26 E-6	- 9.4	357.3	- 11.4	359.0	N	374
2-3, 95-97	5.96	1.43 E-6	+ 0.9	14.2	+ 4.0	10.2	N	308
2-3, 145-147	6.46	7.78 E-7	+ 0.8	12.5	+ 11.6	29.7	N	300
2-4, 36-38	6.87	1.06 E-6	- 11.7	352.2	- 3.9	349.0	N	325
2-4, 95-97	7.46	2.75 E-6	- 48.4	356.8	- 49.9	349.2	N	265
2-4, 145-147	7.96	4.14 E-7	+ 7.7	322.7	+ 10.6	318.7	N	389
2-5, 36-38	8.37	2.00 E-7	+ 59.0	13.5	+ 58.0	5.4	N	>400
2-5, 95-97	8.96	5.32 E-7	- 3.3	351.7	+ 12.7	359.2	N	233
2-5, 143-145	9.44	5.11 E-7	- 9.7	343.3	+ 3.3	341.3	N	399
2-6, 36-38	7.87	1.45 E-6	- 5.8	319.8	- 5.1	319.6	N	330
2-6, 95-97	10.46	2.80 E-6	- 4.1	324.6	- 3.4	324.1	N	310
2-6, 138-140	10.89	1.56 E-6	+ 0.9	314.7	+ 3.1	314.8	N	309
2-7, 36-38	11.37	2.47 E-6	- 9.9	314.0	- 7.9	315.2	N	345
3-1, 8-10	11.59	8.23 E-7	+ 3.6	308.0	+ 7.4	307.2	N	378
3-1, 68-70	12.19	1.11 E-6	- 0.0	308.7	- 0.8	308.9	N	371
3-1, 125-127	12.76	4.28 E-6	- 2.1	355.3	- 2.5	354.6	N	297
3-1, 146-148	12.97	5.07 E-6	+ 0.6	323.3	- 1.9	1.8	N	176
3-2, 35-37	13.36	9.23 E-7	- 20.6	189.8	- 5.7	185.9	R	559
3-2, 85-87	13.86	1.02 E-6	- 13.6	193.6	- 12.5	193.4	R	499
3-2, 135-137	14.36	4.77 E-7	+ 3.6	129.3	+ 52.3	189.0	R	466
3-3, 35-37	14.86	5.04 E-7	- 7.3	196.8	+ 0.2	189.4	R	390
3-3, 85-87	15.36	9.97 E-7	- 4.6	213.1	+ 5.6	202.7	R	463
3-3, 135-137	15.86	1.06 E-6	+ 13.7	212.1	+ 32.4	212.1	R	472
3-4, 35-37	16.36	5.89 E-7	- 30.5	265.4	- 20.6	211.0	R	368
3-4, 85-87	16.86	8.03 E-7	- 29.3	271.8	- 24.2	264.4	N	338
3-4, 135-137	17.36	7.90 E-7	- 22.5	261.4	- 18.1	255.6	N	365
3-5, 6-8	17.57	4.06 E-7	- 14.4	303.5	- 19.9	221.0	R	198
3-5, 35-37	17.86	3.20 E-7	- 20.6	209.1	- 12.8	191.2	R	397
3-5, 85-87	18.36	9.21 E-7	+ 22.1	154.7	+ 5.5	128.6	R	478
3-5, 135-137	18.86	1.82 E-6	+ 2.5	131.9	+ 5.0	133.0	R	399
3-6, 35-37	19.36	2.51 E-6	- 0.4	128.9	- 0.2	130.5	R	347
3-6, 85-87	19.86	4.30 E-6	- 9.2	138.2	- 3.1	138.0	R	361
3-6, 135-137	20.36	1.25 E-6	+ 6.4	148.0	+ 12.6	144.1	R	433
4-1, 101-103	22.02	2.72 E-6	- 7.4	265.9	- 7.1	265.2	R	420
4-1, 144-146	22.45	5.00 E-7	- 32.9	242.2	- 12.4	248.4	R	572
4-2, 35-37	22.86	1.71 E-6	- 2.0	234.8	- 1.9	234.0	R	386
4-2, 87-89	23.38	1.11 E-6	+ 6.1	225.9	+ 8.1	225.2	R	408
4-2, 135-137	23.86	3.19 E-6	- 2.1	213.5	- 3.4	208.7	R	388
4-3, 8-10	24.09	2.05 E-6	+ 6.8	204.4	+ 6.0	200.5	R	364
4-3, 35-37	24.36	1.25 E-6	+ 13.3	194.0	+ 8.4	191.6	R	398
4-3, 87-89	24.88	5.77 E-7	+ 1.2	179.3	+ 4.0	184.7	R	454
4-3, 135-137	25.36	2.61 E-6	+ 0.5	359.5	- 4.1	7.5	N	154
4-4, 35-37	25.86	4.55 E-6	+ 4.0	349.0	+ 3.3	349.8	N	260
4-4, 87-89	26.38	2.25 E-6	+ 6.2	349.6	+ 4.6	347.5	N	256
4-4, 135-137	26.86	3.90 E-6	- 7.0	333.7	- 5.3	335.4	N	248
4-5, 35-37	27.36	1.98 E-7	+ 20.3	184.4	+ 5.0	161.2	R	>700
4-5, 82-84	27.83	1.13 E-6	+ 13.4	176.7	+ 5.8	148.6	R	456
4-5, 135-137	28.36	1.01 E-6	+ 1.2	153.3	+ 7.2	155.9	R	384
4-6, 35-37	28.86	2.30 E-6	+ 1.6	144.4	+ 5.2	143.4	R	441
4-6, 87-89	29.38	1.70 E-6	+ 11.7	142.8	+ 0.8	141.9	R	432
4-6, 135-137	29.86	1.21 E-6	- 6.8	134.3	+ 2.9	135.8	R	473
4-7, 5-7	30.06	1.61 E-6	+ 2.3	132.3	+ 5.5	135.4	R	369
4-7, 32-34	30.33	9.87 E-7	+ 17.4	141.9	+ 13.6	143.3	R	426
5-1, 25-27	30.76	9.86 E-7	- 17.9	18.5	- 16.7	19.6	R	449
5-1, 84-86	31.35	1.46 E-6	- 1.3	49.3	- 0.7	51.5	R	393
5-1, 141-143	31.92	1.23 E-6	+ 1.9	81.5	+ 3.9	80.8	R	403
5-2, 25-27	32.26	1.11 E-6	+ 15.2	94.3	+ 4.2	100.3	R	487
5-2, 84-86	32.85	1.18 E-6	+ 23.8	116.0	+ 10.4	122.2	R	537
5-2, 141-143	33.42	4.73 E-7	+ 7.0	144.6	+ 5.4	144.8	R	422
5-3, 22-24	33.73	1.09 E-6	+ 4.7	148.3	+ 2.4	148.0	R	415

Appendix A. (Continued).

Core-Section (interval in cm)	Sub-bottom depth (m)	J_{NRM} (G)	I_{NRM}	D_{NRM}	I_{stable}	D_{stable}	Polarity	MDF (Oe)
Hole 573 (Cont.)								
5-3, 93-95	34.44	1.32 E-6	+ 15.3	165.4	+ 8.1	168.4	R	388
5-3, 137-139	34.88	2.29 E-6	- 0.7	178.1	- 1.9	180.1	R	440
5-4, 31-33	35.32	1.47 E-6	+ 42.8	199.3	+ 16.2	193.1	R	583
5-4, 85-87	35.86	4.52 E-6	+ 7.9	200.7	+ 6.5	200.9	R	485
5-4, 127-129	36.28	3.69 E-6	- 1.0	24.9	- 2.9	25.1	N	471
5-5, 23-25	36.74	2.33 E-6	+ 4.5	23.8	+ 0.2	26.8	N	263
5-5, 85-87	37.36	2.15 E-6	- 7.7	27.9	- 3.7	29.6	N	218
5-5, 127-129	37.78	4.09 E-6	- 2.6	30.9	+ 0.4	33.1	N	260
5-6, 6-8	38.07	7.06 E-7	+ 9.2	19.3	- 6.3	30.3	N	142
5-6, 32-34	38.33	3.51 E-6	- 6.3	32.3	- 11.0	30.5	N	164
5-6, 85-87	38.86	1.95 E-6	- 1.3	38.7	- 3.1	38.5	N	191
6-1, 128-130	40.59	2.12 E-6	- 0.7	14.7	+ 3.0	16.6	N	235
6-2, 22-24	41.03	2.80 E-6	- 11.6	32.7	- 10.9	31.8	N	226
6-2, 72-74	41.53	2.65 E-6	- 2.7	19.4	- 3.7	17.2	N	232
6-2, 122-124	42.03	2.01 E-6	- 6.4	16.4	- 11.8	14.9	N	201
6-2, 146-148	42.27	7.91 E-7	- 1.2	203.6	+ 3.7	197.8	R	>500
6-3, 22-24	42.53	2.12 E-7	- 46.6	63.6	- 1.6	190.4	R	>1000
6-3, 83-85	43.14	9.83 E-7	+ 10.7	8.8	+ 69.5	84.3	R	63
6-3, 105-107	43.36	4.89 E-6	- 3.3	2.8	- 1.1	1.4	N	268
6-3, 135-137	43.66	3.36 E-6	- 0.3	7.1	+ 6.2	9.0	N	177
6-4, 22-24	44.03	3.13 E-6	- 2.0	2.5	- 4.3	1.0	N	208
6-4, 73-75	44.54	9.15 E-7	+ 31.3	174.1	+ 14.3	180.5	R	391
6-4, 105-107	44.86	6.15 E-7	+ 32.1	175.5	+ 15.0	179.1	R	494
6-4, 135-137	45.16	2.63 E-6	+ 6.7	177.7	+ 3.3	178.8	R	384
6-4, 147-149	45.28	3.46 E-6	+ 0.9	173.7	- 0.3	171.2	R	352
6-5, 12-14	45.43	4.32 E-8	+ 46.0	134.4	+ 46.2	113.9	R	>200
6-5, 61-63	45.92	6.56 E-8	+ 7.5	350.7	+ 32.4	356.9	N	>200
6-5, 114-116	46.45	3.27 E-7	+ 55.3	331.4	+ 53.0	332.4	N	223
6-6, 12-14	46.93	2.18 E-8	+ 18.8	12.4	+ 24.9	2.1	N	98
6-6, 57-59	47.38	1.59 E-7	- 47.6	65.7	- 38.9	68.7	N	>300
6-6, 112-114	47.93	1.77 E-7	- 41.5	40.8	- 38.8	38.2	N	189
Hole 573A								
1-1, 113-115	5.64	1.82 E-6	- 6.2	203.5	- 5.8	8.3	N	169
1-1, 138-140	5.89	8.74 E-7	+ 0.9	58.0	- 2.6	54.4	N	408
1-2, 20-22	6.21	1.56 E-6	+ 9.1	36.7	+ 10.2	33.9	N	385
1-2, 94-96	6.95	5.37 E-6	- 4.4	49.9	- 2.1	48.6	N	332
1-3, 27-29	7.78	3.95 E-6	- 3.3	50.3	- 3.7	49.9	N	455
1-3, 90-92	8.41	3.94 E-6	+ 5.4	46.1	+ 7.6	44.4	N	270
1-4, 45-47	9.46	6.09 E-6	+ 2.3	28.8	+ 1.2	27.1	N	257
1-4, 105-107	10.06	1.22 E-6	+ 2.8	3.3	+ 2.6	2.6	N	302
1-5, 45-47	10.96	4.02 E-6	- 1.1	350.4	+ 0.9	350.8	N	303
1-5, 105-107	11.56	1.48 E-6	+ 5.7	334.6	+ 5.6	334.4	N	373
1-6, 45-47	12.46	1.64 E-6	+ 8.2	309.1	+ 8.7	309.1	N	337
1-6, 105-107	13.06	1.14 E-6	+ 6.2	302.9	- 0.1	302.4	N	358
1-7, 5-7	13.56	5.30 E-6	+ 2.9	300.6	+ 3.5	301.2	N	292
1-7, 29-31	13.80	2.46 E-6	+ 1.4	298.1	- 1.0	298.6	N	241
2-1, 11-13	14.12	1.03 E-6	+ 4.1	354.7	+ 12.9	353.9	N	326
2-1, 37-39	14.38	7.13 E-7	+ 59.3	315.4	+ 61.8	322.0	N	396
2-1, 63-65	14.64	1.03 E-6	+ 81.8	245.3	+ 80.2	270.1	R	371
2-1, 87-89	14.88	6.17 E-7	+ 32.3	158.4	+ 19.2	161.8	R	567
2-1, 115-117	15.16	3.28 E-7	+ 23.2	152.6	+ 0.3	180.3	R	747
2-1, 138-140	15.39	2.32 E-6	+ 4.1	182.9	+ 4.1	183.7	R	654
2-2, 27-29	15.78	2.30 E-7	+ 76.9	318.5	+ 13.7	200.4	R	>1000
2-2, 47-49	15.98	2.30 E-6	+ 7.1	7.8	+ 8.0	6.0	N	169
2-2, 67-69	16.18	1.95 E-6	+ 6.5	14.6	+ 9.3	15.2	N	219
2-2, 112-114	16.63	6.43 E-6	+ 0.5	11.6	+ 1.9	11.9	N	276
2-2, 144-146	16.95	1.50 E-7	+ 45.6	192.5	+ 16.0	197.7	R	>500
2-3, 9-11	17.10	2.99 E-7	+ 29.9	230.3	+ 10.9	199.5	R	>500
2-3, 27-29	17.28	1.62 E-7	+ 35.8	33.2	+ 11.2	192.6	R	>600
2-3, 43-45	17.44	2.74 E-7	+ 46.9	34.6	+ 8.3	191.2	R	>500
2-3, 67-69	17.68	9.23 E-7	+ 21.3	353.3	+ 7.6	189.5	R	658
2-3, 112-114	18.13	1.54 E-6	+ 3.2	4.9	+ 62.9	215.8	R	86
2-4, 27-29	18.78	2.49 E-6	+ 2.7	186.0	+ 2.9	186.7	R	384
2-4, 67-69	19.18	2.46 E-6	+ 1.4	178.3	+ 2.4	181.2	R	360
2-4, 112-114	19.63	4.09 E-6	- 4.2	183.5	- 0.7	182.6	R	398
2-5, 27-29	20.28	8.83 E-7	+ 9.9	176.3	+ 8.8	178.8	R	365
2-5, 67-69	20.68	1.15 E-6	- 8.4	178.8	- 4.0	177.7	R	389

Appendix A. (Continued).

Core-Section (interval in cm)	Sub-bottom depth (m)	J_{NRM} (G)	I_{NRM}	D_{NRM}	I_{stable}	D_{stable}	Polarity	MDF (Oe)
Hole 573A (Cont.)								
2-5, 112-114	21.13	1.18 E-6	+ 17.4	159.6	+ 11.3	170.8	R	542
2-6, 25-27	21.76	2.21 E-6	+ 1.3	163.2	+ 2.0	167.1	R	478
3-1, 53-55	22.64	3.07 E-6	- 19.4	212.0	- 23.5	212.2	R	407
3-1, 88-90	22.99	9.93 E-7	+ 10.0	194.6	+ 10.6	195.1	R	412
3-1, 135-137	23.46	2.85 E-7	- 17.0	203.2	+ 1.8	191.0	R	534
3-2, 17-19	23.78	1.34 E-6	- 2.4	188.3	+ 2.9	187.6	R	426
3-2, 117-119	24.78	1.57 E-6	+ 11.1	159.7	+ 6.3	166.4	R	414
3-3, 16-18	25.27	2.24 E-7	- 62.9	114.4	- 45.6	180.6	R	584
3-3, 36-38	25.47	2.19 E-6	+ 7.8	339.0	+ 1.3	338.7	N	79
3-3, 57-59	25.68	2.87 E-6	- 15.5	338.3	- 14.1	340.8	N	197
3-3, 116-118	26.27	1.98 E-6	- 5.0	343.9	- 5.0	347.5	N	187
3-3, 146-148	26.57	3.59 E-6	- 12.1	347.3	- 13.0	346.1	N	217
3-4, 11-13	26.72	2.28 E-6	+ 6.5	346.1	+ 7.2	342.9	N	64
3-4, 35-37	26.96	7.99 E-7	- 55.0	71.6	- 19.4	160.3	R	452
3-4, 71-73	27.32	1.98 E-6	+ 3.5	182.7	- 1.0	174.2	R	383
3-4, 103-105	27.64	9.47 E-7	+ 19.3	156.9	+ 7.2	164.1	R	365
3-4, 138-140	27.99	1.51 E-6	+ 10.6	180.1	+ 5.7	172.9	R	352
3-5, 35-37	28.46	2.01 E-6	+ 12.2	176.6	+ 5.5	171.0	R	438
3-5, 71-73	28.82	2.01 E-6	- 8.3	161.6	- 6.9	169.5	R	416
3-5, 103-105	29.14	8.40 E-7	- 60.5	102.8	- 16.1	177.8	R	494
3-5, 137-139	29.48	1.17 E-6	- 16.8	185.5	- 3.8	182.2	R	444
3-6, 35-37	29.96	1.22 E-6	- 8.5	206.8	+ 4.8	199.0	R	366
3-6, 71-73	30.32	1.71 E-6	+ 4.1	191.7	- 0.2	199.1	R	478
3-6, 113-115	30.74	8.73 E-7	- 11.3	217.4	- 20.9	203.8	R	399
4-1, 83-85	32.14	3.23 E-7	- 20.7	217.7	- 10.9	219.3	R	451
4-1, 131-133	32.62	3.96 E-7	- 3.7	15.8	+ 10.1	187.4	R	71
4-2, 5-7	32.86	3.20 E-7	+ 0.9	207.8	+ 1.7	197.9	R	536
4-2, 32-34	33.13	6.14 E-7	+ 7.6	198.3	+ 3.2	200.1	R	440
4-2, 83-85	33.64	5.71 E-7	+ 14.6	183.4	+ 14.5	185.9	R	387
4-2, 131-133	34.12	2.24 E-6	+ 11.6	180.6	+ 8.4	182.2	R	473
4-3, 5-7	34.36	2.43 E-6	+ 6.0	177.7	+ 1.2	180.6	R	490
4-3, 32-34	34.63	1.05 E-6	+ 6.3	166.3	+ 7.8	168.1	R	554
4-3, 57-59	34.88	3.49 E-6	+ 2.3	168.5	+ 1.6	167.7	R	471
4-3, 83-85	35.14	2.99 E-6	- 4.5	348.6	- 8.4	350.8	N	275
4-3, 131-133	35.62	2.40 E-6	+ 1.2	339.3	+ 0.1	345.3	N	238
4-4, 32-34	36.13	1.43 E-6	- 3.7	0.8	- 2.5	355.4	N	188
4-4, 83-85	36.64	8.16 E-7	+ 7.8	341.0	+ 0.8	352.2	N	93
4-4, 131-133	37.12	2.39 E-6	- 0.5	354.2	+ 0.9	353.2	N	308
4-5, 32-34	37.63	1.73 E-6	+ 4.3	348.8	- 1.2	349.7	N	175
4-5, 83-85	38.14	2.32 E-6	+ 10.2	350.4	+ 4.0	357.0	N	185
4-5, 131-133	38.62	2.71 E-6	- 9.1	355.0	+ 1.2	351.4	N	232
4-6, 32-34	39.13	2.76 E-6	- 3.1	354.2	+ 3.5	349.1	N	250
4-6, 83-85	39.64	3.07 E-6	+ 6.1	349.2	+ 11.1	353.2	N	242
5-1, 98-100	40.79	4.30 E-6	- 17.1	14.4	- 18.1	11.6	N	232
5-1, 130-132	41.11	1.31 E-6	+ 20.5	211.1	+ 7.9	201.9	R	551
5-2, 25-27	41.56	1.21 E-6	+ 5.4	174.0	+ 1.4	181.3	R	421
5-2, 68-70	41.99	7.47 E-7	- 3.5	8.0	+ 12.9	187.2	R	32
5-2, 113-115	42.44	3.87 E-6	- 1.7	6.0	- 2.6	3.0	N	200
5-2, 146-148	42.77	6.50 E-6	+ 2.8	354.8	+ 3.8	356.8	N	267
5-3, 25-27	43.06	1.15 E-6	- 1.3	9.2	+ 20.5	4.7	N	40
5-3, 68-70	43.49	1.38 E-6	+ 13.4	160.1	+ 14.1	168.8	R	363
5-3, 113-115	43.94	2.71 E-6	- 6.0	181.3	- 1.9	179.5	R	447
5-3, 136-138	44.17	3.31 E-6	+ 6.0	181.3	+ 3.3	179.9	R	383
5-3, 143-145	44.24	3.51 E-6	+ 17.0	171.6	+ 15.2	176.8	R	439
5-4, 45-47	44.76	7.14 E-8	+ 14.8	2.4	no stable			399
5-4, 131-133	45.62	6.23 E-8	- 15.1	6.5	no stable			277
5-5, 51-53	46.32	3.96 E-8	+ 58.7	283.8	no stable			
5-5, 115-117	46.96	2.60 E-8	+ 74.3	345.5	no stable			
5-6, 8-10	47.39	1.04 E-7	+ 35.3	1.4	no stable			
5-6, 90-92	48.21	6.26 E-8	+ 8.9	118.5	no stable			
6-1, 65-67	49.86	4.45 E-7	- 8.8	177.2	no stable			105
6-2, 61-63	51.32	9.76 E-8	+ 71.4	254.1	no stable			31
6-3, 81-83	53.02	3.52 E-8	+ 57.0	289.6	no stable			
6-4, 58-60	54.29	2.96 E-8	- 42.6	294.0	no stable			
6-5, 90-92	56.11	1.05 E-7	+ 82.6	336.5	no stable			
6-6, 18-20	56.89	2.15 E-8	+ 15.8	323.0	no stable			
Hole 574								
1-1, 79-81	0.80	4.54 E-6	- 1.5	16.2	+ 0.9	14.0	N	250
1-1, 129-131	1.30	3.37 E-6	+ 6.2	16.0	+ 5.5	13.9	N	201

Appendix A. (Continued).

Core-Section (interval in cm)	Sub-bottom depth (m)	J_{NRM} (G)	I_{NRM}	D_{NRM}	I_{stable}	D_{stable}	Polarity	MDF (Oe)
Hole 574 (Cont.)								
1-2, 29-31	1.80	5.51 E-6	+ 12.0	5.5	+ 12.4	1.6	N	156
1-2, 54-56	2.05	4.39 E-6	+ 11.1	4.2	+ 6.8	1.0	N	147
1-2, 104-106	2.55	4.72 E-6	+ 2.8	0.7	- 0.6	356.7	N	196
1-2, 129-131	2.80	5.75 E-6	+ 15.0	336.5	+ 13.6	348.9	N	225
1-3, 4-6	3.05	3.10 E-6	+ 4.9	12.1	+ 5.6	11.3	N	198
1-3, 29-31	3.30	6.61 E-6	+ 0.1	355.5	+ 5.5	353.8	N	216
1-3, 54-56	3.55	4.20 E-6	+ 24.4	351.5	+ 9.5	352.9	N	95
1-3, 79-81	3.80	4.21 E-6	+ 7.1	355.3	+ 6.0	347.2	N	131
1-3, 104-106	4.05	1.14 E-6	- 7.2	38.5	+ 10.6	351.5	N	464
1-3, 129-131	4.30	1.78 E-6	+ 7.2	345.9	+ 8.9	350.8	N	280
2-1, 14-16	4.65	2.93 E-6	- 68.5	242.7	- 79.5	231.4	R	290
2-1, 37-39	4.88	2.27 E-7	- 63.2	277.8	+ 28.9	261.0	R	19
2-1, 67-69	5.18	2.05 E-6	+ 18.9	202.1	- 28.9	164.1	R	285
2-1, 94-96	5.45	2.34 E-6	+ 2.9	149.0	- 0.1	151.3	R	418
2-1, 119-121	5.70	2.73 E-6	- 3.8	157.4	- 3.3	161.0	R	508
2-2, 4-6	6.05	1.13 E-6	- 8.4	328.9	- 2.2	167.5	R	510
2-2, 29-31	6.30	2.06 E-6	- 5.6	165.5	- 6.1	165.9	R	388
2-2, 54-56	6.55	3.37 E-6	+ 3.4	176.5	- 2.4	172.3	R	434
2-2, 79-81	6.80	1.58 E-6	+ 4.0	152.5	- 1.3	166.0	R	468
2-2, 104-106	7.05	1.53 E-6	- 1.0	172.0	- 2.5	171.9	R	429
2-2, 129-131	7.30	5.01 E-7	+ 2.8	163.3	+ 8.7	179.7	R	521
2-3, 4-6	7.55	1.28 E-6	- 0.2	178.1	- 7.9	179.0	R	442
2-3, 29-31	7.80	1.60 E-6	- 14.3	164.7	- 12.4	174.2	R	421
2-3, 54-56	8.05	3.84 E-6	19.7	9.6	+ 5.8	10.7	N	121
2-3, 79-81	8.30	5.66 E-6	+ 9.7	10.3	+ 9.1	11.1	N	161
2-3, 104-106	8.55	5.73 E-6	+ 10.4	3.9	+ 12.6	4.9	N	173
2-3, 129-131	8.80	5.68 E-6	+ 5.4	8.0	+ 8.4	12.3	N	171
2-4, 4-6	9.05	9.31 E-7	- 12.4	184.2	- 5.7	185.6	R	467
2-4, 29-31	9.30	8.64 E-7	+ 0.3	193.7	- 1.6	181.3	R	456
2-4, 54-56	9.55	2.19 E-6	+ 3.2	195.1	- 4.9	185.2	R	398
2-4, 79-81	9.80	4.39 E-7	- 29.7	354.7	- 6.6	183.5	R	552
2-4, 104-106	10.05	1.57 E-6	- 10.7	185.5	- 9.8	185.2	R	416
2-4, 129-131	10.30	1.91 E-6	- 31.5	186.4	- 15.8	184.3	R	392
2-5, 4-6	10.55	1.16 E-6	+ 5.8	182.0	- 6.8	184.1	R	440
2-5, 29-31	10.80	3.12 E-7	+ 9.3	168.8	- 8.6	180.1	R	560
2-5, 54-56	11.05	5.70 E-7	+ 20.6	214.9	+ 8.3	179.0	R	599
2-5, 79-81	11.30	5.49 E-7	- 4.5	177.8	- 9.6	178.0	R	493
2-5, 104-106	11.55	2.64 E-6	+ 0.8	152.6	+ 1.5	161.1	R	431
2-5, 129-131	11.80	6.73 E-7	+ 14.5	5.8	+ 45.5	38.7	N	49
2-6, 4-6	12.05	2.05 E-6	+ 11.3	1.2	+ 8.8	14.0	N	144
2-6, 29-31	12.30	2.09 E-6	+ 14.0	10.9	+ 14.3	13.0	N	186
2-6, 54-56	12.55	2.61 E-6	+ 3.6	357.9	+ 16.7	3.6	N	74
2-6, 79-81	12.80	4.06 E-6	+ 8.1	9.2	+ 3.1	13.2	N	75
2-6, 104-106	13.05	5.25 E-6	+ 10.8	359.2	+ 13.8	8.1	N	135
2-6, 129-131	13.30	7.02 E-6	+ 5.2	8.7	+ 4.6	11.0	N	159
2-7, 4-6	13.55	6.30 E-6	+ 5.4	18.1	+ 6.4	23.1	N	103
2-7, 29-31	13.80	5.80 E-6	+ 11.1	15.9	+ 15.7	17.4	N	95
3-1, 75-77	14.76	9.45 E-6	- 86.2	249.2	- 85.0	217.7	R	274
3-1, 97-99	14.98	5.15 E-7	+ 11.2	321.5	- 29.5	254.8	R	348
3-1, 118-120	15.19	1.74 E-6	- 39.0	330.4	- 41.8	295.1	R	217
3-2, 16-18	15.67	1.83 E-6	- 17.8	126.3	- 6.1	137.2	R	388
3-2, 87-89	16.38	2.81 E-6	- 80.5	130.1	- 78.2	125.5	R	321
3-2, 136-138	16.87	1.25 E-6	- 61.8	65.3	- 30.0	60.4	N	315
3-3, 15-17	17.16	1.67 E-6	+ 14.6	332.3	+ 6.2	305.9	N	88
3-3, 39-41	17.40	2.49 E-6	+ 11.6	352.8	+ 9.8	351.8	N	208
3-3, 112-114	18.13	3.34 E-6	- 66.3	335.4	- 68.8	346.5	N	300
3-3, 136-138	18.37	1.06 E-6	- 46.2	231.8	- 49.5	210.9	R	299
3-4, 8-10	18.59	2.20 E-6	- 67.4	115.9	- 63.7	136.2	R	284
3-4, 29-31	18.80	6.45 E-7	- 18.0	147.6	- 4.6	148.5	R	449
3-4, 54-56	19.05	1.52 E-6	+ 2.5	146.0	+ 5.3	152.3	R	462
3-4, 79-81	19.30	1.16 E-6	+ 0.7	153.9	+ 3.7	160.4	R	418
3-4, 104-106	19.55	2.62 E-7	+ 79.6	239.4	+ 4.6	162.6	R	> 1000
3-4, 129-131	19.80	9.06 E-7	- 5.5	159.9	- 2.2	164.0	R	498
3-5, 4-6	20.05	1.13 E-6	- 3.0	144.1	- 1.5	165.3	R	443
3-5, 29-31	20.30	2.41 E-6	+ 8.2	179.6	+ 2.7	180.4	R	424
3-5, 54-56	20.55	1.54 E-6	1.3	171.5	+ 0.1	177.6	R	384
3-5, 75-77	20.76	1.99 E-6	+ 2.9	181.4	- 0.9	181.0	R	390
3-5, 104-106	21.05	1.87 E-6	+ 0.7	179.2	- 4.9	178.0	R	396
3-5, 129-131	21.30	6.86 E-7	+ 8.4	133.4	- 3.1	179.0	R	495
3-6, 4-6	21.55	1.51 E-6	+ 5.3	174.6	- 0.6	189.5	R	437
3-6, 29-31	21.80	1.67 E-6	- 12.3	186.2	- 8.7	191.0	R	449
3-6, 54-56	22.05	1.42 E-6	- 4.5	193.1	- 5.3	197.4	R	401
3-6, 79-81	22.30	2.39 E-6	- 13.6	180.0	- 8.9	190.3	R	424

Appendix A. (Continued).

Core-Section (interval in cm)	Sub-bottom depth (m)	J_{NRM} (G)	I_{NRM}	D_{NRM}	I_{stable}	D_{stable}	Polarity	MDF (Oe)
Hole 574 (Cont.)								
3-6, 104-106	22.55	1.17 E-6	-5.7	193.5	+0.8	202.2	R	500
3-6, 129-131	22.80	1.06 E-6	+57.8	86.5	+6.3	207.7	R	487
3-7, 4-6	23.05	7.27 E-7	-44.5	193.2	-4.8	202.9	R	532
3-7, 29-31	23.30	4.60 E-7	+4.3	105.3	-10.0	204.2	R	694
4-1, 12-14	23.63	6.45 E-6	-80.7	40.9	-75.0	62.9	N	307
4-1, 50-52	24.01	7.09 E-7	-1.3	50.2	-18.8	35.3	N	267
4-1, 91-93	24.42	2.76 E-7	-2.4	13.5	-3.0	7.8	N	287
4-1, 123-125	24.74	9.82 E-7	+18.5	18.9	+10.1	27.2	N	273
4-2, 15-17	25.16	2.36 E-6	+13.5	17.1	+1.8	28.5	N	142
4-2, 48-50	25.49	1.29 E-6	+21.0	15.2	+17.5	17.2	N	176
4-2, 85-87	25.86	2.37 E-6	+64.3	345.8	+44.0	13.0	N	304
4-2, 102-104	26.03	8.50 E-7	-31.9	320.1	-22.3	133.9	R	341
4-3, 6-8	26.57	9.37 E-7	+35.5	332.7	-15.8	164.0	R	23
4-3, 64-66	27.15	3.66 E-7	+39.2	226.8	-1.0	172.3	R	676
4-3, 89-91	27.40	7.21 E-7	+49.7	15.9	+3.2	164.5	R	378
4-3, 114-116	27.65	5.37 E-6	+6.1	350.0	+4.8	355.6	N	130
4-3, 139-141	27.90	5.10 E-6	+8.8	350.2	+4.9	351.2	N	189
4-4, 4-6	28.05	4.91 E-6	+4.5	354.3	+5.9	358.1	N	235
4-4, 29-31	28.30	4.47 E-6	+5.3	348.6	+7.2	354.9	N	159
4-4, 54-56	28.55	6.05 E-6	+4.7	346.3	+2.9	350.2	N	188
4-4, 79-81	28.80	5.49 E-7	+42.6	2.8	+14.2	169.4	R	48
4-4, 104-106	29.05	1.16 E-6	+51.5	178.3	+7.1	173.1	R	393
4-4, 129-131	29.30	3.06 E-7	+32.6	231.9	+8.8	176.5	R	699
4-5, 4-6	29.55	2.54 E-7	+70.0	201.3	+10.4	182.8	R	699
4-5, 29-31	29.80	5.82 E-7	+62.0	125.9	+4.8	173.5	R	499
4-5, 54-56	30.05	1.33 E-6	+22.1	186.4	-4.9	183.0	R	403
4-5, 79-81	30.30	7.84 E-7	+11.7	167.6	-2.4	185.9	R	476
4-5, 104-106	30.55	4.08 E-6	+4.5	357.4	-2.2	3.5	N	86
4-5, 129-131	30.80	5.74 E-6	+7.8	0.6	+7.0	8.1	N	160
4-6, 4-6	31.05	1.34 E-6	+25.6	332.0	+17.4	191.9	R	47
4-6, 29-31	31.30	7.32 E-7	+25.0	308.0	+13.5	193.9	R	> 500
4-6, 54-56	31.55	1.40 E-6	+6.7	359.4	+14.8	352.4	N	56
4-6, 79-81	31.80	4.78 E-6	+5.1	6.3	+8.5	9.8	N	205
44-6, 104-106	32.05	3.09 E-6	+1.6	0.8	+4.2	9.1	N	121
4-6, 139-141	32.40	5.28 E-6	+9.4	5.5	+7.1	4.7	N	234
4-7, 4-6	32.55	3.51 E-6	-19.3	354.1	+7.3	355.4	N	199
4-7, 27-29	32.78	4.94 E-6	-0.7	337.1	+3.7	350.1	N	123
5-1, 14-16	33.15	7.77 E-7	+69.5	260.0	+74.5	177.6	R	314
5-1, 36-38	33.37	9.93 E-7	-26.5	200.3	-24.4	176.4	R	431
5-1, 60-62	33.61	1.07 E-6	-35.7	74.5	-62.5	108.7	R	72
5-1, 100-102	34.01	7.00 E-6	+60.3	186.4	+61.2	186.7	R	47
5-1, 134-136	34.35	4.17 E-7	+25.0	311.1	-11.9	178.4	R	635
5-2, 4-6	34.55	1.43 E-6	+20.1	221.8	+0.4	176.6	R	464
5-2, 29-31	34.80	5.26 E-7	-4.9	332.9	-3.7	167.7	R	706
5-2, 54-56	35.05	4.56 E-7	+20.4	229.1	-1.1	161.9	R	680
5-2, 79-81	35.30	7.00 E-6	-42.6	298.5	+7.1	326.9	R	214
5-2, 104-106	35.55	7.35 E-7	+14.1	199.3	+2.0	166.8	R	772
5-2, 129-131	35.80	1.79 E-6	+21.7	342.7	-2.8	154.7	R	49
5-3, 4-6	36.05	9.19 E-7	-25.7	299.9	-13.3	165.7	R	496
5-3, 29-31	36.30	1.57 E-6	-36.3	209.9	-12.3	159.9	R	526
5-3, 54-56	36.55	1.96 E-6	-2.0	187.3	-4.5	156.7	R	433
5-3, 79-81	36.80	1.51 E-6	+43.4	2.0	-1.6	153.6	R	418
5-3, 104-106	37.05	1.09 E-6	-36.8	171.9	-9.7	162.4	R	677
5-3, 129-131	37.30	1.11 E-6	+24.0	171.8	+9.2	157.0	R	604
5-4, 4-6	37.55	1.30 E-6	-35.2	63.9	-6.9	161.7	R	462
5-4, 29-31	37.80	6.97 E-7	-20.6	329.6	-1.8	165.4	R	762
5-4, 54-56	38.05	2.04 E-6	+52.8	316.9	+4.4	169.8	R	485
5-4, 79-81	38.30	1.27 E-6	-63.2	315.2	-11.4	160.9	R	597
5-4, 104-106	38.55	2.77 E-6	+11.4	188.0	-2.9	169.5	R	446
5-4, 129-131	38.80	1.41 E-6	+66.1	310.6	+4.0	170.1	R	506
5-5, 4-6	39.05	1.22 E-6	+44.4	298.8	+3.6	187.2	R	572
5-5, 29-31	39.30	1.90 E-6	+16.8	43.3	+13.0	183.9	R	347
5-5, 54-56	39.55	6.69 E-7	-38.3	241.0	-6.7	191.5	R	575
5-5, 79-81	39.80	1.81 E-6	+27.1	340.4	-1.3	192.0	R	347
5-5, 104-106	40.05	2.05 E-6	+26.0	358.0	-7.5	190.0	R	27
5-5, 129-131	40.30	2.76 E-6	+13.3	3.0	-4.9	182.7	R	31
5-6, 4-6	40.55	5.32 E-6	-1.7	19.2	+4.6	28.1	N	81
5-6, 29-31	40.80	7.06 E-6	+11.8	20.2	+7.9	28.8	N	175
5-6, 54-56	41.05	3.71 E-6	-1.1	19.0	+10.4	30.4	N	71
5-6, 79-81	41.30	4.45 E-6	-0.2	23.4	+2.8	34.2	N	90
5-6, 104-106	41.55	3.80 E-6	+6.8	21.4	-14.1	35.0	N	66
5-6, 129-131	41.80	4.31 E-6	+5.0	23.9	-5.1	36.6	N	87

Appendix A. (Continued).

Core-Section (interval in cm)	Sub-bottom depth (m)	J_{NRM} (G)	I_{NRM}	D_{NRM}	I_{stable}	D_{stable}	Polarity	MDF (Oe)
Hole 574 (Cont.)								
5-7, 4-6	42.05	3.51 E-6	+ 2.2	23.1	+ 6.3	35.2	N	81
5-7, 29-31	42.30	3.27 E-6	- 1.4	35.7	+ 6.8	43.2	N	153
6-1, 15-17	42.66	8.54 E-7	- 32.2	316.4	- 70.6	113.7	N	484
6-1, 52-54	43.03	1.53 E-6	+ 3.5	19.7	- 34.2	32.8	N	179
6-1, 77-79	43.28	6.82 E-7	+ 29.8	0.7	+ 40.8	34.3	N	124
6-1, 119-121	43.70	7.06 E-7	- 30.6	332.9	+ 39.8	182.3	R	28
6-1, 142-144	43.93	1.05 E-6	+ 2.2	173.9	+ 2.2	160.8	R	703
6-2, 4-6	44.05	2.45 E-6	+ 24.0	2.5	+ 29.4	94.0	N	40
6-2, 29-31	44.30	4.28 E-6	+ 5.5	351.7	+ 1.8	352.7	N	227
6-2, 54-56	44.55	5.03 E-6	+ 11.8	337.1	+ 12.4	344.4	N	181
6-2, 79-81	44.80	5.75 E-6	+ 4.5	348.1	- 0.5	346.9	N	92
6-2, 104-106	45.05	5.92 E-6	+ 7.6	340.3	+ 7.4	344.7	N	208
6-2, 129-131	45.30	4.35 E-6	+ 10.0	347.3	+ 11.4	0.7	N	86
6-3, 4-6	45.55	2.47 E-6	- 5.8	349.2	+ 14.2	35.4	N	47
6-3, 29-31	45.80	5.83 E-6	+ 0.6	353.4	+ 2.9	359.5	N	285
6-3, 54-56	46.05	2.54 E-6	- 1.8	345.6	- 4.6	2.3	N	50
6-3, 79-81	46.30	4.48 E-6	+ 3.6	350.5	+ 5.9	356.1	N	158
6-3, 104-106	46.55	5.24 E-6	- 6.4	358.3	- 3.3	4.1	N	139
6-3, 129-131	46.80	4.65 E-6	+ 6.2	0.9	+ 6.0	7.3		138
6-4, 4-6	47.05	4.68 E-6	+ 5.4	359.1	+ 5.3	358.8	N	150
6-4, 29-31	47.30	1.33 E-6	+ 10.8	187.1	+ 3.4	186.1	R	473
6-4, 54-56	47.55	8.94 E-8	- 36.0	174.1	+ 0.8	182.3	R	>300
6-4, 79-81	47.80	4.05 E-8	+ 27.1	348.4	no stable			
6-4, 99-101	48.00	4.08 E-7	+ 17.1	16.6	+ 29.5	15.8	N	387
6-4, 129-131	48.30	1.11 E-8	- 17.7	236.7	no stable			
6-5, 30-32	48.81	1.93 E-7	+ 19.7	132.7	+ 9.6	202.0	R	23
6-5, 70-72	49.21	8.84 E-8	+ 44.7	202.5	no stable			
6-5, 116-118	49.67	1.46 E-7	- 41.4	254.9	no stable			
6-6, 30-32	50.31	1.45 E-7	- 27.8	261.9	no stable			
6-6, 70-72	50.71	1.57 E-7	- 31.0	241.9	no stable			
6-6, 116-118	51.17	2.34 E-7	- 59.2	258.7	no stable			
6-7, 30-32	51.81	1.84 E-7	- 55.8	258.3	no stable			44
7-1, 85-87	52.86	2.60 E-7	+ 0.7	2.0	no stable			
7-2, 56-58	54.07	1.46 E-7	- 5.2	36.5	no stable			
7-2, 65-67	54.16	1.75 E-7	- 52.4	194.7	no stable			
7-2, 130-132	54.81	1.59 E-7	+ 2.0	61.0	no stable			
7-3, 55-57	55.56	1.73 E-7	+ 2.3	38.8	no stable			19
7-4, 15-17	56.66	1.59 E-7	+ 12.9	37.5	no stable			73
7-4, 65-67	57.16	1.38 E-7	- 37.1	174.2	no stable			
7-4, 97-99	57.48	2.68 E-7	+ 14.6	24.1	no stable			18
7-5, 34-36	58.35	1.30 E-7	+ 75.7	57.5	no stable			
7-5, 133-135	59.34	7.38 E-8	+ 1.1	36.2	no stable			
7-6, 13-15	59.64	7.62 E-7	+ 2.1	53.7	no stable			14
8-1, 92-94	61.93	1.59 E-7	+ 15.6	45.9	no stable			
8-2, 69-71	63.20	2.73 E-7	+ 2.0	48.5	no stable			17
8-2, 115-117	63.66	3.05 E-7	+ 3.4	32.9	no stable			126
8-3, 33-35	64.34	2.44 E-7	- 7.8	40.7	no stable			
8-3, 113-115	65.14	1.33 E-7	- 37.1	168.3	no stable			
8-4, 29-31	65.80	4.81 E-7	+ 29.2	202.2	no stable			205
8-4, 130-132	66.81	1.46 E-7	- 7.3	28.2	no stable			
8-5, 117-119	68.18	1.58 E-7	+ 19.6	46.5	no stable			
8-6, 9-11	68.60	1.95 E-7	+ 11.6	34.5	no stable			
8-6, 38-40	68.89	1.08 E-7	- 32.7	172.2	no stable			
8-6, 125-127	69.76	1.65 E-7	+ 12.0	41.0	no stable			
9-1, 65-67	71.16	3.64 E-7	- 0.3	44.8	no stable			
9-2, 5-7	72.06	1.90 E-7	+ 12.8	26.8	no stable			43
9-2, 34-36	72.35	1.40 E-7	- 43.9	72.1	no stable			
9-3, 30-32	73.81	2.58 E-7	+ 14.8	35.8	no stable			38
9-3, 144-146	74.95	2.20 E-7	+ 7.1	32.4	no stable			
9-4, 35-37	75.36	3.65 E-7	+ 0.2	76.6	no stable			85
9-4, 58-60	75.59	1.61 E-7	- 44.5	100.8	no stable			
9-4, 85-87	75.86	5.88 E-6	- 0.3	172.8	- 0.6	173.0	R	288
9-4, 118-120	76.19	1.41 E-6	+ 29.2	152.9	+ 5.6	169.8	R	>1000
9-4, 135-137	76.36	2.55 E-6	+ 18.9	351.6	+ 42.4	169.2	R	69
9-5, 9-11	76.60	1.00 E-6	- 8.8	52.0	- 1.6	172.8	R	361
9-5, 34-36	76.85	3.34 E-6	- 3.5	16.2	- 7.9	3.7	N	52
9-5, 58-60	77.09	4.86 E-6	- 4.4	10.2	- 8.1	3.8	N	69
9-5, 85-87	77.36	5.66 E-6	- 4.1	18.0	- 2.3	9.8	N	97
9-5, 118-120	77.69	2.22 E-6	+ 0.9	31.0	+ 17.0	173.0	R	31
9-6, 9-11	78.10	2.40 E-6	- 12.4	24.0	- 36.3	152.7	R	27

Appendix A. (Continued).

Core-Section (interval in cm)	Sub-bottom depth (m)	J_{NRM} (G)	I_{NRM}	D_{NRM}	I_{stable}	D_{stable}	Polarity	MDF (Oe)
Hole 574 (Cont.)								
9-6, 34-36	78.35	3.91 E-6	-10.0	6.9	-11.9	357.0	N	99
9-6, 58-60	78.59	4.13 E-6	-7.8	9.7	-6.0	1.7	N	97
9-6, 85-87	78.86	6.29 E-6	+4.4	16.7	+9.6	6.8	N	128
9-6, 118-120	79.19	5.09 E-6	+4.5	4.0	+4.8	354.9	N	105
9-7, 9-11	79.60	2.20 E-6	-9.8	33.7	-6.8	19.8	N	46
9-7, 34-36	79.85	3.82 E-6	-3.9	24.2	-0.3	10.1	N	89
10-1, 23-25	80.24	1.81 E-6	+8.1	9.6	+7.7	13.2	N	151
10-1, 50-52	80.51	2.38 E-6	+0.8	10.1	-0.1	10.4	N	204
10-1, 77-79	80.78	2.50 E-6	+2.7	4.6	+0.5	4.8	N	163
10-1, 102-104	81.03	1.01 E-6	-4.1	10.0	-3.6	13.2	N	57
10-1, 125-127	81.26	1.97 E-6	+0.4	2.0	-3.2	2.2	N	150
10-1, 147-149	81.48	1.47 E-6	+5.3	357.2	+5.4	6.0	N	180
10-2, 23-25	81.74	2.01 E-6	-0.1	2.0	+1.2	5.6	N	182
10-2, 50-52	82.01	2.58 E-6	-9.6	0.0	-6.0	0.3	N	245
10-2, 77-79	82.28	3.36 E-6	-2.6	352.1	-1.4	353.9	N	238
10-2, 102-104	82.53	2.51 E-6	-5.7	354.0	-7.1	359.9	N	76
10-2, 125-127	82.76	6.32 E-6	-2.2	346.4	-0.8	351.2	N	93
10-2, 147-149	82.98	6.98 E-6	+0.3	345.9	+4.9	353.2	N	157
10-3, 23-25	83.24	4.90 E-6	+0.8	351.5	+2.6	353.6	N	188
10-3, 50-52	83.51	4.45 E-6	-2.0	344.4	+3.6	349.2	N	122
10-3, 77-79	83.78	4.84 E-6	+1.0	340.2	+7.6	350.7	N	73
10-3, 102-104	84.03	8.96 E-6	+4.0	343.1	+3.5	347.6	N	131
10-3, 125-127	84.26	1.32 E-7	+43.1	308.2	no stable			
10-4, 13-15	84.46	2.91 E-7	+7.8	292.8	no stable			
10-4, 103-105	85.54	6.03 E-7	-7.2	305.0	no stable			
10-5, 115-117	87.16	4.49 E-7	-3.0	285.7	no stable			
10-6, 30-32	87.81	3.45 E-7	+14.2	262.8	no stable			
10-6, 129-131	88.80	4.62 E-7	+2.6	283.5	no stable			
Hole 574A								
2-1, 14-16	6.45	1.53 E-6	+0.7	172.2	-1.7	168.4	R	536
2-1, 40-42	6.71	1.90 E-6	-7.2	166.9	-8.6	163.4	R	478
2-1, 64-66	6.95	1.20 E-6	+6.5	160.8	-0.5	159.6	R	410
2-1, 89-91	7.20	2.02 E-6	+6.2	161.7	+7.5	159.0	R	440
2-1, 114-116	7.45	4.95 E-6	-2.1	152.0	-2.3	151.4	R	361
2-1, 140-142	7.71	1.76 E-6	-17.6	166.5	-9.6	157.7	R	406
2-2, 15-17	7.96	7.68 E-7	-6.8	158.9	-0.6	151.1	R	444
2-2, 41-43	8.22	2.86 E-6	+1.7	173.9	-4.2	170.1	R	380
2-2, 65-67	8.46	1.39 E-6	+2.2	166.7	-0.6	163.4	R	398
2-2, 90-92	8.71	5.20 E-6	+0.7	345.1	+0.1	353.4	N	111
2-2, 115-117	8.96	6.70 E-6	+7.7	347.6	+4.2	351.4	N	191
2-2, 141-143	9.22	4.39 E-6	+13.2	351.6	+13.1	354.8	N	231
2-3, 15-17	9.46	2.05 E-6	-0.4	335.0	-13.8	340.4	N	38
2-3, 41-43	9.72	1.23 E-6	+7.7	197.9	+0.1	175.8	R	426
2-3, 65-67	9.96	1.93 E-6	-7.6	220.7	-8.2	199.4	R	401
2-3, 90-92	10.21	2.59 E-6	-8.3	201.9	-7.9	211.6	R	365
2-3, 115-117	10.46	1.90 E-6	-16.7	213.9	-6.4	228.2	R	370
2-3, 141-143	10.72	2.03 E-6	-24.1	217.7	-15.9	229.4	R	358
2-4, 18-20	10.99	1.33 E-6	-24.7	64.1	-30.9	71.2	N	294
2-4, 85-87	11.66	1.70 E-6	+13.7	44.1	+8.5	45.5	N	224
2-5, 109-111	13.40	1.22 E-6	-25.3	351.3	-27.6	346.7	N	214
2-5, 134-136	13.65	3.61 E-6	-4.1	2.8	-2.6	10.8	N	164
2-6, 14-16	13.95	3.88 E-6	+8.0	14.0	+7.9	14.5	N	202
2-6, 40-42	14.21	5.30 E-6	+0.2	7.2	+4.9	13.0	N	178
2-6, 64-66	14.45	6.05 E-6	+6.9	16.2	+2.5	17.6	N	238
2-6, 89-91	14.70	5.26 E-6	+12.6	13.4	+7.5	12.1	N	225
2-6, 109-111	14.90	4.20 E-6	+2.5	10.5	+4.9	10.2	N	226
2-6, 134-136	15.15	7.31 E-7	+13.7	190.4	+6.8	188.3	R	488
3-1, 24-26	15.75	8.50 E-7	-31.2	223.0	-16.9	225.6	R	430
3-1, 49-51	16.00	3.32 E-7	+38.8	246.0	-2.4	221.0	R	638
3-1, 74-76	16.25	5.26 E-7	+14.3	223.4	-2.9	219.9	R	523
3-1, 100-102	16.51	1.28 E-6	-6.4	227.6	-9.1	220.9	R	388
3-1, 124-126	16.75	1.10 E-6	+17.7	222.8	+6.8	217.1	R	397
3-2, 2-4	17.03	1.41 E-6	-1.6	204.1	-5.8	201.8	R	437
3-2, 24-26	17.25	2.01 E-6	-2.8	211.0	-8.3	207.6	R	373
3-2, 49-51	17.50	2.35 E-6	+0.7	207.4	+0.3	205.1	R	423
3-2, 80-82	17.81	1.88 E-6	-20.0	200.4	-17.3	197.5	R	419
3-2, 104-106	18.05	4.04 E-7	+6.5	225.5	-5.5	186.7	R	496
3-2, 134-136	18.35	2.24 E-6	-0.6	194.4	-3.9	186.0	R	375
3-3, 14-16	18.65	1.53 E-6	+17.4	185.2	+7.1	177.9	R	408
3-3, 40-42	18.91	2.02 E-6	-12.2	182.6	-12.3	175.9	R	395

Appendix A. (Continued).

Core-Section (interval in cm)	Sub-bottom depth (m)	J_{NRM} (G)	I_{NRM}	D_{NRM}	I_{stable}	D_{stable}	Polarity	MDF (Oe)
Hole 574A (Cont.)								
3-3, 64-66	19.15	2.43 E-6	-1.1	177.0	-7.7	169.7	R	403
3-3, 89-91	19.40	2.20 E-6	-0.2	175.6	-3.6	164.0	R	420
3-3, 114-116	19.65	2.22 E-6	+12.8	184.6	-4.4	166.6	R	440
3-3, 139-141	19.90	1.59 E-6	+41.0	151.2	+12.8	160.6	R	476
3-4, 14-16	20.15	1.95 E-6	-11.9	156.3	-8.2	150.4	R	439
3-4, 40-42	20.41	7.77 E-7	+15.0	235.6	-0.9	152.3	R	459
3-4, 64-66	20.65	1.35 E-6	-2.9	141.5	-3.6	145.2	R	441
3-4, 89-91	20.90	1.11 E-6	-14.1	298.6	-8.3	143.2	R	338
3-4, 114-116	21.15	1.18 E-6	+0.0	162.2	-0.8	143.5	R	476
3-4, 140-142	21.41	3.31 E-6	+16.7	334.2	+13.9	336.2	N	82
3-5, 14-16	21.65	4.08 E-6	+14.1	325.3	+12.5	321.0	N	117
3-5, 40-42	21.91	1.57 E-7	+30.7	332.8	+38.0	329.6	N	514
3-5, 108-110	22.59	5.75 E-7	+74.0	84.1	+61.0	81.1	N	377
3-5, 136-138	22.87	6.40 E-7	+38.4	113.0	no stable			311
3-6, 14-16	23.15	5.36 E-7	-53.0	249.7	no stable			
3-6, 80-82	23.81	3.00 E-7	-11.1	226.8	no stable			
4-1, 10-12	24.01	1.74 E-6	-63.2	154.7	no stable			334
4-1, 49-51	24.40	1.14 E-6	-56.8	167.8	-26.5	290.9	N	46
4-1, 80-82	24.71	4.68 E-6	-8.0	359.4	-14.8	4.1	N	144
4-1, 103-105	24.94	8.13 E-7	+46.5	220.9	-1.2	182.1	R	463
4-1, 129-131	25.20	4.33 E-7	+23.1	238.7	-8.7	166.4	R	>500
4-2, 4-6	25.45	7.53 E-7	+41.3	216.6	-6.0	164.3	R	529
4-2, 29-31	25.70	1.39 E-6	+44.9	197.1	+6.6	166.0	R	496
4-2, 54-56	25.95	8.99 E-7	+47.1	335.7	-3.2	172.6	R	451
4-2, 80-82	26.21	4.22 E-7	-11.3	303.8	-14.4	174.0	R	539
4-2, 104-106	26.45	7.76 E-7	-6.4	162.0	-15.2	179.0	R	532
4-2, 129-131	26.70	3.40 E-7	-23.1	236.2	-6.5	173.3	R	584
4-3, 4-6	26.95	4.29 E-6	+10.8	5.5	+1.7	5.8	N	108
4-3, 29-31	27.20	4.63 E-6	+12.1	7.3	+5.0	8.5	N	142
4-3, 54-56	27.45	4.94 E-6	+10.5	8.2	+9.7	6.1	N	211
4-3, 80-82	27.71	6.16 E-6	+15.5	5.0	+14.3	5.6	N	208
4-3, 104-106	27.95	8.60 E-7	-18.2	194.3	-26.3	184.4	R	486
4-3, 129-131	28.20	8.74 E-7	+5.1	187.2	-9.5	182.2	R	439
4-4, 4-6	28.45	9.54 E-7	+10.2	2.2	-17.4	177.6	R	42
4-4, 29-31	28.70	2.85 E-7	+33.7	197.8	-11.3	182.7	R	600
4-4, 54-56	28.95	1.38 E-6	-10.1	3.9	-26.7	190.8	R	30
4-4, 80-82	29.21	5.31 E-6	+10.5	356.1	+3.8	0.9	N	117
4-4, 104-106	29.45	3.13 E-6	+13.3	357.6	+7.2	357.9	N	68
4-4, 129-131	29.70	1.55 E-6	+22.5	350.4	+52.1	175.3	R	48
4-5, 4-6	29.95	5.96 E-7	+26.6	11.1	-13.0	179.9	R	461
4-5, 37-39	30.28	2.90 E-6	+6.4	0.4	-7.7	4.8	N	73
4-5, 68-70	30.59	3.44 E-6	+4.1	356.8	+6.2	355.4	N	120
4-5, 113-115	31.04	3.43 E-6	+12.6	2.4	+9.8	1.8	N	189
4-5, 135-137	31.26	3.07 E-6	+6.6	3.7	+2.7	2.3	N	90
4-6, 5-7	31.46	3.10 E-6	+4.0	4.3	+6.1	6.8	N	139
4-6, 27-29	31.68	7.23 E-7	+17.4	162.6	-4.6	180.9	R	417
4-6, 51-53	31.92	3.25 E-7	+10.6	181.8	-8.2	185.2	R	472
4-6, 75-77	32.16	1.02 E-6	+26.3	128.7	+1.1	184.9	R	312
4-6, 104-106	32.45	2.67 E-6	+48.4	111.9	no stable			266
5-1, 115-117	34.26	3.34 E-7	+42.4	290.6	-9.5	188.3	R	>600
5-1, 142-144	34.53	1.20 E-6	-32.7	176.3	-15.3	183.9	R	513
5-2, 14-16	34.75	5.04 E-7	+55.2	356.0	-10.4	176.5	R	550
5-2, 40-42	35.01	1.14 E-6	+33.4	172.2	-1.5	187.7	R	480
5-2, 64-66	35.25	9.91 E-7	+19.4	281.4	-0.6	178.0	R	522
5-2, 89-91	35.50	7.74 E-7	-9.0	127.9	-15.5	180.7	R	553
5-2, 114-116	35.75	1.96 E-6	+14.5	197.2	-5.6	185.7	R	488
5-2, 140-142	36.01	5.97 E-7	+20.2	194.3	-11.7	176.7	R	496
5-3, 14-16	36.25	1.03 E-6	+21.4	143.6	-0.6	181.6	R	577
5-3, 40-42	36.51	9.56 E-7	-4.6	178.2	-1.6	178.8	R	625
5-3, 64-66	36.75	2.50 E-6	-10.2	176.4	-7.8	180.8	R	517
5-3, 89-91	37.00	2.20 E-6	+4.6	173.6	-1.3	183.4	R	488
5-3, 114-116	37.25	1.40 E-6	-15.7	179.1	-1.8	174.2	R	497
5-3, 140-142	37.51	1.33 E-6	-3.9	170.0	-2.4	178.1	R	571
5-4, 14-16	37.75	1.06 E-6	+21.3	177.7	+3.5	181.4	R	615
5-4, 40-42	38.01	6.63 E-7	+41.6	217.7	-7.5	188.5	R	630
5-4, 64-66	38.25	1.21 E-6	+70.5	49.6	+7.1	186.9	R	471
5-4, 89-91	38.50	1.40 E-6	-28.0	174.3	-10.6	191.5	R	522
5-4, 114-116	38.75	3.84 E-7	+29.6	297.8	+3.9	210.1	R	>800
5-4, 140-142	39.01	4.96 E-7	+6.8	189.0	-6.7	185.7	R	>800
5-5, 14-16	39.25	1.68 E-6	+31.1	345.1	+19.7	199.0	R	33
5-5, 40-42	39.51	2.31 E-6	+2.5	347.8	+6.0	345.7	N	85
5-5, 64-66	39.75	5.20 E-6	+10.3	1.0	+15.6	353.7	N	180

Appendix A. (Continued).

Core-Section (interval in cm)	Sub-bottom depth (m)	J_{NRM} (G)	I_{NRM}	D_{NRM}	I_{stable}	D_{stable}	Polarity	MDF (Oe)
Hole 574A (Cont.)								
5-5, 89-91	40.00	3.65 E-6	+ 24.0	357.9	+ 22.8	342.6	N	73
5-5, 114-116	40.25	4.69 E-6	+ 15.4	347.3	+ 9.7	349.8	N	165
5-5, 140-142	40.51	2.54 E-6	+ 3.0	354.8	+ 7.1	346.1	N	82
5-6, 14-16	40.75	2.87 E-6	+ 1.3	5.5	- 0.8	350.6	N	89
5-6, 40-42	41.01	3.07 E-6	+ 13.0	3.1	+ 14.8	355.6	N	97
5-6, 64-66	41.25	3.95 E-6	+ 9.9	349.4	+ 2.5	352.2	N	181
5-6, 89-91	41.50	1.88 E-6	+ 8.7	6.1	- 4.6	346.5	N	70
5-6, 122-124	41.83	8.82 E-7	+ 33.5	32.6	+ 1.9	185.9	R	42
5-6, 144-146	42.05	9.30 E-7	+ 16.6	148.2	- 9.0	184.0	R	635
5-7, 9-11	42.20	1.29 E-6	- 63.3	333.0	- 11.5	86.2	R	328
6-1, 13-15	42.54	3.94 E-6	- 0.4	358.2	- 5.3	358.5	N	133
6-1, 41-43	42.82	3.75 E-6	- 0.3	354.0	- 14.2	353.9	N	129
6-1, 65-67	43.06	2.84 E-6	+ 3.3	319.8	+ 1.9	4.3	N	85
6-1, 90-92	43.31	3.25 E-6	+ 6.9	1.3	+ 6.7	1.4	N	197
6-1, 115-117	43.56	3.74 E-6	+ 16.1	355.7	+ 15.1	356.3	N	150
6-1, 141-143	43.82	1.48 E-7	- 17.1	181.9	- 20.5	185.8	R	362
6-2, 11-13	44.02	1.14 E-7	- 27.7	189.2	- 28.0	190.6	R	>400
6-2, 41-43	44.32	2.07 E-7	- 38.9	181.8	- 1.9	180.9	R	353
6-2, 65-67	44.56	1.11 E-7	- 11.0	177.4	- 35.4	180.7	R	463
6-2, 90-92	44.81	2.41 E-7	+ 6.6	334.8	- 1.8	329.0	N	381
6-2, 115-117	45.06	6.41 E-8	- 24.7	195.9	- 11.3	196.7	R	87
6-2, 140-142	45.31	4.40 E-8	- 52.8	138.5	- 4.2	170.0	R	20
6-3, 13-15	45.54	1.20 E-7	+ 51.0	248.4	no stable			68
6-3, 41-43	45.82	6.06 E-8	- 4.1	165.2	no stable			
6-3, 68-70	46.09	3.54 E-8	- 66.5	8.0	no stable			
6-3, 85-87	46.26	6.98 E-8	+ 80.6	194.9	no stable			39
6-3, 130-132	46.71	4.46 E-8	- 65.6	39.9	no stable			
6-4, 13-15	47.04	5.50 E-7	+ 13.4	80.3	no stable			
6-4, 55-57	47.46	2.20 E-7	+ 13.1	95.6	no stable			
6-4, 95-97	47.86	4.63 E-8	+ 36.2	216.3	no stable			
6-4, 137-139	48.28	2.07 E-7	+ 31.6	106.3	no stable			
6-5, 13-15	48.54	5.70 E-8	+ 18.6	88.9	no stable			
6-5, 57-59	48.98	1.49 E-7	- 68.7	56.4	no stable			
6-5, 105-107	49.46	1.06 E-7	- 53.2	121.7	no stable			
6-5, 137-139	49.78	1.63 E-7	- 80.5	143.3	no stable			
6-6, 13-15	50.04	8.01 E-8	- 10.0	156.7	no stable			
6-6, 84-86	50.75	6.56 E-8	+ 35.1	88.8	no stable			
6-6, 118-120	51.09	1.28 E-7	- 62.0	125.2	no stable			
7-1, 85-87	52.76	1.44 E-7	- 48.3	149.9	no stable			
7-1, 126-128	53.17	2.06 E-7	+ 51.1	187.4	no stable			
7-2, 8-10	53.49	9.96 E-8	- 46.1	23.6	no stable			
7-2, 45-47	53.86	3.14 E-7	- 63.0	45.6	no stable			
7-2, 85-87	54.26	2.95 E-7	- 83.4	354.9	no stable			
7-2, 125-127	54.66	3.64 E-7	- 52.9	42.4	no stable			
7-3, 8-10	54.99	1.61 E-7	- 59.9	302.7	no stable			
7-3, 35-37	55.26	1.03 E-7	+ 63.4	259.8	no stable			
7-3, 69-71	55.60	6.60 E-8	+ 39.5	348.7	no stable			
7-3, 108-110	55.99	5.80 E-8	- 31.0	111.3	no stable			
7-4, 15-17	56.56	1.87 E-7	- 35.9	253.0	no stable			
7-4, 51-53	56.92	5.78 E-8	- 46.4	38.4	no stable			
7-4, 86-88	57.27	6.61 E-8	+ 41.0	83.5	no stable			
7-4, 121-123	57.62	4.95 E-8	- 63.7	142.7	no stable			
7-5, 15-17	58.06	6.47 E-8	+ 26.5	173.4	no stable			
7-5, 51-53	58.42	1.19 E-7	+ 51.7	153.3	no stable			
7-5, 96-98	58.87	1.50 E-7	- 55.9	180.1	no stable			
7-5, 134-136	59.25	2.05 E-8	+ 31.3	234.5	no stable			
7-6, 17-19	59.58	5.44 E-8	+ 46.7	185.5	no stable			
7-6, 53-55	59.94	1.45 E-7	+ 80.6	234.9	no stable			
7-6, 65-67	60.06	4.36 E-8	- 19.5	99.6	no stable			
7-6, 97-99	60.38	7.05 E-8	- 78.1	105.5	no stable			
7-6, 134-136	60.75	5.98 E-8	- 69.9	15.0	no stable			
8-1, 95-97	62.36	1.50 E-7	- 80.6	263.0	no stable			
8-1, 134-136	62.75	5.86 E-8	+ 27.5	90.4	no stable			
8-2, 32-34	63.23	4.74 E-8	- 20.2	324.9	no stable			
8-2, 108-110	63.99	1.96 E-8	- 15.5	22.7	no stable			
8-3, 64-66	65.05	1.10 E-7	- 16.2	264.6	no stable			
8-3, 103-105	65.44	4.54 E-8	- 30.7	55.0	no stable			
8-3, 144-146	65.85	1.40 E-7	+ 52.7	81.3	no stable			
8-4, 44-46	66.35	1.29 E-7	- 51.2	239.5	no stable			
8-4, 68-70	66.59	2.99 E-8	- 1.0	43.9	no stable			
8-4, 103-105	66.94	1.21 E-7	- 38.3	165.7	no stable			

Appendix A. (Continued).

Core-Section (interval in cm)	Sub-bottom depth (m)	J_{NRM} (G)	I_{NRM}	D_{NRM}	I_{stable}	D_{stable}	Polarity	MDF (Oe)
Hole 574A (Cont.)								
8-4, 145-147	67.36	3.71 E-8	+ 54.5	356.3			no stable	
8-5, 23-25	67.64	6.01 E-8	- 24.1	336.6			no stable	
8-5, 52-54	67.93	1.35 E-7	- 70.1	94.3			no stable	
8-5, 91-93	68.32	1.77 E-8	- 53.5	28.3			no stable	
8-5, 123-125	68.64	1.12 E-7	- 75.9	98.0			no stable	
8-6, 15-17	69.06	9.21 E-8	- 35.5	260.9			no stable	
8-6, 46-48	69.37	2.18 E-7	+ 23.0	180.1			no stable	
8-6, 78-80	69.69	1.46 E-7	+ 77.8	174.5			no stable	
8-6, 112-114	70.03	1.04 E-7	+ 37.3	356.4			no stable	
9-1, 25-27	70.66	2.27 E-7	+ 19.6	204.9			no stable	
9-1, 128-130	71.69	1.21 E-7	- 50.6	174.7			no stable	
9-2, 105-107	72.96	1.93 E-7	+ 14.4	227.0			no stable	
9-3, 67-69	74.08	1.87 E-7	+ 3.4	222.9			no stable	
9-3, 135-137	74.76	9.09 E-8	+ 32.1	266.1			no stable	
9-3, 143-145	74.84	2.43 E-7	- 9.4	211.0			no stable	
9-4, 26-28	75.17	6.87 E-8	- 16.2	72.8			no stable	
9-4, 70-72	75.61	2.38 E-8	- 56.3	38.8			no stable	
9-4, 115-117	76.06	6.65 E-6	- 21.6	168.0	- 21.0	169.0	R	287
9-4, 144-146	76.35	6.34 E-7	+ 48.0	355.3	- 15.1	173.7	R	>600
9-5, 15-17	76.56	9.82 E-7	+ 23.4	316.7	+ 3.5	166.5	R	366
9-5, 41-43	76.82	1.13 E-6	+ 4.4	334.1	- 14.2	158.7	R	28
9-5, 66-68	77.07	5.66 E-6	+ 15.7	345.8	+ 19.5	352.1	N	127
9-5, 90-92	77.31	5.56 E-6	- 1.0	350.1	- 1.0	358.3	N	124
9-5, 114-116	77.55	5.05 E-6	+ 4.6	356.2	+ 11.1	358.1	N	89
9-5, 135-137	77.76	5.85 E-7	- 3.2	211.6	- 0.8	174.0	R	462
9-6, 15-17	78.06	3.74 E-6	- 3.9	351.4	- 10.7	355.8	N	84
9-6, 41-43	78.32	3.67 E-6	+ 7.4	357.6	+ 9.9	3.3	N	184
9-6, 66-68	78.57	3.94 E-6	+ 1.6	1.7	+ 5.1	7.2	N	153
9-6, 90-92	78.81	3.56 E-6	- 0.7	6.9	+ 4.7	13.9	N	90
9-6, 114-116	79.05	5.43 E-6	- 2.8	16.4	- 3.8	19.6	N	177
9-6, 135-137	79.26	5.06 E-6	+ 0.6	15.5	+ 3.7	17.1	N	203
9-7, 8-10	79.49	6.69 E-7	+ 4.2	351.7	- 13.8	220.9	R	35
9-7, 32-34	79.73	3.07 E-6	- 4.4	23.0	+ 1.5	24.8	N	219
10-1, 15-17	80.06	2.61 E-6	- 2.3	352.1	- 9.9	351.7	N	177
10-1, 41-43	80.32	1.44 E-6	+ 0.9	8.7	- 1.7	8.3	N	198
10-1, 65-67	80.56	1.03 E-6	- 27.6	355.5	- 30.9	0.6	N	228
10-1, 90-92	80.81	1.17 E-6	- 29.3	353.2	- 31.0	0.5	N	214
10-1, 115-117	81.06	1.07 E-6	- 6.2	2.3	- 10.1	13.4	N	250
10-1, 141-143	81.32	6.12 E-7	- 1.4	352.6	- 20.2	10.5	N	198
10-2, 15-17	81.56	1.13 E-6	+ 8.9	357.8	+ 4.1	1.2	N	224
10-2, 41-43	81.82	1.66 E-6	+ 17.6	60.9	+ 28.5	24.2	N	115
10-2, 65-67	82.06	6.62 E-7	- 21.7	354.5	- 12.8	360.0	N	281
10-2, 90-92	82.31	8.09 E-7	- 20.0	348.8	- 17.9	355.3	N	282
10-3, 15-17	83.06	5.81 E-7	- 49.6	82.5	- 41.4	25.1	N	195
10-3, 41-43	83.32	7.34 E-7	- 0.2	343.3	- 3.5	350.5	N	230
10-3, 65-67	83.56	1.94 E-6	+ 1.2	329.0	+ 3.5	331.3	N	255
10-3, 90-92	83.81	4.95 E-6	+ 31.4	339.0	+ 28.9	343.3	N	203
10-3, 119-121	84.10	4.59 E-6	- 11.8	349.9	- 7.7	356.0	N	199
10-3, 143-145	84.34	5.24 E-6	+ 15.1	342.7	+ 15.3	345.3	N	96
10-4, 15-17	84.56	9.25 E-8	+ 14.1	336.4			no stable	
10-4, 45-47	84.86	1.34 E-7	+ 8.7	352.9			no stable	
10-4, 87-89	85.28	5.72 E-8	+ 52.5	4.4			no stable	
10-4, 117-119	85.58	2.18 E-7	+ 33.5	354.3			no stable	
10-5, 50-52	86.41	1.26 E-7	+ 81.9	321.3			no stable	
10-5, 107-109	86.98	1.52 E-7	+ 51.6	343.0			no stable	
10-6, 18-20	87.59	7.61 E-8	- 85.1	337.4			no stable	
10-6, 51-53	87.92	5.89 E-8	- 52.3	311.7			no stable	
10-6, 83-85	88.24	1.85 E-7	+ 70.5	2.3			no stable	
10-6, 118-120	88.59	6.76 E-8	+ 53.2	339.6			no stable	
11-1, 45-47	89.66	1.80 E-7	+ 25.9	14.5			no stable	
11-1, 95-97	90.16	1.38 E-7	+ 84.4	319.9			no stable	
11-1, 115-117	90.36	2.83 E-7	- 5.6	42.0			no stable	
11-2, 64-66	91.35	1.76 E-7	- 15.0	64.9			no stable	
11-2, 95-97	91.66	1.05 E-7	+ 62.4	5.9			no stable	
11-3, 95-97	93.16	3.46 E-7	+ 51.7	5.8			no stable	
11-3, 144-146	93.65	1.74 E-7	- 1.4	42.8			no stable	
11-4, 10-12	93.81	1.95 E-7	+ 13.1	10.8			no stable	
11-4, 95-97	94.66	1.35 E-7	+ 77.5	349.5			no stable	
11-5, 30-32	95.51	1.64 E-7	- 14.3	42.1			no stable	
11-5, 95-97	96.16	1.66 E-7	+ 68.1	20.4			no stable	
11-6, 95-97	97.66	6.17 E-8	- 29.5	196.9			no stable	
11-6, 131-133	98.02	9.20 E-8	+ 64.1	80.5			no stable	

Appendix A. (Continued).

Core-Section (interval in cm)	Sub-bottom depth (m)	J_{NRM} (G)	I_{NRM}	D_{NRM}	I_{stable}	D_{stable}	Polarity	MDF (Oe)
Hole 575								
1-1, 24-26	0.25	1.94 E-6	- 25.5	48.0	- 9.4	17.3	N	187
1-1, 34-36	0.35	4.17 E-6	+ 26.1	21.0	+ 14.4	28.1	N	287
1-1, 44-46	0.45	4.76 E-6	- 5.3	15.3	+ 7.0	27.1	N	276
1-1, 54-56	0.55	7.30 E-6	- 5.3	39.0	+ 4.4	35.4	N	259
1-1, 64-66	0.65	4.80 E-6	+ 22.4	21.0	+ 14.3	28.7	N	289
1-1, 84-86	0.85	4.81 E-6	+ 29.1	29.3	+ 17.5	27.1	N	225
1-1, 94-96	0.95	7.04 E-6	+ 29.0	22.6	+ 13.5	26.3	N	238
1-1, 104-106	1.05	9.05 E-6	+ 24.9	36.0	+ 15.2	33.0	N	231
1-1, 114-116	1.15	5.35 E-6	+ 14.7	26.4	+ 11.6	30.4	N	254
1-1, 124-126	1.25	8.26 E-6	+ 0.9	37.0	+ 7.2	25.1	N	156
1-1, 134-136	1.35	7.67 E-6	+ 8.7	42.4	+ 13.0	30.2	N	185
1-2, 4-6	1.55	4.50 E-6	+ 4.5	28.6	+ 8.9	34.6	N	254
1-2, 14-16	1.65	2.39 E-6	- 0.4	23.6	+ 3.4	29.4	N	260
1-2, 24-26	1.75	3.90 E-6	- 2.8	31.9	+ 7.1	26.0	N	227
1-2, 34-36	1.85	5.91 E-6	+ 17.7	13.1	+ 13.4	22.1	N	254
1-2, 44-46	1.95	9.89 E-6	+ 20.0	20.5	+ 8.4	24.0	N	225
1-2, 54-56	2.05	7.15 E-6	+ 3.1	13.9	+ 12.5	20.7	N	238
1-2, 64-66	2.15	4.36 E-6	- 1.8	30.8	+ 6.9	24.9	N	194
1-2, 84-86	2.35	9.35 E-6	+ 14.9	11.4	+ 16.0	20.8	N	253
1-2, 94-96	2.45	8.20 E-6	- 6.1	20.8	+ 7.4	20.9	N	174
1-2, 114-116	2.65	4.08 E-6	+ 21.2	23.7	+ 51.4	10.7	N	45
1-2, 124-126	2.75	4.06 E-6	+ 13.6	150.6	- 7.9	173.5	R	353
1-2, 134-136	2.85	2.61 E-6	- 43.5	140.8	- 21.8	177.1	R	322
1-2, 144-146	2.95	2.49 E-6	- 32.2	243.4	- 16.6	182.1	R	315
1-3, 4-6	3.05	2.95 E-6	+ 43.5	299.1	+ 4.0	215.8	R	33
1-3, 14-16	3.15	2.74 E-6	- 13.7	3.1	+ 35.4	357.8	N	57
1-3, 24-26	3.25	2.26 E-6	+ 34.2	228.7	- 4.6	188.8	R	323
1-3, 34-36	3.35	1.85 E-6	+ 26.6	263.4	- 0.4	192.5	R	256
1-3, 44-46	3.45	2.46 E-6	+ 40.3	267.8	+ 0.1	188.4	R	267
1-3, 54-56	3.55	3.16 E-6	- 41.0	137.5	- 12.2	177.2	R	305
1-3, 64-66	3.65	2.34 E-6	- 11.0	218.6	- 12.3	180.4	R	373
1-3, 84-86	3.85	2.18 E-6	- 8.8	201.2	- 7.0	178.9	R	407
1-3, 94-96	3.95	1.93 E-6	- 20.4	209.7	- 15.9	176.1	R	380
1-3, 104-106	4.05	1.93 E-6	- 23.1	140.1	- 8.9	167.0	R	350
1-3, 114-116	4.15	4.75 E-6	+ 15.9	312.5	+ 35.1	331.8	N	43
1-3, 124-126	4.25	3.01 E-6	+ 33.9	33.9	- 65.0	10.2	N	36
1-3, 134-136	4.35	1.52 E-6	- 59.8	220.0	- 6.4	168.2	R	435
1-3, 144-146	4.45	2.01 E-6	- 48.5	250.9	- 14.7	184.0	R	301
1-4, 4-6	4.55	1.98 E-6	- 30.1	173.5	- 9.1	169.4	R	345
1-4, 14-16	4.65	5.91 E-7	+ 19.7	181.2	+ 5.8	165.5	R	401
1-4, 24-26	4.75	9.48 E-7	- 51.5	235.4	- 12.0	171.4	R	371
1-4, 34-36	4.85	2.16 E-6	+ 8.8	191.9	- 0.3	167.6	R	405
1-4, 44-46	4.95	1.52 E-6	+ 32.0	249.5	+ 5.8	169.3	R	360
1-4, 55-57	5.06	1.95 E-6	- 1.6	198.3	- 14.6	159.7	R	406
1-4, 64-66	5.15	2.54 E-6	- 29.7	148.3	- 11.4	156.9	R	344
1-4, 84-86	5.35	5.58 E-7	+ 18.5	207.5	- 4.9	171.4	R	357
1-4, 94-96	5.45	9.33 E-7	+ 4.5	4.2	+ 17.5	339.1	N	142
1-4, 104-106	5.55	2.39 E-6	- 7.3	344.6	+ 3.9	340.8	N	161
1-4, 114-116	5.65	1.51 E-6	- 11.2	351.1	+ 7.4	340.0	N	155
1-4, 124-126	5.75	1.69 E-6	- 9.8	328.2	+ 0.4	335.2	N	87
1-4, 134-136	5.85	6.39 E-6	+ 14.4	320.5	+ 5.8	330.1	N	93
1-4, 144-146	5.95	7.86 E-6	- 5.7	315.7	- 1.1	327.1	N	76
1-5, 4-6	6.05	6.62 E-6	- 6.8	352.2	+ 4.5	343.9	N	197
1-5, 14-16	6.15	9.01 E-6	+ 28.0	319.9	+ 18.6	336.1	N	79
1-5, 24-26	6.25	8.78 E-6	+ 26.5	329.9	+ 14.2	338.0	N	125
1-5, 34-36	6.35	8.26 E-6	- 3.9	327.3	+ 4.5	336.3	N	164
1-5, 44-46	6.45	9.10 E-6	+ 17.2	319.8	+ 11.6	328.4	N	130
1-5, 54-56	6.55	4.68 E-6	- 18.3	336.3	+ 5.1	329.6	N	86
1-5, 64-66	6.65	3.14 E-6	+ 29.0	304.1	+ 10.3	203.3	R	30
1-5, 84-86	6.85	8.66 E-7	+ 46.4	284.7	- 1.6	158.9	R	33
1-5, 94-96	6.95	3.75 E-6	- 12.8	343.0	+ 4.9	333.9	N	155
1-5, 104-106	7.05	5.17 E-6	- 11.4	340.2	- 1.9	336.3	N	153
1-5, 114-116	7.15	3.23 E-6	- 2.4	328.2	+ 6.4	328.5	N	137
1-5, 122-124	7.23	4.32 E-6	+ 15.0	220.0	+ 7.7	206.3	R	107
1-5, 127-129	7.28	2.35 E-6	- 4.9	209.0	- 7.4	211.4	R	46
2-1, 3-5	7.34	3.25 E-6	- 84.3	39.1	- 77.3	12.4	N	267
2-1, 19-21	7.50	3.25 E-6	- 44.8	282.4	- 68.9	296.8	N	44
2-1, 29-31	7.60	1.85 E-6	- 37.4	54.8	- 45.5	350.9	N	37
2-1, 39-41	7.70	2.67 E-6	+ 51.4	21.3	- 63.8	152.5	R	30
2-1, 49-51	7.80	6.81 E-6	- 21.6	276.3	- 13.2	190.4	R	39
2-1, 59-61	7.90	3.56 E-6	+ 20.7	288.8	- 10.3	209.7	R	24
2-1, 69-71	8.00	2.95 E-6	+ 40.5	73.4	- 11.8	158.9	R	45
2-1, 79-81	8.10	3.11 E-6	- 5.3	64.7	- 22.4	153.2	R	39

Appendix A. (Continued).

Core-Section (interval in cm)	Sub-bottom depth (m)	J_{NRM} (G)	I_{NRM}	D_{NRM}	I_{stable}	D_{stable}	Polarity	MDF (Oe)
Hole 575 (Cont.)								
2-1, 89-91	8.20	3.45 E-6	-66.6	1.4	-45.3	166.2	R	23
2-1, 99-101	8.30	3.65 E-6	+33.8	286.3	-3.0	187.7	R	45
2-1, 109-111	8.40	3.65 E-6	+66.6	307.5	-0.8	176.4	R	39
2-1, 119-121	8.50	3.47 E-6	+6.3	95.3	-7.2	168.1	R	250
2-1, 129-131	8.60	3.41 E-6	-56.7	291.7	-31.9	192.0	R	44
2-1, 140-142	8.71	2.34 E-6	+29.4	62.7	-23.2	168.1	R	41
2-2, 19-21	9.00	3.33 E-6	-21.3	260.8	-4.4	186.8	R	246
2-2, 29-31	9.10	3.23 E-6	-13.0	69.1	-16.3	162.3	R	274
2-2, 39-41	9.20	3.20 E-6	-18.2	66.4	-18.6	162.3	R	43
2-2, 49-51	9.30	4.38 E-6	-75.4	0.9	-31.5	167.7	R	45
2-2, 59-61	9.40	4.03 E-6	-58.3	80.1	-22.7	169.6	R	228
2-2, 69-71	9.50	2.07 E-6	-48.3	334.6	-17.4	185.5	R	286
2-2, 79-81	9.60	3.39 E-6	+36.8	291.2	-4.9	190.6	R	243
2-2, 89-91	9.70	4.54 E-6	+24.0	297.2	-7.5	199.8	R	35
2-2, 99-101	9.80	3.86 E-6	-53.8	41.5	-33.5	180.2	R	33
2-2, 109-111	9.90	3.78 E-6	-63.9	43.6	-28.9	178.5	R	39
2-2, 119-121	10.00	4.97 E-6	+56.3	315.5	-8.3	195.8	R	29
2-2, 129-131	10.10	4.68 E-6	+37.3	304.0	-10.9	223.6	R	30
2-2, 139-141	10.20	5.85 E-6	+11.9	81.0	-26.2	156.8	R	32
2-3, 3-5	10.34	4.44 E-6	+29.6	11.9	+28.4	10.7	N	38
2-3, 20-22	10.51	3.25 E-6	+0.7	2.2	+4.4	6.3	N	83
2-3, 29-31	10.60	5.20 E-6	+52.6	315.1	+29.8	344.6	N	44
2-3, 41-43	10.72	3.53 E-6	+60.3	3.5	+14.4	349.3	N	38
2-3, 59-61	10.90	4.00 E-6	+38.2	31.8	+21.7	8.6	N	50
2-3, 69-71	11.00	2.96 E-6	+11.1	305.8	-26.2	328.3	N	36
2-3, 82-84	11.13	3.79 E-6	+16.5	304.5	-4.5	333.3	N	36
2-3, 89-91	11.20	3.84 E-6	-2.7	60.6	+2.0	11.4	N	42
2-3, 99-101	11.30	4.72 E-6	+42.2	317.4	+30.5	347.1	N	46
2-3, 109-111	11.40	5.21 E-6	+66.6	10.2	+29.0	353.0	N	38
2-3, 119-121	11.50	3.87 E-6	+21.9	315.1	+11.3	347.2	N	42
2-3, 129-131	11.60	5.15 E-6	+51.8	319.4	+23.1	350.3	N	37
2-3, 146-148	11.77	4.12 E-6	+14.4	350.2	+20.3	5.0	N	69
2-4, 25-27	12.06	4.95 E-6	+18.8	329.9	+6.1	350.9	N	52
2-4, 87-89	12.68	3.17 E-6	+13.4	0.4	-20.1	4.7	N	73
2-4, 127-129	13.08	6.37 E-6	-62.1	305.4	-49.7	308.5	N	402
2-4, 144-146	13.25	2.34 E-6	+22.7	321.2	+2.7	245.2	R	32
2-5, 9-11	13.40	1.26 E-6	+7.4	325.4	-23.3	235.0	R	45
2-5, 19-21	13.50	1.28 E-6	-13.3	310.8	-16.7	227.6	R	47
2-5, 29-31	13.60	1.19 E-6	-1.9	316.0	-5.4	230.4	R	322
2-5, 39-41	13.70	2.38 E-6	-58.7	77.5	-20.7	207.8	R	252
2-5, 49-51	13.80	2.00 E-6	+52.8	353.3	+3.7	252.0	R	29
2-5, 59-61	13.90	1.28 E-6	+8.1	335.8	-12.2	242.8	R	36
2-5, 69-71	14.00	2.01 E-6	+12.8	276.8	-8.3	221.8	R	303
2-5, 79-81	14.10	1.48 E-6	-38.7	307.9	-25.2	221.7	R	331
2-5, 89-91	14.20	2.09 E-6	+55.8	344.2	+17.1	218.2	R	31
2-5, 99-101	14.30	1.94 E-6	+61.6	284.3	+4.3	215.6	R	46
2-5, 109-111	14.40	1.79 E-6	-23.6	330.9	-8.8	235.4	R	29
2-5, 119-121	14.50	3.01 E-6	+53.2	302.3	+7.0	224.3	R	34
2-5, 129-131	14.60	1.70 E-6	+63.1	11.8	-1.8	208.5	R	42
2-5, 139-141	14.70	1.19 E-6	-40.7	97.7	-13.7	187.1	R	343
2-6, 9-11	14.90	1.39 E-6	+9.4	264.5	-14.3	204.1	R	49
2-6, 19-21	15.00	1.74 E-6	-38.9	257.3	-24.0	203.9	R	282
2-6, 29-31	15.10	7.88 E-7	+25.2	318.8	-29.7	262.1	R	38
2-6, 39-41	15.20	8.46 E-7	-32.8	99.0	-30.6	183.5	R	269
2-6, 49-51	15.30	9.38 E-7	-19.5	318.5	-38.0	224.8	N	49
2-6, 59-61	15.40	4.57 E-7	-40.4	51.2	-55.6	210.3	N	39
2-6, 69-71	15.50	5.63 E-7	-73.5	30.7	-50.5	209.5	N	40
2-6, 79-81	15.60	3.73 E-7	+33.1	279.9	+1.7	207.4	R	306
2-6, 89-91	15.70	6.53 E-7	+66.7	265.8	+6.8	198.3	R	258
2-6, 99-101	15.80	8.37 E-7	+88.5	58.1	+5.4	202.8	R	317
2-6, 109-111	15.90	1.00 E-6	-69.2	338.8	-36.7	194.2	R	35
2-6, 119-121	16.00	8.54 E-7	+0.4	292.0	-27.0	215.3	R	38
2-6, 129-131	16.10	4.44 E-7	-19.3	12.6	-37.9	208.8	R	42
2-6, 139-141	16.20	8.01 E-7	-42.8	41.9	-62.3	359.6	N	40
2-7, 5-7	16.36	1.04 E-6	+23.8	347.0	-12.7	339.7	N	50
2-7, 16-18	16.47	1.39 E-6	-41.9	336.9	-30.2	342.0	N	50
2-7, 25-27	16.56	1.95 E-6	-42.5	353.4	-33.7	351.7	N	66
2-7, 36-38	16.67	8.27 E-7	-33.7	349.2	-20.0	329.7	N	43
2-7, 45-47	16.76	1.24 E-6	-12.3	322.7	-28.2	332.0	N	41
2-7, 49-51	16.80	1.27 E-6	+57.9	0.7	+27.7	291.5	N	142
3-1, 9-11	16.90	1.35 E-6	-78.6	82.8	-80.8	31.2	N	49
3-1, 19-21	17.00	1.76 E-6	-58.0	55.2	-59.9	57.4	N	62
3-1, 29-31	17.10	9.40 E-7	-70.3	36.1	-69.0	35.9	N	74

Appendix A. (Continued).

Core-Section (interval in cm)	Sub-bottom depth (m)	J_{NRM} (G)	I_{NRM}	D_{NRM}	I_{stable}	D_{stable}	Polarity	MDF (Oe)
Hole 575 (Cont.)								
3-1, 79-81	17.60	5.24 E-7	-11.4	54.3	-63.6	117.9	N	203
3-1, 89-91	17.70	1.30 E-6	-30.3	61.3	-42.1	64.1	N	146
3-1, 99-101	17.80	1.66 E-6	-23.5	279.7	-59.1	172.2	N	208
3-1, 109-111	17.90	3.39 E-6	-54.2	350.6	-56.7	50.6	N	46
3-1, 119-121	18.00	2.43 E-6	-70.5	47.1	-71.3	93.1	N	117
3-2, 19-21	18.50	2.63 E-6	-50.4	25.0	-59.1	24.7	N	45
3-2, 29-31	18.60	2.57 E-6	-19.0	43.8	-71.5	87.0	N	44
3-2, 79-81	19.10	3.12 E-6	-42.0	41.0	-27.9	41.4	N	45
3-2, 99-101	19.30	2.71 E-6	-31.4	46.0	-40.4	29.4	N	73
3-2, 129-131	19.60	1.21 E-6	+32.0	344.2	-41.5	38.3	N	299
3-2, 139-141	19.70	2.03 E-6	+52.2	336.3	-35.7	24.3	N	42
3-3, 29-31	20.10	3.03 E-6	-26.1	21.8	-54.1	0.9	N	83
3-3, 39-41	20.20	9.58 E-7	-19.3	20.2	-50.3	61.9	N	292
3-3, 59-61	20.40	2.25 E-6	-31.0	298.9	-73.5	10.6	N	94
3-3, 69-71	20.50	1.48 E-6	-3.4	289.0	-45.0	360.0	N	190
3-3, 79-81	20.60	2.12 E-6	+34.3	8.6	+8.5	49.4	N	41
3-3, 89-91	20.70	2.27 E-6	+47.5	41.6	+10.9	38.8	N	45
3-3, 99-101	20.80	1.48 E-6	-50.6	319.1	-52.4	13.9	N	61
3-3, 109-111	20.90	1.19 E-6	-42.5	54.4	-45.3	34.4	N	85
3-3, 119-121	21.00	1.52 E-6	-45.3	43.4	-51.9	59.5	N	72
3-3, 129-131	21.10	5.68 E-7	+24.7	26.8	-61.1	44.1	N	268
3-3, 139-141	21.20	1.79 E-6	-59.5	37.2	-38.6	49.7	N	50
3-4, 29-31	21.60	2.00 E-6	-69.4	39.1	-40.8	34.7	N	95
3-4, 49-51	21.80	3.01 E-7	-11.4	99.1	-56.2	63.3	N	546
3-4, 59-61	21.90	1.93 E-6	-46.9	42.8	-64.2	52.2	N	90
3-4, 69-71	22.00	7.68 E-7	-71.8	211.9	-50.4	80.5	N	286
3-4, 79-81	22.10	2.01 E-7	-75.5	87.4	-31.8	63.4	N	549
3-4, 99-101	22.30	1.95 E-6	-26.7	86.8	-26.8	98.8	N	58
3-4, 109-111	22.40	2.04 E-6	-50.9	59.1	-44.2	59.2	N	48
3-4, 138-140	22.69	7.13 E-7	+45.3	70.2	+72.5	22.7	N	187
3-5, 4-6	22.85	1.84 E-6	+47.8	176.0	+47.8	176.0	R	42
3-5, 89-91	23.70	5.16 E-7	+83.7	179.0	-22.5	150.0	R	41
3-5, 107-109	23.88	1.42 E-7	+30.1	317.7	-4.9	105.3	R	376
3-5, 123-125	24.04	1.10 E-6	+82.0	83.2	+47.7	120.7	R	41
3-5, 139-141	24.20	1.10 E-6	-51.4	45.9	-27.5	105.5	R	38
3-6, 9-11	24.40	1.52 E-6	-14.7	62.1	-18.3	169.2	R	35
3-6, 19-21	24.50	6.28 E-7	-19.4	53.0	-1.6	171.6	R	36
3-6, 29-31	24.60	1.33 E-6	+49.4	43.5	+37.1	130.4	R	43
3-6, 39-41	24.70	6.92 E-7	+64.9	289.2	-5.2	181.0	R	40
3-6, 49-51	24.80	1.39 E-6	-30.0	48.8	-29.2	152.1	R	33
3-6, 59-61	24.90	9.39 E-7	+89.3	28.2	+6.3	202.6	R	143
3-6, 69-71	25.00	1.02 E-6	+42.2	78.3	+3.2	179.3	R	39
3-6, 79-81	25.10	9.72 E-7	+26.6	65.9	+11.6	146.8	R	35
3-6, 89-91	25.20	1.26 E-6	+58.3	235.5	+6.6	180.3	R	41
3-6, 99-101	25.30	1.56 E-6	-55.8	73.2	-3.9	192.0	R	258
3-6, 109-111	25.40	6.86 E-7	+44.3	240.5	-15.7	177.8	R	46
3-6, 119-121	25.50	1.43 E-6	-28.5	64.8	-28.4	182.9	R	42
3-6, 129-131	25.60	1.45 E-6	-25.0	70.5	-36.1	185.3	R	259
3-6, 139-141	25.70	1.93 E-6	-4.3	71.5	-13.4	187.5	R	278
3-7, 9-11	25.90	4.79 E-6	-5.0	50.3	-47.8	51.7	N	37
3-7, 19-21	26.00	3.07 E-6	+27.7	57.1	-22.7	159.8	R	32
3-7, 29-31	26.10	2.36 E-6	-16.4	73.1	-3.4	203.7	R	40
3-7, 39-41	26.20	1.76 E-6	-71.8	101.8	-18.8	213.0	R	310
4-1, 9-11	26.40	2.75 E-6	-37.7	345.0	-19.8	199.8	R	93
4-1, 18-20	26.49	1.38 E-6	-25.7	221.8	-23.8	168.0	R	428
4-1, 29-31	26.60	2.22 E-6	+38.9	355.7	+44.9	192.1	R	832
4-1, 38-40	26.69	2.50 E-6	-70.7	44.2	-7.8	190.9	R	41
4-1, 49-51	26.80	2.94 E-6	+49.9	19.0	+1.8	188.2	R	36
4-1, 59-61	26.90	4.99 E-6	+24.4	322.1	+17.2	322.4	N	40
4-1, 69-71	27.00	3.56 E-6	-14.2	318.6	+30.0	330.1	N	47
4-1, 90-92	27.21	5.94 E-6	-13.9	142.3	-18.8	124.6	R	47
4-1, 110-112	27.41	3.21 E-6	-5.5	158.9	-6.2	153.8	R	67
4-1, 130-132	27.61	3.96 E-6	+8.5	159.4	-11.9	173.4	R	91
4-1, 145-147	27.76	3.61 E-6	-7.1	150.1	-13.6	145.9	R	78
4-2, 6-8	27.87	3.34 E-6	-2.9	182.0	-23.7	172.1	R	67
4-2, 32-34	28.13	3.34 E-6	+14.8	16.5	-8.3	4.0	N	56
4-2, 89-91	28.70	2.84 E-6	-26.2	209.9	-24.1	216.5	R	429
4-2, 133-135	29.14	4.02 E-6	+5.2	176.6	+5.0	180.0	R	104
4-3, 19-21	29.50	3.73 E-6	+9.3	357.2	+9.4	10.7	N	150
4-3, 29-31	29.60	2.48 E-6	+10.9	347.3	+17.7	359.4	N	70
4-3, 39-41	29.70	3.96 E-6	+42.1	340.2	+27.2	350.3	N	48
4-3, 49-51	29.80	1.17 E-6	-14.6	28.4	+13.1	169.2	R	37
4-3, 59-61	29.90	1.91 E-6	+46.6	345.8	+6.0	177.7	R	32
4-3, 69-71	30.00	2.93 E-6	-4.9	355.0	+7.0	0.7	N	57

Appendix A. (Continued).

Core-Section (interval in cm)	Sub-bottom depth (m)	J_{NRM} (G)	I_{NRM}	D_{NRM}	I_{stable}	D_{stable}	Polarity	MDF (Oe)
Hole 575 (Cont.)								
4-3, 79-81	30.10	1.15 E-6	+ 39.6	41.7	+ 13.5	166.1	R	30
4-3, 89-91	30.20	1.22 E-6	+ 37.4	343.7	+ 18.3	145.9	R	33
4-3, 99-101	30.30	1.22 E-6	- 6.5	342.9	- 23.2	128.4	R	36
4-3, 109-111	30.40	1.34 E-6	+ 42.3	317.5	- 23.2	186.8	R	30
4-3, 119-121	30.50	9.44 E-7	- 23.0	282.6	- 8.9	179.2	R	317
4-3, 129-131	30.60	1.21 E-6	+ 39.0	83.3	- 2.4	181.7	R	34
4-3, 139-141	30.70	1.70 E-6	+ 29.1	57.3	+ 24.3	39.1	N	34
4-4, 4-6	30.85	3.72 E-6	- 4.4	353.4	- 8.1	5.3	N	48
4-4, 14-16	30.95	3.04 E-6	+ 8.7	31.9	- 6.0	26.6	N	46
4-4, 24-26	31.05	9.17 E-7	+ 21.3	67.0	+ 3.8	184.7	R	40
4-4, 34-36	31.15	8.89 E-7	+ 42.8	191.0	+ 59.1	167.1	R	35
4-4, 44-46	31.25	5.61 E-7	- 15.7	1.0	- 14.8	160.3	R	35
4-4, 54-56	31.35	1.07 E-6	- 5.3	40.2	- 0.5	35.5	N	37
4-4, 64-66	31.45	1.59 E-6	+ 34.8	20.3	+ 35.9	14.4	N	35
4-4, 74-76	31.55	1.31 E-6	+ 29.7	346.9	+ 4.8	179.9	R	30
4-4, 84-86	31.65	5.42 E-7	- 16.5	55.7	- 12.2	173.0	R	36
4-4, 94-96	31.75	5.07 E-7	+ 19.8	332.9	- 4.1	180.4	R	28
4-4, 104-106	31.85	6.04 E-7	- 5.8	56.6	+ 1.8	172.2	R	39
4-4, 114-116	31.95	6.91 E-7	+ 40.3	340.9	- 16.0	166.0	R	29
4-4, 124-126	32.05	4.28 E-7	- 42.2	342.5	- 3.8	171.6	R	22
4-4, 134-136	32.15	7.12 E-7	+ 26.7	40.1	+ 15.4	38.8	N	36
4-4, 144-146	32.25	3.85 E-7	+ 22.2	41.7	+ 24.3	47.5	N	41
4-5, 8-10	32.39	3.48 E-7	- 57.8	211.6	- 14.6	354.6	N	>250
4-5, 64-66	32.95	3.70 E-7	+ 11.2	207.4	+ 11.2	207.4	R	46
4-5, 90-92	33.21	1.76 E-7	- 39.4	177.0	- 35.8	180.0	N	26
4-5, 133-135	33.64	1.98 E-7	+ 32.2	2.2	+ 15.0	0.1	N	>300
4-6, 10-12	33.91	3.75 E-7	- 1.6	342.8	- 0.2	359.3	N	>300
4-6, 38-40	34.19	4.46 E-7	+ 20.9	188.9	+ 7.0	3.6	N	37
4-6, 47-49	34.28	4.55 E-7	+ 61.2	27.8	- 15.6	183.9	R	30
4-6, 59-61	34.40	4.07 E-7	+ 25.7	77.2	- 33.0	158.3	R	42
4-6, 70-72	34.51	6.09 E-7	- 10.2	78.0	+ 31.1	143.7	R	45
4-6, 82-84	34.63	6.95 E-7	- 64.0	347.4	- 5.9	167.0	R	45
4-6, 94-96	34.75	4.24 E-7	+ 56.0	325.9	- 14.1	181.7	R	389
4-6, 94-96	34.75	4.24 E-7	+ 56.0	325.9	- 14.1	181.7	R	389
Hole 575B								
1-1, 10-12	3.41	3.76 E-6	+ 30.7	346.0	+ 41.9	345.0	N	159
1-1, 20-22	3.51	5.23 E-6	+ 17.2	350.2	+ 22.0	351.5	N	97
1-1, 30-32	3.61	8.52 E-6	+ 13.7	358.4	+ 14.2	357.9	N	135
1-1, 40-42	3.71	3.19 E-6	- 10.2	354.4	- 15.1	357.6	N	128
1-1, 50-52	3.81	1.66 E-6	+ 6.7	3.9	+ 3.6	355.4	N	249
1-1, 60-62	3.91	1.83 E-6	+ 14.0	358.4	+ 14.3	4.9	N	188
1-1, 70-72	4.01	2.11 E-6	+ 24.6	337.7	+ 17.9	344.2	N	284
1-1, 100-102	4.31	6.17 E-6	+ 15.3	1.9	+ 18.7	4.1	N	206
1-1, 110-112	4.41	7.63 E-6	+ 11.0	3.5	+ 18.1	359.9	N	279
1-1, 120-122	4.51	6.19 E-6	+ 10.4	359.7	+ 15.5	358.8	N	126
1-1, 130-132	4.61	4.00 E-6	+ 11.8	357.0	+ 16.0	357.4	N	172
1-1, 140-142	4.71	5.20 E-6	+ 8.4	2.8	+ 13.6	3.1	N	163
1-2, 10-12	4.91	6.17 E-6	+ 15.3	343.0	+ 23.8	352.0	N	50
1-2, 20-22	5.01	1.67 E-6	+ 39.4	351.3	+ 19.1	184.1	R	339
1-2, 30-32	5.11	1.77 E-6	+ 28.8	2.0	+ 3.7	187.9	R	344
1-2, 40-42	5.21	6.93 E-7	- 16.2	200.0	- 10.3	186.2	R	645
1-2, 50-52	5.31	1.47 E-6	+ 29.4	183.6	+ 0.4	185.4	R	525
1-2, 60-62	5.41	1.64 E-6	+ 9.7	6.6	+ 5.4	187.7	R	349
1-2, 70-72	5.51	3.74 E-6	+ 5.6	13.7	+ 32.4	359.5	N	43
1-2, 100-102	5.81	1.42 E-6	- 47.5	46.9	+ 22.6	207.7	R	31
1-2, 112-114	5.93	1.55 E-6	- 69.3	20.6	- 21.3	188.7	R	379
1-2, 122-124	6.03	1.45 E-6	+ 55.7	317.0	+ 60.6	157.7	R	187
1-2, 133-135	6.14	1.38 E-6	- 67.6	277.0	- 39.4	191.5	R	349
1-2, 144-146	6.25	6.05 E-7	- 29.7	183.0	- 4.7	176.8	R	497
1-3, 2-4	6.33	6.91 E-7	+ 15.8	231.5	+ 3.4	170.5	R	317
1-3, 10-12	6.41	1.16 E-6	- 44.0	259.2	- 19.0	187.0	R	266
1-4, 13-15	7.94	1.96 E-6	- 49.9	287.9	- 55.3	340.3	N	83
1-5, 12-14	9.43	6.84 E-7	- 26.0	252.3	no stable			>500
1-5, 97-99	10.28	5.35 E-6	- 7.0	2.5	no stable			40
1-6, 69-71	11.50	1.79 E-6	- 38.7	276.7	no stable			254
1-6, 141-143	12.22	2.71 E-6	- 10.1	306.5	no stable			75
2-1, 80-82	12.81	3.01 E-6	+ 8.1	43.6	+ 40.5	32.4	N	38
2-1, 90-92	12.91	4.43 E-6	+ 6.3	30.6	+ 9.6	6.3	N	50
2-1, 100-102	13.01	4.50 E-6	+ 12.3	32.3	+ 13.0	15.4	N	43
2-1, 110-112	13.11	2.93 E-6	+ 7.4	39.1	- 9.9	178.1	R	29
2-1, 120-122	13.21	3.29 E-6	+ 12.4	35.9	- 18.6	181.8	R	28
2-1, 130-132	13.31	2.12 E-6	+ 4.4	54.8	- 17.0	186.9	R	48

Appendix A. (Continued).

Core-Section (interval in cm)	Sub-bottom depth (m)	J_{NRM} (G)	I_{NRM}	D_{NRM}	I_{stable}	D_{stable}	Polarity	MDF (Oe)
Hole 575B (Cont.)								
2-1, 140-142	13.41	2.40 E-6	-9.7	47.3	-29.2	186.1	R	43
2-2, 2-4	13.53	3.65 E-6	+20.5	71.0	-23.8	173.0	R	43
2-2, 12-14	13.63	3.09 E-6	+28.8	55.4	-0.2	166.6	R	46
2-2, 22-24	13.73	2.28 E-6	+27.5	71.5	-4.3	170.1	R	325
2-2, 32-34	13.83	1.98 E-6	+23.0	84.2	-3.9	166.1	R	355
2-2, 42-44	13.93	1.95 E-6	+24.4	77.5	-0.4	173.5	R	339
2-2, 52-54	14.03	2.41 E-6	+41.0	86.5	+12.2	172.7	R	341
2-2, 62-64	14.13	2.41 E-6	+17.3	113.8	-3.7	170.1	R	365
2-2, 72-74	14.23	2.21 E-6	+27.5	98.8	+2.4	174.0	R	352
2-2, 82-84	14.33	2.44 E-6	+8.2	111.7	-3.5	167.3	R	342
2-2, 92-94	14.43	2.01 E-6	+2.1	110.4	-9.5	173.2	R	345
2-2, 102-104	14.53	1.54 E-6	-1.0	65.7	-3.0	168.1	R	381
2-2, 112-114	14.63	3.05 E-6	+7.8	23.6	+8.3	168.2	R	33
2-2, 122-124	14.73	3.61 E-6	-2.5	15.9	+11.5	347.4	N	43
2-2, 132-134	14.83	4.49 E-6	-1.8	20.8	+4.4	358.3	N	64
2-2, 142-144	14.93	3.88 E-6	+4.6	15.2	+19.3	355.6	N	56
2-3, 2-4	15.03	5.17 E-6	+30.4	23.7	+64.3	347.8	N	36
2-3, 12-14	15.13	5.03 E-6	+22.9	21.5	+27.2	358.7	N	44
2-3, 22-24	15.23	4.87 E-6	+17.6	18.1	+12.0	357.6	N	48
2-3, 32-34	15.33	5.29 E-6	+15.6	15.3	+10.5	358.9	N	53
2-3, 42-44	15.43	5.02 E-6	+15.4	22.3	+17.5	2.7	N	63
2-3, 52-54	15.53	5.68 E-6	+17.3	13.1	+13.3	355.0	N	79
2-3, 62-64	15.63	4.37 E-6	+13.4	18.6	+21.1	356.2	N	67
2-3, 72-74	15.73	2.90 E-6	+10.8	19.0	+14.4	350.2	N	55
2-3, 82-84	15.83	1.67 E-6	+6.3	35.4	-5.6	184.8	R	41
2-3, 92-94	15.93	1.42 E-6	+13.3	47.0	+3.2	183.6	R	41
2-3, 102-104	16.03	1.29 E-6	-0.9	81.8	-5.0	178.6	R	337
2-3, 112-114	16.13	1.63 E-6	-7.4	118.4	-10.8	176.4	R	329
2-3, 122-124	16.23	1.29 E-6	-14.4	97.4	-5.9	174.9	R	314
2-3, 132-134	16.33	1.18 E-6	+5.1	65.7	+11.7	176.6	R	40
2-3, 142-144	16.43	1.42 E-6	-3.3	46.5	+7.1	174.0	R	41
2-4, 2-4	16.53	4.47 E-6	+26.7	35.6	+16.1	180.3	R	32
2-4, 12-14	16.63	5.35 E-6	+16.5	24.5	+28.2	10.1	N	43
2-4, 22-24	16.73	4.77 E-6	+12.5	24.2	+16.4	1.1	N	50
2-4, 32-34	16.83	5.57 E-6	16.6	21.4	+15.2	359.4	N	58
2-4, 42-44	16.93	5.93 E-6	+12.9	18.7	+8.2	357.4	N	74
2-4, 52-54	17.03	6.63 E-6	+13.3	19.7	+14.2	6.0	N	84
2-4, 72-74	17.23	3.07 E-6	+0.5	47.8	-39.3	156.4	N	37
2-4, 82-84	17.33	3.74 E-6	+18.3	20.2	+28.2	348.1	N	54
2-4, 92-94	17.43	4.77 E-6	+20.7	31.9	+26.1	15.0	N	81
2-4, 102-104	17.53	4.75 E-6	-45.5	11.4	-67.6	304.4	N	374
2-4, 122-124	17.63	4.08 E-6	+11.7	19.8	+16.1	7.5	N	93
2-4, 122-124	17.73	3.99 E-6	+10.7	25.9	+12.5	2.2	N	97
2-4, 132-134	17.83	2.81 E-6	+11.6	20.3	+19.1	352.7	N	99
2-4, 142-144	17.93	3.77 E-6	+11.3	25.9	+18.6	359.7	N	127
2-5, 2-4	18.03	3.59 E-6	+33.9	41.6	+33.5	359.7	N	45
2-5, 12-14	18.13	3.59 E-6	+32.8	54.9	+54.5	30.7	N	40
2-5, 22-24	18.23	2.97 E-6	+36.7	74.0	+13.8	181.3	R	34
2-5, 32-34	18.33	2.32 E-6	+22.7	47.1	+19.0	184.8	R	34
2-5, 42-44	18.43	2.20 E-6	+18.6	41.9	+13.7	180.7	R	31
2-5, 52-54	18.53	3.75 E-6	+24.8	51.6	+4.2	180.6	R	31
2-5, 62-64	18.63	3.02 E-6	+28.1	52.2	+15.8	191.7	R	34
2-5, 72-74	18.73	2.39 E-6	+34.0	62.5	+19.9	186.5	R	38
2-5, 82-84	18.83	2.03 E-6	+27.5	42.0	+47.5	196.3	R	43
2-5, 92-94	18.93	1.52 E-6	+25.3	51.7	+20.4	188.4	R	39
2-5, 102-104	19.03	1.09 E-6	+20.9	94.0	-7.8	186.6	R	364
2-5, 112-114	19.13	1.54 E-6	+31.9	76.4	+14.6	194.5	R	270
2-5, 122-124	19.23	1.58 E-6	+38.2	64.0	+37.5	192.0	R	88
2-5, 132-134	19.33	1.06 E-6	+16.2	69.5	+18.9	180.1	R	49
2-5, 142-144	19.43	9.28 E-7	+29.1	87.0	+23.3	195.4	R	316
2-6, 2-4	19.53	1.17 E-6	+38.9	79.8	+12.2	188.5	R	46
2-6, 12-14	19.63	1.64 E-6	+26.8	60.6	+17.3	189.6	R	40
2-6, 22-24	19.73	1.43 E-6	+22.8	73.6	-14.0	200.9	R	31
2-6, 32-34	19.83	1.28 E-6	+24.4	75.2	-8.7	199.2	R	36
2-6, 42-44	19.93	8.76 E-7	+30.4	98.0	-0.5	182.7	R	300
2-6, 52-54	20.03	8.29 E-7	+19.4	112.6	+5.5	185.0	R	44
2-6, 62-64	20.13	1.15 E-6	+24.6	120.1	+17.6	175.3	R	74
2-6, 72-74	20.23	1.07 E-6	+11.5	59.0	+25.5	165.7	R	44
2-6, 82-84	20.33	7.47 E-7	+16.6	68.4	+0.5	161.0	R	349
2-6, 92-94	20.43	1.17 E-6	-3.1	70.7	-23.5	132.6	R	38
2-6, 102-104	20.53	6.39 E-7	+4.2	45.0	+4.2	45.0	R	333
2-6, 112-114	20.63	7.04 E-7	+15.3	56.7	+63.7	185.4	R	48
2-6, 122-124	20.73	6.29 E-7	+16.1	78.3	+6.8	180.4	R	37
2-6, 132-134	20.83	4.46 E-7	+11.9	89.4	+29.0	164.8	R	118
2-6, 142-144	20.93	3.29 E-7	+14.4	65.0	+83.0	210.6	R	90

Appendix A. (Continued).

Core-Section (interval in cm)	Sub-bottom depth (m)	J_{NRM} (G)	I_{NRM}	D_{NRM}	I_{stable}	D_{stable}	Polarity	MDF (Oe)
Hole 575B (Cont.)								
2-7, 2-4	21.03	3.48 E-7	+ 29.0	67.8	no stable			
2-7, 12-14	21.13	4.43 E-7	+ 45.3	9.5	+ 43.6	10.0	N	63
2-7, 22-24	21.23	2.95 E-7	+ 45.5	9.4	+ 51.3	12.9	N	99
2-7, 32-34	21.33	2.57 E-7	+ 64.3	15.4	+ 62.7	14.2	N	134
2-7, 42-44	21.43	4.44 E-7	+ 56.2	327.3	+ 60.3	320.8	N	213
3-1, 58-60	21.59	1.70 E-6	+ 47.1	43.4	+ 48.9	353.2		37
3-1, 68-70	21.69	5.34 E-7	+ 38.7	356.9	+ 31.2	352.4		220
3-1, 78-80	21.79	7.86 E-6	+ 12.3	46.4	- 49.1	96.4		41
3-1, 88-90	21.89	7.37 E-7	+ 1.4	39.1	- 30.4	35.3		65
3-1, 98-100	21.99	7.82 E-7	+ 7.2	45.8	+ 8.3	40.4		97
3-1, 108-110	22.09	9.46 E-7	+ 12.2	51.8	- 15.0	48.2		75
3-1, 118-120	22.19	9.97 E-7	- 6.2	25.7	- 11.9	23.2		109
3-1, 128-130	22.29	2.97 E-6	- 3.0	14.5	- 23.6	12.6		61
3-1, 138-140	22.39	2.21 E-6	- 14.7	23.0	- 48.6	15.5		97
3-2, 8-10	22.59	1.98 E-6	- 3.2	23.3	- 80.6	353.6		37
3-2, 30-32	22.81	2.00 E-6	+ 4.4	29.7	- 67.4	192.0		34
3-2, 50-52	23.01	2.19 E-6	+ 7.5	30.3	- 77.9	150.1		33
3-2, 136-138	23.87	2.22 E-6	- 29.0	23.4	- 61.6	18.0		98
3-3, 12-14	24.13	2.94 E-6	- 23.7	15.7	- 70.0	13.7		74
3-3, 106-108	25.07	1.44 E-6	- 8.5	4.2	- 38.8	9.3		220
3-4, 11-13	25.62	1.33 E-6	- 12.1	11.9	- 26.4	3.8		52
3-4, 39-41	25.90	1.32 E-6	- 18.2	15.3	- 51.0	12.4		47
3-4, 59-61	26.10	1.84 E-6	+ 16.5	18.0	+ 33.5	359.7		139
3-4, 100-102	26.51	2.06 E-6	- 3.6	1.8	- 15.6	14.5		96
3-4, 110-112	26.61	1.96 E-6	- 0.5	1.6	+ 10.3	346.2		93
3-4, 120-122	26.71	3.04 E-6	+ 17.4	352.9	+ 21.6	330.9		99
3-4, 130-132	26.81	2.36 E-6	+ 18.2	346.2	+ 20.6	334.3		89
3-4, 140-142	26.91	2.68 E-6	+ 17.1	347.3	+ 20.7	335.0		91
3-5, 8-10	27.09	2.86 E-6	+ 41.7	16.3	+ 29.7	356.2		42
3-5, 18-20	27.19	2.58 E-6	+ 41.7	5.8	+ 25.5	339.3		51
3-5, 28-30	27.29	2.51 E-6	+ 45.0	25.6	+ 31.2	340.4		48
3-5, 38-40	27.39	3.56 E-6	+ 16.9	352.9	+ 19.5	335.7		64
3-5, 48-50	27.49	3.02 E-6	+ 11.2	349.6	+ 10.3	332.7		98
3-5, 58-60	27.59	2.94 E-6	+ 13.5	346.5	+ 15.7	334.2		107
3-5, 68-70	27.69	1.66 E-6	+ 21.2	359.1	+ 32.7	351.0		71
3-5, 78-80	27.79	1.72 E-6	+ 19.5	349.7	+ 27.9	332.2		96
3-5, 88-90	27.89	1.76 E-6	+ 12.3	349.5	+ 16.7	337.1		205
3-5, 98-100	27.99	1.20 E-6	+ 23.9	353.5	+ 26.9	350.3		177
3-5, 108-110	28.09	7.34 E-7	+ 16.4	7.1	+ 25.4	356.5		228
3-5, 118-120	28.19	7.57 E-7	+ 8.8	356.8	+ 26.7	348.3		208
3-5, 128-130	28.29	9.83 E-7	+ 12.5	355.0	+ 26.6	340.4		246
3-5, 138-140	28.39	7.31 E-7	+ 22.1	359.4	+ 26.3	348.3		235
3-5, 146-148	28.47	1.71 E-6	+ 12.4	292.8	+ 9.3	316.0		87
3-6, 8-10	28.59	2.50 E-6	+ 25.4	6.2	+ 18.6	344.2		75
3-6, 18-20	28.69	1.47 E-6	+ 17.7	6.4	+ 26.5	345.4		98
3-6, 28-30	28.79	1.79 E-6	+ 14.1	353.8	+ 16.7	335.1		178
3-6, 38-40	28.89	7.94 E-7	+ 24.7	7.6	+ 31.8	346.4		163
3-6, 48-50	28.99	8.12 E-7	+ 30.0	34.6	+ 35.8	28.5		99
3-6, 58-60	29.09	7.92 E-7	+ 27.6	53.7	+ 42.7	64.9		137
3-6, 68-70	29.19	6.77 E-7	+ 30.2	42.7	+ 40.7	15.1		188
3-6, 82-84	29.33	7.48 E-7	+ 48.5	51.5	+ 39.0	35.5		213
3-6, 95-97	29.46	6.08 E-7	+ 7.1	7.7	+ 20.4	8.5		145
3-6, 105-107	29.56	6.55 E-7	+ 2.3	18.1	+ 27.4	18.2		173
4-1, 26-28	29.77	10.0 E-7	+ 22.8	21.4	+ 44.2	337.7		149
4-1, 41-43	29.92	9.75 E-7	+ 22.0	13.8	+ 62.8	320.6		120
4-1, 56-58	30.07	9.25 E-7	+ 27.2	5.8	+ 59.0	357.9		173
4-1, 74-76	30.25	9.52 E-7	+ 25.3	352.1	+ 52.5	345.3		223
4-1, 92-94	30.43	6.79 E-7	+ 32.4	0.2	+ 50.8	349.4		255
4-1, 114-116	30.65	7.22 E-7	+ 24.1	5.2	+ 40.7	351.3		309
4-1, 136-138	30.87	6.48 E-7	+ 33.7	359.3	+ 42.8	355.6		313
4-2, 11-13	31.12	6.62 E-7	+ 31.6	2.7	+ 45.0	0.7		207
4-2, 26-28	31.27	8.57 E-7	+ 31.7	10.1	+ 44.9	3.9		286
4-2, 41-43	31.42	8.55 E-7	+ 35.2	3.5	+ 57.2	348.2		291
4-2, 56-58	31.57	1.10 E-6	+ 46.7	5.4	+ 46.0	9.1		266
4-2, 71-73	31.72	7.94 E-7	+ 36.3	1.1	+ 39.7	359.3		298
4-2, 86-88	31.87	1.00 E-6	+ 41.0	11.5	+ 34.9	2.9		316
4-2, 101-103	32.02	5.92 E-7	+ 46.6	358.3	+ 45.9	355.9		355
4-2, 116-118	32.17	8.46 E-7	+ 69.3	37.0	+ 61.8	359.7		305
4-2, 131-133	32.32	7.28 E-7	+ 83.7	81.7	+ 69.0	334.7		328
4-2, 146-148	32.47	1.01 E-6	+ 57.3	46.0	+ 53.7	355.9		306
4-3, 11-13	32.62	1.96 E-6	+ 52.2	24.3	+ 65.0	28.5		50
4-3, 26-28	32.77	1.61 E-6	+ 46.7	10.3	+ 54.7	5.1		97
4-3, 41-43	32.92	1.52 E-6	+ 35.1	11.7	+ 38.7	4.8		163

Appendix A. (Continued).

Core-Section (interval in cm)	Sub-bottom depth (m)	J_{NRM} (G)	I_{NRM}	D_{NRM}	I_{stable}	D_{stable}	Polarity	MDF (Oe)
Hole 575B (Cont.)								
4-3, 56-58	33.07	9.81 E-7	+ 37.9	16.2	+ 48.1	2.9		236
4-3, 71-73	33.22	9.30 E-7	+ 25.4	5.8	+ 35.3	356.1		195
4-3, 91-93	33.42	1.93 E-6	+ 44.2	13.7	+ 46.9	1.0		239
4-3, 114-116	33.65	1.29 E-6	+ 34.1	12.2	+ 43.0	4.0		208
4-3, 136-138	33.87	2.10 E-6	+ 37.1	16.5	+ 39.8	356.8		235
4-4, 11-13	34.12	4.29 E-6	+ 42.9	12.1	+ 52.8	30.6		45
4-4, 26-28	34.27	3.32 E-6	+ 55.9	3.5	+ 67.4	9.8		100
4-4, 41-43	34.42	3.05 E-6	+ 52.2	10.8	+ 60.1	15.2		171
4-4, 56-58	34.57	2.77 E-6	+ 49.9	19.9	+ 50.3	24.8		203
4-4, 71-73	34.72	2.04 E-6	+ 54.7	331.5	+ 67.8	354.9		215
4-4, 86-88	34.87	1.97 E-6	+ 68.1	8.6	+ 73.5	340.7		198
4-4, 101-103	35.02	1.39 E-6	+ 81.3	242.3	+ 67.2	223.0		260
4-4, 116-118	35.17	1.75 E-6	+ 82.8	279.1	+ 71.7	274.9		276
4-4, 131-133	35.32	2.04 E-6	+ 82.0	32.9	+ 76.2	311.4		265
4-4, 146-148	35.47	2.37 E-6	+ 81.2	242.3	+ 66.5	257.9		261
4-5, 11-13	35.62	1.84 E-6	+ 81.2	225.0	+ 69.4	244.5		222
4-5, 26-28	35.77	2.24 E-6	+ 53.0	175.7	+ 50.3	214.8		210
4-5, 41-43	35.92	2.62 E-6	+ 62.9	163.4	+ 68.4	230.4		180
4-5, 56-58	36.07	9.97 E-7	+ 84.0	66.1	+ 75.3	321.4		277
4-5, 71-73	36.22	8.08 E-7	+ 68.2	45.8	+ 74.0	348.9		306
4-5, 86-88	36.37	1.35 E-6	+ 50.8	32.6	+ 51.7	16.1		269
4-5, 101-103	36.52	6.71 E-7	+ 83.3	35.0	+ 69.0	285.5		264
4-5, 116-118	36.67	1.13 E-6	+ 40.3	195.0	+ 48.4	228.0		292
4-5, 131-133	36.82	6.27 E-7	+ 49.8	130.2	+ 69.9	323.5		358
4-5, 146-148	36.97	7.31 E-7	+ 43.3	107.5	+ 74.4	335.6		280
4-6, 11-13	37.12	3.07 E-6	+ 52.4	8.9	+ 59.4	7.3		40
4-6, 26-28	37.27	1.13 E-6	+ 84.2	231.2	- 11.2	194.3		388
4-6, 41-43	37.42	2.05 E-6	+ 64.6	359.9	+ 68.7	262.6		56
4-6, 56-58	37.57	1.88 E-6	+ 76.0	336.7	+ 52.0	239.4		85
4-6, 71-73	37.72	1.38 E-6	+ 79.6	327.4	+ 52.3	243.0		121
4-6, 86-88	37.87	1.92 E-6	+ 76.9	173.9	+ 46.6	213.6		130
4-6, 101-103	38.02	1.20 E-6	+ 72.2	186.2	+ 50.5	235.3		142
4-6, 116-118	38.17	1.21 E-6	+ 57.2	202.1	+ 25.2	221.9		235
4-6, 131-133	38.32	1.22 E-6	+ 54.5	190.8	+ 22.8	217.8		219
4-6, 146-148	38.47	1.22 E-6	+ 51.1	179.8	+ 22.6	225.1		191
4-7, 11-13	38.62	9.08 E-7	+ 51.2	200.5	+ 30.4	221.7		241
4-7, 26-28	38.77	1.36 E-6	+ 40.0	202.9	+ 23.1	227.2		191
4-7, 41-43	38.92	1.79 E-6	+ 37.2	176.6	+ 20.6	212.4		88
Hole 575C								
1-1, 5-7	0.06	4.10 E-6	+ 34.2	307.1	+ 32.5	286.0	N	310
1-1, 15-17	0.16	2.86 E-6	+ 24.1	314.6	+ 19.1	291.1	N	287
1-1, 25-27	0.26	1.66 E-6	+ 32.2	305.1	+ 28.2	284.9	N	289
1-1, 35-37	0.36	1.85 E-6	+ 19.5	304.7	+ 26.5	287.4	N	281
1-1, 45-47	0.46	4.37 E-6	+ 16.6	294.3	+ 6.6	274.7	N	242
1-1, 55-57	0.56	4.44 E-6	+ 18.5	300.0	+ 17.8	284.5	N	175
1-1, 65-67	0.66	5.18 E-6	+ 19.6	300.4	+ 12.7	276.3	N	197
1-1, 75-77	0.76	4.81 E-6	+ 21.6	291.9	+ 13.3	274.4	N	268
1-1, 85-87	0.86	5.71 E-6	+ 19.7	307.8	+ 11.7	286.5	N	210
1-1, 95-97	0.96	5.27 E-6	+ 20.2	338.1	+ 20.5	307.1	N	209
1-1, 105-107	1.06	8.11 E-6	+ 15.1	330.6	+ 14.1	318.0	N	203
1-1, 115-117	1.16	6.72 E-6	+ 8.2	339.4	+ 10.5	321.2	N	194
1-1, 125-127	1.26	7.24 E-6	+ 6.6	337.2	+ 8.5	326.6	N	221
1-1, 135-137	1.36	8.75 E-6	+ 16.3	335.2	+ 15.7	324.5	N	227
1-1, 145-147	1.46	4.84 E-6	+ 4.5	335.2	+ 5.3	321.8	N	183
1-2, 5-7	1.56	8.28 E-6	+ 14.6	358.1	+ 13.9	349.6	N	132
1-2, 15-17	1.66	4.46 E-6	+ 12.1	5.8	+ 13.3	349.5	N	154
1-2, 25-27	1.76	2.42 E-6	+ 11.3	352.9	+ 14.6	342.8	N	224
1-2, 35-37	1.86	4.46 E-6	+ 10.1	4.7	+ 16.4	354.1	N	221
1-2, 45-47	1.96	6.70 E-6	+ 15.8	359.7	+ 15.7	350.7	N	214
1-2, 55-57	2.06	7.26 E-6	+ 9.4	5.4	+ 13.1	358.1	N	179
1-2, 65-67	2.16	4.43 E-6	+ 6.4	12.3	+ 11.3	357.3	N	157
1-2, 75-77	2.26	3.62 E-6	+ 3.6	9.6	+ 13.6	350.3	N	194
1-2, 85-87	2.36	7.45 E-6	+ 5.4	356.3	+ 11.4	349.6	N	226
1-2, 95-97	2.46	7.19 E-6	+ 9.7	358.4	+ 21.5	346.5	N	242
1-2, 105-107	2.56	2.92 E-6	- 9.1	17.8	+ 26.1	351.8	N	103
1-2, 115-117	2.66	1.83 E-6	- 13.8	61.4	+ 31.5	211.5	R	50
1-2, 125-127	2.76	1.41 E-6	- 15.7	96.5	+ 14.6	199.5	R	394
1-2, 135-137	2.86	1.73 E-6	- 64.4	142.4	- 12.3	200.4	R	394
1-2, 145-147	2.96	1.81 E-6	- 33.3	192.0	- 2.7	215.2	R	418
1-3, 5-7	3.06	1.71 E-6	+ 13.2	40.4	- 8.4	226.0	R	330
1-3, 15-17	3.16	4.84 E-6	+ 11.6	36.0	+ 36.5	34.1	N	58
1-3, 25-27	3.26	1.08 E-6	- 9.2	54.1	- 0.1	222.1	R	413
1-3, 35-37	3.36	1.37 E-6	- 9.1	51.8	- 0.3	220.3	R	381

Appendix A. (Continued).

Core-Section (interval in cm)	Sub-bottom depth (m)	J_{NRM} (G)	I_{NRM}	D_{NRM}	I_{stable}	D_{stable}	Polarity	MDF (Oe)
Hole 575C (Cont.)								
1-3, 45-47	3.46	1.29 E-6	-57.6	71.4	-17.8	222.1	R	450
1-3, 55-57	3.56	5.91 E-7	+2.7	64.0	+2.4	220.4	R	629
1-3, 65-67	3.66	9.33 E-7	-47.1	202.8	-8.3	226.2	R	561
1-3, 75-77	3.76	1.13 E-6	-56.6	215.5	-9.1	233.4	R	491
1-3, 85-87	3.86	1.08 E-6	-26.4	209.2	-6.5	226.2	R	466
1-3, 95-97	3.96	2.66 E-6	-13.6	215.6	-6.6	221.9	R	374
1-3, 105-107	4.06	1.86 E-6	-13.1	217.4	-3.6	228.3	R	432
1-3, 115-117	4.16	2.66 E-6	-8.7	51.5	+12.0	22.6	N	33
1-3, 125-127	4.26	7.32 E-7	-48.7	132.3	-5.5	232.8	R	478
1-3, 135-137	4.36	1.31 E-6	-28.9	70.0	-5.2	230.4	R	339
1-3, 145-147	4.46	9.68 E-7	-45.8	211.9	-9.4	229.7	R	417
1-4, 5-7	4.56	4.20 E-7	-47.0	155.0	-4.1	234.7	R	498
1-4, 15-17	4.66	6.27 E-7	-16.7	88.8	-0.9	237.8	R	449
1-4, 25-27	4.76	6.67 E-7	+27.4	265.4	-2.8	241.7	R	555
1-4, 35-37	4.86	5.49 E-7	-21.0	126.9	-6.4	237.0	R	452
1-4, 45-47	4.96	1.52 E-6	-19.1	222.9	+1.3	241.1	R	424
1-4, 55-57	5.06	1.56 E-6	-25.6	227.6	-4.9	233.7	R	411
1-4, 65-67	5.16	2.17 E-6	-22.9	226.4	-5.5	235.4	R	413
1-4, 75-77	5.26	5.38 E-7	-21.2	224.5	+6.8	236.4	R	428
1-4, 85-87	5.36	1.21 E-6	-9.2	71.6	+8.9	62.2	N	109
1-4, 95-97	5.46	2.34 E-6	-2.5	72.7	+13.3	61.7	N	107
1-4, 105-107	5.56	1.58 E-6	-5.1	71.8	+11.9	61.2	N	95
1-4, 115-117	5.66	2.39 E-6	-12.5	71.7	+7.9	57.2	N	79
1-4, 125-127	5.76	4.45 E-6	-6.7	70.0	+10.9	59.7	N	84
1-4, 135-137	5.86	8.15 E-6	-4.8	76.9	+10.8	65.4	N	113
1-4, 145-147	5.96	9.39 E-6	-7.5	69.6	+10.6	62.4	N	95
1-5, 15-17	6.16	8.85 E-6	-6.0	66.8	+11.4	55.8	N	86
1-5, 22-24	6.23	5.18 E-6	-18.5	341.1	no stable			174
2-1, 5-7	6.36	1.51 E-6	-35.9	41.5	-78.7	6.5	N	56
2-1, 25-27	6.56	2.74 E-6	+3.1	6.9	+7.2	1.7	N	96
2-1, 45-47	6.76	1.45 E-6	+51.9	345.7	-7.6	199.6	R	47
2-1, 55-57	6.86	2.61 E-6	+40.5	6.8	+17.7	195.5	R	30
2-1, 65-67	6.96	3.08 E-6	+16.8	19.9	+7.3	16.4	N	37
2-1, 75-77	7.06	2.62 E-6	+40.2	14.9	+32.9	13.6	N	48
2-1, 85-87	7.16	2.47 E-6	+36.1	40.6	-12.7	193.4	R	22
2-1, 95-97	7.26	1.92 E-6	+54.9	9.2	-14.5	194.8	R	356
2-1, 105-107	7.36	4.53 E-6	-20.3	28.2	-57.7	185.5	R	36
2-1, 115-117	7.46	5.61 E-6	-13.0	21.6	+6.3	2.4	N	48
2-1, 125-127	7.56	5.15 E-6	-10.7	25.8	+9.4	11.1	N	51
2-1, 135-137	7.66	4.76 E-6	-17.7	21.8	+5.0	9.4	N	43
2-1, 145-147	7.76	4.84 E-6	-15.2	27.0	+18.6	9.5	N	42
2-2, 5-7	7.86	7.17 E-6	+13.5	356.2	+2.6	1.8	N	41
2-2, 15-17	7.96	3.98 E-6	+4.3	329.3	-2.4	7.2	N	48
2-2, 25-27	8.06	4.20 E-6	+3.8	354.8	-27.8	191.9	R	32
2-2, 35-37	8.16	3.01 E-6	-11.8	10.8	-16.7	177.9	R	29
2-2, 45-47	8.26	1.96 E-6	+33.5	6.4	-27.0	185.1	R	47
2-2, 55-57	8.36	2.04 E-6	+20.4	23.4	-17.2	167.7	R	433
2-2, 65-67	8.46	2.06 E-6	+37.1	50.3	-12.4	167.8	R	469
2-2, 75-77	8.56	9.32 E-7	+7.0	131.1	-15.6	179.7	R	375
2-2, 85-87	8.66	1.83 E-6	+21.2	0.6	-21.8	180.2	R	42
2-2, 95-97	8.76	1.92 E-6	+19.4	13.5	-20.3	179.7	R	324
2-2, 105-107	8.86	2.48 E-6	-2.9	18.3	+5.9	168.1	R	34
2-2, 115-117	8.96	1.11 E-6	-24.8	22.2	-8.9	169.4	R	386
2-2, 125-127	9.06	9.84 E-7	-22.3	35.9	-2.8	171.2	R	446
2-2, 135-137	9.16	9.72 E-7	-35.4	72.1	-2.9	172.4	R	472
2-2, 145-147	9.26	6.54 E-7	-35.3	85.1	-2.8	174.8	R	541
2-3, 5-7	9.36	2.29 E-6	+13.6	12.2	-0.2	196.1	R	363
2-3, 15-17	9.46	2.19 E-6	+8.8	22.2	+0.7	195.1	R	363
2-3, 25-27	9.56	2.06 E-6	+2.8	10.0	-0.3	200.7	R	382
2-3, 35-37	9.66	3.94 E-6	-5.4	21.5	-6.8	196.7	R	29
2-3, 45-47	9.76	3.35 E-6	+39.2	355.0	-4.0	200.2	R	29
2-3, 55-57	9.86	4.48 E-6	+27.9	357.8	+14.7	221.8	R	34
2-3, 65-67	9.96	4.71 E-6	+19.7	351.7	+3.5	345.4	N	43
2-3, 75-77	10.06	5.12 E-6	+26.7	6.7	+24.0	359.4	N	48
2-3, 85-87	10.16	4.18 E-6	+33.1	0.4	+33.0	356.1	N	37
2-3, 95-97	10.26	4.74 E-6	+22.7	1.5	+13.7	355.7	N	48
2-3, 105-107	10.36	4.58 E-6	+1.6	12.5	+13.8	356.5	N	44
2-3, 115-117	10.46	5.63 E-6	+0.1	4.1	+13.3	350.3	N	49
2-3, 125-127	10.56	5.80 E-6	+2.4	357.9	+12.5	351.9	N	51
2-3, 135-137	10.66	4.56 E-6	+6.3	359.0	+19.7	349.3	N	47
2-3, 145-147	10.76	3.25 E-6	+1.2	345.1	+11.7	335.2	N	41
2-4, 5-7	10.86	4.01 E-6	+16.0	10.2	+23.0	3.3	N	35
2-4, 15-17	10.96	3.38 E-6	+10.9	5.3	-3.5	196.4	R	28
2-4, 25-27	11.06	2.39 E-6	+19.6	359.7	+3.5	200.8	R	293

Appendix A. (Continued).

Core-Section (interval in cm)	Sub-bottom depth (m)	J_{NRM} (G)	I_{NRM}	D_{NRM}	I_{stable}	D_{stable}	Polarity	MDF (Oe)
Hole 575C (Cont.)								
2-4, 35-37	11.16	3.47 E-6	+ 21.9	358.4	+ 6.4	201.2	R	30
2-4, 45-47	11.26	1.27 E-6	+ 22.9	286.0	+ 2.9	191.0	R	293
2-4, 55-57	11.36	2.41 E-6	+ 62.7	320.4	+ 10.6	191.3	R	258
2-4, 65-67	11.46	3.66 E-6	+ 42.5	348.6	- 2.8	204.3	R	32
2-4, 75-77	11.56	4.72 E-6	+ 35.5	356.6	+ 42.0	345.4	N	41
2-4, 85-87	11.66	4.93 E-6	+ 20.7	342.5	+ 13.0	347.6	N	49
2-4, 95-97	11.76	5.69 E-6	+ 23.2	354.0	+ 21.2	2.8	N	61
2-4, 105-107	11.86	7.48 E-6	- 6.9	281.3	- 8.5	243.6	N	897
2-4, 115-117	11.96	5.11 E-6	+ 5.8	1.6	+ 17.9	346.6	N	44
2-4, 125-127	12.06	5.09 E-6	- 24.1	338.4	no stable			91
2-5, 5-7	12.36	6.09 E-6	- 9.8	359.2	+ 13.6	343.4	N	49
2-5, 15-17	12.46	5.41 E-6	+ 9.4	350.3	+ 14.6	340.8	N	54
2-5, 25-27	12.56	5.64 E-6	+ 9.2	350.1	+ 15.7	340.4	N	61
2-5, 35-37	12.66	3.85 E-6	+ 7.2	353.9	+ 21.0	312.6	N	41
2-5, 45-47	12.76	2.47 E-6	+ 13.6	313.4	+ 14.7	215.6	R	40
2-5, 55-57	12.86	2.42 E-6	+ 44.0	337.2	+ 14.5	180.1	R	34
2-5, 65-67	12.96	1.98 E-6	+ 43.6	330.9	+ 16.2	173.0	R	42
2-5, 75-77	13.06	1.48 E-6	+ 43.7	332.2	+ 11.8	173.8	R	46
2-5, 85-87	13.16	1.90 E-6	+ 42.6	335.9	+ 18.3	172.0	R	36
2-5, 95-97	13.26	1.29 E-6	+ 27.0	333.1	- 2.7	186.2	R	34
2-5, 105-107	13.36	6.36 E-7	- 16.8	33.9	- 6.5	166.5	R	455
2-5, 115-117	13.46	7.46 E-7	+ 3.8	66.4	+ 6.7	164.8	R	494
2-5, 125-127	13.56	9.29 E-7	- 7.2	12.6	- 5.7	173.6	R	34
2-5, 135-137	13.66	8.16 E-7	+ 2.6	31.2	+ 3.6	168.1	R	378
2-5, 145-147	13.76	1.90 E-6	+ 0.3	357.2	+ 32.1	190.8	R	42
2-6, 5-7	13.86	3.04 E-6	+ 21.2	345.4	- 7.9	175.5	R	30
2-6, 15-17	13.96	1.99 E-6	+ 12.4	345.1	- 0.8	173.8	R	29
2-6, 25-27	14.06	1.32 E-6	+ 7.9	349.2	- 2.4	171.0	R	28
2-6, 35-37	14.16	1.58 E-6	+ 17.5	344.2	+ 14.1	176.8	R	30
2-6, 45-47	14.26	1.54 E-6	+ 0.4	357.7	- 3.8	173.2	R	34
2-6, 55-57	14.36	1.53 E-6	+ 12.8	0.8	+ 20.9	171.9	R	35
2-6, 65-67	14.46	8.90 E-7	+ 1.0	346.4	no stable			42
2-6, 75-77	14.56	6.84 E-7	+ 9.1	347.7	+ 12.8	179.5	R	34
2-6, 85-87	14.66	7.30 E-7	+ 8.9	345.1	+ 16.2	194.3	R	39
2-6, 95-97	14.76	5.82 E-7	+ 12.1	353.5	+ 59.2	215.9	R	40
2-6, 105-107	14.86	5.51 E-7	+ 6.1	351.1	+ 31.6	208.0	R	43
2-6, 115-117	14.96	5.46 E-7	- 8.0	350.4	- 19.7	148.5	R	30
2-6, 125-127	15.06	5.33 E-7	- 1.8	19.2	- 3.1	142.7	R	38
2-6, 135-137	15.16	3.40 E-7	+ 32.0	5.5	+ 9.7	179.9	R	369
2-6, 145-147	15.26	7.58 E-7	+ 9.6	3.8	+ 43.2	218.8	R	43
2-7, 5-7	15.36	3.70 E-7	+ 38.1	30.9	+ 22.8	210.1	R	298
2-7, 15-17	15.46	4.36 E-7	+ 12.7	34.1	+ 6.9	231.6	R	39
2-7, 25-27	15.56	5.84 E-7	+ 13.9	37.2	+ 40.9	293.2	N	49
2-7, 35-37	15.66	5.59 E-7	- 4.3	73.1	+ 13.8	27.3	N	61

Notes: J = intensity; I = inclination, D = declination (+ = downward, - = upward); polarity is as derived from stable inclinations and declinations (N = normal, R = reversed).

APPENDIX B
Paleomagnetic Data Derived from Oligocene to Late Miocene Leg 85 Samples (samples were measured at HIG, after demagnetization at 50 Oe)

Sub-bottom depth (m)	Declination (°)	Inclination (°)	Intensity (G)
Hole 572A			
120.00	-30.75	-33.14	0.4140 E-6
121.11	-9.93	7.01	0.1202 E-5
122.61	-8.75	27.17	0.7416 E-6
124.11	-32.03	-13.53	0.6314 E-6
125.61	-11.06	-0.03	0.7462 E-6
127.11	-84.24	-13.65	0.9357 E-6
129.17	-24.49	-16.97	0.6278 E-6
130.33	-16.79	-17.00	0.6634 E-6
131.81	-176.09	-26.31	0.3915 E-5
133.31	2.04	-3.32	0.9725 E-6
134.81	-6.53	6.61	0.9195 E-6
136.31	-15.47	3.35	0.6878 E-6
139.09	-14.29	19.42	0.1012 E-5
140.59	-2.18	12.06	0.5413 E-6
142.09	48.59	-6.87	0.2807 E-5
143.59	-9.26	9.35	0.6088 E-6
145.09	-25.83	6.86	0.7711 E-6
145.80	-79.61	21.75	0.8132 E-5
147.30	-20.03	-27.25	0.9364 E-6
148.80	-1.25	8.03	0.9587 E-6
150.30	-20.42	-12.81	0.7407 E-6
151.80	-133.48	-17.92	0.6038 E-6
153.30	-16.85	17.63	0.9806 E-6
Hole 572B			
154.11	-31.58	-3.65	0.8671 E-6
154.51	-55.50	81.87	0.2193 E-4
155.31	-2.58	-13.63	0.7255 E-6
155.41	-79.98	1.14	0.2373 E-5
155.61	-17.23	-21.52	0.1098 E-5
156.01	-4.34	-5.84	0.1374 E-5
156.41	-13.61	-19.50	0.1121 E-5
156.81	-37.85	-0.95	0.7004 E-6
157.11	12.39	-35.88	0.7492 E-6
157.51	-14.07	20.42	0.1170 E-5
157.91	-13.78	-9.99	0.1745 E-5
158.31	-36.01	42.77	0.2268 E-5
158.61	46.52	-24.13	0.5915 E-5
159.78	-9.95	8.73	0.9883 E-6
161.28	-0.51	3.84	0.8560 E-6
163.32	-120.34	58.39	0.6165 E-5
164.70	-68.68	8.22	0.1372 E-5
166.20	-4.29	-0.79	0.1081 E-5
167.70	-63.76	-12.48	0.2251 E-5
169.29	0.88	15.08	0.7037 E-6
170.79	10.01	-14.63	0.6568 E-6
Hole 572C			
121.40	-8.39	3.66	0.6006 E-6
121.80	-178.13	-50.26	0.1208 E-5
122.40	-19.47	-6.02	0.9384 E-6
122.90	-13.51	-2.08	0.1071 E-5
123.30	48.00	-56.07	0.8916 E-6
123.90	-14.94	-19.92	0.9925 E-6
124.40	-24.54	-17.11	0.4741 E-6
124.80	-21.71	-16.45	0.5465 E-6
125.40	-17.22	-12.78	0.1005 E-5
125.90	-6.50	-0.03	0.9885 E-6
126.30	-15.13	5.02	0.9938 E-6
126.90	-1.16	0.02	0.1164 E-5
127.40	-8.24	-1.76	0.8270 E-6
127.80	-2.11	-19.44	0.1110 E-5
128.40	-10.85	0.93	0.1046 E-5
128.90	-15.52	2.04	0.7333 E-6
129.30	-15.32	-12.64	0.9309 E-6
129.90	-17.16	-12.20	0.7775 E-6
131.19	-30.40	-14.41	0.6704 E-6
131.69	-21.07	-18.65	0.9621 E-6

Appendix B. (Continued).

Sub-bottom depth (m)	Declination (°)	Inclination (°)	Intensity (G)
Hole 572C (Cont.)			
132.19	-32.58	-35.89	0.4285 E-6
132.69	-22.28	-17.31	0.6186 E-6
133.19	-11.94	-28.12	0.8788 E-6
133.69	-20.07	2.97	0.8102 E-6
134.19	-16.21	3.71	0.7840 E-6
134.69	-18.81	-18.69	0.8381 E-6
135.19	-25.23	0.56	0.1240 E-5
135.69	-32.16	-19.57	0.6772 E-6
136.19	-11.76	-19.97	0.1198 E-5
136.69	-5.75	-30.89	0.7144 E-6
137.19	-52.12	62.14	0.1279 E-5
137.69	-11.48	-2.73	0.7534 E-6
138.19	-11.70	-4.61	0.1042 E-5
138.69	-33.83	25.88	0.5139 E-6
139.19	-11.53	7.91	0.9498 E-6
139.69	-11.38	-4.01	0.9837 E-6
140.77	-4.19	-8.91	0.9177 E-6
140.80	-12.22	1.04	0.8669 E-6
141.29	-7.29	20.13	0.8724 E-6
142.30	-13.14	3.52	0.7377 E-6
142.79	-2.13	-10.84	0.8356 E-6
143.28	-13.44	4.43	0.7186 E-6
144.00	-10.69	-6.76	0.9705 E-6
144.70	-28.97	-2.50	0.5550 E-6
145.10	-12.16	3.56	0.8993 E-6
145.62	-6.63	-4.89	0.9526 E-6
150.73	-8.89	-0.78	0.1100 E-5
151.35	-10.10	2.13	0.8162 E-6
151.89	-38.46	63.84	0.8778 E-6
152.39	-12.47	15.45	0.6561 E-6
152.85	36.43	-51.98	0.5028 E-6
153.39	-12.34	-9.72	0.7096 E-6
153.89	-10.87	7.47	0.9266 E-6
154.35	-2.11	5.25	0.1255 E-5
154.89	-12.30	-23.57	0.1481 E-5
155.39	-7.84	12.71	0.7945 E-6
155.85	-19.01	-28.72	0.4982 E-6
156.39	-24.48	-28.81	0.8046 E-6
156.89	-16.39	-37.02	0.5728 E-6
157.35	-8.40	2.59	0.1009 E-5
157.70	-45.08	-26.67	0.2735 E-6
158.25	-4.34	-14.06	0.8719 E-6
158.61	-167.35	-39.02	0.7069 E-6
163.89	-14.38	-3.12	0.1297 E-5
164.24	-17.10	-16.14	0.1020 E-5
164.65	-39.85	-13.52	0.5896 E-6
165.01	-18.33	-17.82	0.9418 E-6
165.48	-13.68	-16.83	0.8960 E-6
165.92	-12.09	-32.99	0.9920 E-6
166.33	-10.31	14.86	0.7394 E-6
166.85	-49.97	1.01	0.1625 E-5
167.35	-41.09	-1.07	0.1269 E-5
167.83	-11.07	-6.81	0.8448 E-6
168.24	-33.38	-1.47	0.6688 E-6
Hole 572D			
155.21	-3.82	53.57	0.3624 E-5
155.71	-38.52	-37.92	0.4579 E-6
160.70	-15.98	-31.89	0.1086 E-5
161.41	-11.58	-8.63	0.5493 E-6
166.46	-8.68	-14.22	0.7600 E-6
167.33	-18.01	-23.65	0.7482 E-6
170.15	5.01	-14.65	0.2276 E-5
174.88	-17.08	-14.75	0.7485 E-6
179.61	-14.80	-13.99	0.3772 E-6
195.17	-15.52	-27.21	0.8771 E-6
196.56	-31.45	26.45	0.4452 E-6
206.71	-18.77	-30.71	0.5987 E-6
207.29	-16.08	-13.08	0.5534 E-6

Appendix B. (Continued).

Sub-bottom depth (m)	Declination (°)	Inclination (°)	Intensity (G)
----------------------	-----------------	-----------------	---------------

Hole 572D (Cont.)

207.81	-16.52	-20.30	0.6360 E-6
209.85	-9.52	-24.14	0.7813 E-6
210.81	-7.75	-1.15	0.5789 E-6
211.85	-2.28	-21.83	0.7976 E-6
212.43	-12.73	-5.40	0.6967 E-6
213.17	-17.53	-18.95	0.8165 E-6
215.20	-22.97	18.59	0.4700 E-6
215.91	-14.07	-7.39	0.6630 E-6
216.59	-13.90	-36.75	0.8534 E-6
217.70	-67.48	-15.51	0.1477 E-5
218.90	-20.94	-8.88	0.5221 E-6
219.58	-14.39	-21.04	0.8489 E-6
221.33	-1.23	-42.77	0.3744 E-6
221.75	-13.96	-29.20	0.5950 E-6
222.96	-33.83	-27.70	0.3443 E-6
224.27	-20.36	-34.81	0.6797 E-6
224.78	-16.39	-7.72	0.7839 E-6
225.57	-9.91	-35.13	0.5328 E-6
226.00	-68.72	9.64	0.1311 E-5
226.42	-9.87	-14.00	0.5632 E-6
227.26	8.46	-19.50	0.7741 E-6
227.71	-22.81	-22.63	0.7773 E-6
228.82	12.18	-29.71	0.6925 E-6
229.67	-20.08	-23.08	0.9788 E-6
230.61	-18.42	-18.40	0.7743 E-6
231.25	-8.98	-21.49	0.6186 E-6
231.75	-19.82	0.46	0.4861 E-6
236.61	-20.27	-4.66	0.6795 E-6
237.34	0.12	-15.09	0.6262 E-6
238.84	-14.81	-16.79	0.6937 E-6
240.73	-11.52	-13.60	0.4501 E-6
241.30	-25.25	-22.29	0.7709 E-6
241.84	-16.91	-15.83	0.5727 E-6
242.78	0.39	21.02	0.7595 E-6
243.58	-11.07	16.97	0.6840 E-6
244.41	34.50	-18.63	0.3768 E-6
245.35	-22.48	-19.93	0.5722 E-6
245.78	-19.38	-25.11	0.5653 E-6
246.05	-42.82	-7.09	0.6969 E-6
247.03	-26.75	-18.28	0.4328 E-6
248.38	-90.44	1.06	0.8393 E-4
249.69	1.80	-2.46	0.8809 E-6
250.87	-7.92	25.23	0.8604 E-6
251.66	-10.69	24.56	0.5116 E-6
252.68	-159.02	39.25	0.2302 E-6
253.45	-26.03	-14.16	0.7069 E-6
254.18	10.47	-19.19	0.1020 E-5
254.90	-3.75	-2.36	0.4406 E-6
255.47	-22.86	-15.24	0.7378 E-6
255.67	-6.19	-26.16	0.9569 E-6
256.75	-0.07	-5.65	0.1362 E-4
257.21	-60.13	-28.01	0.9167 E-5
257.82	157.88	-17.59	0.1356 E-4
258.25	-1.74	-25.32	0.8024 E-6
259.29	-16.69	-11.11	0.6727 E-6
260.21	33.21	4.53	0.2305 E-5
261.12	7.33	-4.43	0.7210 E-5
265.63	37.35	-7.17	0.1404 E-5
267.51	-0.35	-21.99	0.4359 E-6
267.61	14.02	5.31	0.1126 E-5
268.40	-7.66	-15.32	0.9872 E-6
270.72	17.49	-51.30	0.6518 E-5
272.32	-3.35	0.12	0.1596 E-5
277.35	83.04	10.26	0.3377 E-4
279.31	-24.17	2.89	0.1902 E-4
281.15	-140.64	-1.92	0.1147 E-4
281.74	9.48	-7.15	0.2453 E-4
284.14	4.36	-5.18	0.1032 E-5
287.41	-0.23	-29.87	0.9808 E-6
294.08	-152.02	4.50	0.6370 E-5
295.23	79.83	-1.39	0.2974 E-4
296.20	-47.31	-8.45	0.2746 E-4
296.71	59.33	6.36	0.2152 E-4
297.24	179.33	-33.50	0.3539 E-5

Appendix B. (Continued).

Sub-bottom depth (m)	Declination (°)	Inclination (°)	Intensity (G)
----------------------	-----------------	-----------------	---------------

Hole 572D (Cont.)

297.76	88.49	-0.95	0.2232 E-4
298.21	37.56	-8.58	0.1265 E-4
299.17	-10.25	-13.36	0.7184 E-6
299.75	-0.23	-7.25	0.6949 E-6
300.56	14.08	-37.07	0.8316 E-6
301.25	42.67	-2.65	0.2334 E-5
302.73	-6.59	-24.36	0.7178 E-6
303.27	-2.32	4.13	0.1181 E-5
304.16	-1.69	-42.06	0.7279 E-6
304.77	-20.14	-49.43	0.6524 E-6
306.20	71.75	-33.87	0.9729 E-6
312.82	-11.89	12.27	0.5565 E-6
313.82	-2.27	-17.47	0.6279 E-6
314.45	-6.03	-13.49	0.6298 E-6
314.93	-14.27	-24.38	0.5363 E-6
315.94	-10.78	-12.21	0.5764 E-6
316.54	-12.43	-12.81	0.5911 E-6
317.44	-16.07	-23.90	0.5329 E-6
318.94	-17.59	-26.50	0.5720 E-6
319.59	-2.07	3.86	0.4699 E-6
320.44	-9.79	-6.63	0.6976 E-6
322.40	-19.62	-16.64	0.6988 E-6
324.25	0.18	-39.53	0.6960 E-6
332.60	149.09	-35.53	0.2580 E-5
333.68	6.39	-19.14	0.6672 E-5
334.66	14.93	-58.26	0.5477 E-5
350.76	4.80	-67.87	0.8096 E-6
351.90	-2.52	-48.04	0.9978 E-6
353.40	-16.92	-42.49	0.1132 E-5
353.77	-5.51	-48.53	0.1057 E-5
354.51	1.20	-42.32	0.9772 E-6
360.77	-31.21	-46.29	0.8072 E-6
360.78	-37.95	-41.04	0.5761 E-6
361.42	-30.14	-31.41	0.4309 E-6
361.76	-11.99	-21.42	0.6691 E-6
362.85	-94.32	-25.47	0.2501 E-5
363.30	-149.29	-22.49	0.6058 E-5
363.73	-50.64	5.85	0.5503 E-5
364.38	-113.67	2.46	0.1272 E-4
364.63	37.70	-11.31	0.1325 E-4
365.27	41.58	-13.36	0.6311 E-5
365.74	-4.31	-31.31	0.6006 E-5
366.21	-17.64	-25.08	0.3020 E-5
367.39	-101.55	-16.96	0.1570 E-5
369.85	101.21	-17.11	0.6478 E-5
370.36	85.91	19.77	0.1123 E-4
370.81	176.37	12.82	0.1045 E-4
371.15	-45.87	-2.95	0.2160 E-4
372.46	58.66	3.92	0.7981 E-5
372.52	105.06	-2.49	0.1124 E-4
373.47	-154.67	-3.41	0.1896 E-4
375.37	-129.14	-8.00	0.1711 E-4
376.23	125.76	5.12	0.2589 E-4
376.37	-156.34	2.18	0.3179 E-4
377.33	61.67	5.57	0.7119 E-5
377.98	54.95	-5.27	0.4237 E-4
379.46	-18.95	4.64	0.1736 E-4
380.06	19.66	5.84	0.2397 E-4
381.36	71.52	-12.66	0.1707 E-4
381.89	125.02	-6.01	0.4127 E-5
382.99	-82.29	-11.77	0.1304 E-4
383.39	116.50	0.92	0.7968 E-5
383.83	73.63	-15.91	0.3317 E-4
384.96	22.98	7.39	0.3002 E-4
385.39	135.63	-72.27	0.3861 E-5
386.21	130.77	-9.36	0.1759 E-4
386.59	162.53	8.45	0.2731 E-4
387.85	-150.65	-4.91	0.2652 E-4
388.27	89.50	-17.95	0.2685 E-4
388.93	-144.08	0.62	0.2755 E-4
389.45	-24.05	-22.78	0.6259 E-5
389.96	-156.88	-20.57	0.2103 E-4
390.26	177.93	-6.46	0.1528 E-4
390.82	-170.43	-2.12	0.1305 E-4

Appendix B. (Continued).

Sub-bottom depth (m)	Declination (°)	Inclination (°)	Intensity (G)
----------------------	-----------------	-----------------	---------------

Hole 572D (Cont.)

391.46	-89.16	-12.73	0.2910 E-4
391.60	-11.69	-11.06	0.2916 E-4
392.47	-5.17	-16.95	0.5982 E-5
392.81	-42.85	-20.42	0.1181 E-4
393.41	168.78	-72.74	0.5074 E-5
393.98	74.84	-9.07	0.1589 E-4
394.44	57.33	-0.95	0.2508 E-4
396.03	-50.87	-7.89	0.2516 E-4
396.31	-62.94	-26.79	0.4312 E-5
396.55	-39.29	-49.79	0.3632 E-5
397.45	-40.25	-60.94	0.1318 E-5
398.24	-140.23	3.26	0.1535 E-4
398.69	-62.93	11.04	0.1686 E-4
399.14	150.05	17.28	0.1288 E-4
399.76	-130.77	11.69	0.1786 E-4
400.31	98.51	-6.22	0.1764 E-4
400.73	23.20	-10.12	0.2191 E-4
401.22	-6.49	-2.11	0.2828 E-4
401.81	3.82	-6.78	0.3381 E-4
402.22	137.23	-18.17	0.2363 E-4
402.73	-178.00	1.76	0.1924 E-4
403.21	103.32	-43.26	0.4757 E-5
403.72	75.32	-4.21	0.1925 E-4
404.24	-78.95	-13.28	0.2303 E-4
404.76	46.58	-4.72	0.2728 E-4
405.24	-127.99	-11.63	0.1532 E-4
405.74	134.91	22.31	0.1872 E-4
406.26	-173.93	11.89	0.1482 E-4
406.74	-54.19	13.15	0.2112 E-4
407.24	-78.33	-1.88	0.2048 E-4
407.59	97.09	-0.89	0.2335 E-4
407.93	-23.41	-0.92	0.4579 E-5
408.51	-158.76	34.16	0.3397 E-5
409.22	-81.47	5.65	0.2485 E-5
409.63	66.65	0.82	0.3848 E-4
410.07	56.95	-1.68	0.7768 E-5
410.59	133.86	-6.82	0.2093 E-4
411.16	70.15	-2.24	0.2894 E-4
411.57	-109.14	-12.89	0.7080 E-5
412.09	15.58	24.43	0.2724 E-5
412.87	54.80	-8.48	0.6336 E-5
413.38	148.94	-12.43	0.8179 E-5
413.86	-124.15	-17.40	0.3058 E-4
414.36	99.58	2.04	0.8275 E-5
417.32	98.54	-23.62	0.6353 E-5
417.85	178.02	-12.27	0.3399 E-5
418.35	-38.30	4.25	0.2667 E-4
418.83	-162.49	-31.43	0.2654 E-4
419.34	175.35	4.65	0.2616 E-4
419.85	-125.56	-4.44	0.1622 E-4
420.35	73.75	-9.61	0.2971 E-4
420.84	-40.35	3.36	0.2615 E-4
421.27	86.85	-14.11	0.2953 E-4
421.85	20.22	-9.65	0.6591 E-5
422.34	80.44	-7.40	0.2809 E-4
422.83	-12.24	-2.45	0.1523 E-4
423.38	-72.92	8.32	0.2177 E-4
427.76	-45.64	1.60	0.1204 E-4
429.08	-10.27	-33.85	0.1698 E-4
429.55	50.94	-40.31	0.2571 E-5
430.13	176.79	-26.51	0.8744 E-5
430.58	137.05	-7.67	0.9320 E-5
431.05	45.85	-17.25	0.1393 E-4
431.63	92.42	-12.47	0.2017 E-4
432.08	14.73	-25.41	0.1083 E-4
432.55	61.16	-3.76	0.1575 E-4
433.13	-60.18	-13.79	0.1636 E-4
433.58	115.41	-27.16	0.1550 E-4
434.05	76.03	-11.87	0.2365 E-4
434.63	71.58	-27.52	0.1131 E-4
436.13	-6.23	-6.49	0.5424 E-5
436.71	107.11	0.81	0.3451 E-4
437.22	96.46	-10.45	0.1157 E-4
437.62	128.74	-4.40	0.4012 E-4

Appendix B. (Continued).

Sub-bottom depth (m)	Declination (°)	Inclination (°)	Intensity (G)
----------------------	-----------------	-----------------	---------------

Hole 572D (Cont.)

438.51	46.73	0.51	0.5201 E-4
438.78	-78.05	2.87	0.3231 E-4
439.27	83.08	-6.39	0.6410 E-4
439.83	-141.86	5.24	0.3502 E-4
441.02	45.37	13.30	0.4477 E-4
441.61	53.81	-1.41	0.1811 E-4
442.20	61.70	0.51	0.3093 E-4
443.18	-171.07	17.29	0.2928 E-4
443.81	-126.31	12.38	0.4142 E-4
445.63	30.23	13.44	0.4874 E-4
446.32	-71.31	-36.34	0.7333 E-5
446.69	-11.51	-23.65	0.7505 E-6
447.31	23.53	-35.48	0.9180 E-6
448.49	-118.56	-2.09	0.4200 E-5
450.41	14.08	0.98	0.3600 E-4
451.02	76.11	-5.69	0.3831 E-4
451.38	-14.94	2.83	0.5979 E-4
451.61	136.38	-18.41	0.4659 E-4
452.01	163.55	-2.47	0.4647 E-4
452.55	-60.05	5.24	0.4595 E-4
452.94	48.25	-6.44	0.7193 E-4
453.15	-85.56	1.03	0.4306 E-4
453.64	-130.66	3.68	0.3380 E-4
455.31	-63.25	-0.78	0.5773 E-4
455.71	-50.25	-0.61	0.5391 E-4
456.18	166.31	1.99	0.3136 E-4
456.61	-50.23	-11.23	0.2431 E-4
457.31	6.88	-17.91	0.2098 E-4
457.56	66.30	0.24	0.3146 E-4
458.73	17.09	-18.95	0.2549 E-4
459.38	-69.94	12.30	0.5609 E-5
459.91	-106.51	21.59	0.2369 E-5
461.00	-21.26	21.40	0.1292 E-5
461.91	95.69	-3.38	0.1422 E-4
462.33	-162.62	0.72	0.1164 E-4
463.36	-63.33	1.89	0.3102 E-4
463.96	-71.69	-1.50	0.4524 E-4
464.16	-95.37	3.56	0.3286 E-4
464.41	-80.51	3.40	0.8191 E-5
86.21	23.72	-19.22	0.9955 E-6
87.81	27.88	-19.91	0.1026 E-5
88.54	24.77	-16.80	0.1072 E-5
89.15	28.41	-5.22	0.8568 E-6
89.43	24.21	-8.47	0.9709 E-6
89.85	23.55	-14.10	0.1104 E-5
90.51	22.69	-7.38	0.1111 E-5
90.92	30.24	-22.56	0.1188 E-5
91.32	33.94	-6.29	0.8573 E-6
92.01	25.22	-11.98	0.1053 E-5
92.43	27.47	-3.91	0.9334 E-6
92.82	21.10	-14.77	0.8963 E-6
93.01	26.90	-22.95	0.9816 E-6
93.93	25.43	-14.17	0.9546 E-6
94.32	23.73	-19.88	0.9472 E-6
95.64	24.91	-10.49	0.9491 E-6
96.03	16.62	-14.74	0.9864 E-6
96.44	25.62	-11.32	0.1093 E-5
97.01	32.12	-9.29	0.8938 E-6
97.43	41.21	-0.47	0.9953 E-6
97.94	21.35	-13.89	0.1012 E-5
98.51	31.04	-7.38	0.8489 E-6
98.93	23.04	-3.07	0.9959 E-6
99.44	59.54	-18.85	0.7823 E-6
100.01	42.33	8.23	0.7683 E-6
100.43	30.72	-2.32	0.8443 E-6
100.94	34.81	-9.78	0.8179 E-6
101.51	23.96	-21.32	0.1053 E-5
101.93	44.61	-5.53	0.1017 E-5
102.44	43.06	-41.63	0.8287 E-6
103.01	25.43	-13.11	0.9394 E-6
103.43	35.21	-23.91	0.8869 E-6

Appendix B. (Continued).

Sub-bottom depth (m)	Declination (°)	Inclination (°)	Intensity (G)
----------------------	-----------------	-----------------	---------------

Hole 573 (Cont.)

103.94	35.85	9.47	0.9653 E-6
105.40	25.45	0.96	0.9804 E-6
105.82	31.99	6.00	0.8664 E-6
106.22	27.52	-17.34	0.9700 E-6
106.63	31.45	12.87	0.9875 E-6
107.32	31.51	-0.87	0.9585 E-6
107.72	13.01	-4.14	0.8362 E-6
108.13	26.22	3.83	0.9893 E-6
108.82	76.76	-9.58	0.1185 E-5
109.22	39.59	13.03	0.7803 E-6
109.63	19.69	2.05	0.1078 E-5
110.31	26.58	2.99	0.9746 E-6
110.72	22.80	2.98	0.9987 E-6
111.82	20.95	-11.44	0.8673 E-6
112.22	24.11	2.60	0.9206 E-6
112.63	30.47	-3.26	0.8608 E-6
113.04	49.52	10.16	0.1032 E-5
113.45	27.40	3.48	0.7606 E-6
113.87	38.93	34.22	0.9630 E-6
114.54	21.83	9.72	0.9329 E-6
114.95	24.04	-6.69	0.9261 E-6
115.37	27.16	30.72	0.1442 E-5
116.04	2.25	-18.19	0.4428 E-6
116.45	31.44	12.46	0.9073 E-6
116.87	37.53	-14.76	0.7448 E-6
117.54	32.80	20.03	0.8411 E-6
117.95	29.00	5.21	0.1104 E-5
118.37	32.30	6.29	0.9178 E-6
119.04	45.01	1.69	0.2398 E-5
119.45	24.29	7.48	0.9006 E-6
119.87	28.06	1.50	0.9696 E-6
120.54	21.75	5.83	0.1006 E-5
120.95	51.48	-2.96	0.1089 E-5
121.37	33.07	0.96	0.8907 E-6
121.72	34.28	2.15	0.9283 E-6
122.41	22.64	5.30	0.9404 E-6
122.82	61.89	37.45	0.7244 E-6
123.22	44.85	33.44	0.6481 E-6
123.91	-46.36	-33.53	0.1648 E-5
124.32	40.05	-6.55	0.8978 E-6
124.72	69.17	1.57	0.3192 E-5
125.41	20.61	-26.06	0.8318 E-6
125.82	26.05	8.35	0.1318 E-5
126.22	31.07	26.91	0.1052 E-5
126.91	42.66	27.79	0.1101 E-5
127.32	29.47	7.04	0.1297 E-5
127.72	18.92	-20.03	0.1878 E-5
128.41	33.21	3.78	0.1601 E-5
128.82	26.15	13.52	0.1567 E-5
129.22	10.43	14.17	0.1365 E-5
129.91	9.68	-7.14	0.1353 E-5
130.32	19.98	14.18	0.1084 E-5
130.72	16.39	11.46	0.1040 E-5
131.61	39.01	24.43	0.1875 E-5
132.01	17.06	-11.45	0.3362 E-5
132.53	7.31	5.15	0.1368 E-5
133.52	15.21	8.16	0.1292 E-5
135.02	6.37	4.74	0.1430 E-5
136.52	14.48	14.71	0.1188 E-5
138.02	5.75	-2.56	0.1616 E-5
139.52	11.62	-7.76	0.1586 E-5
140.81	19.50	4.25	0.7739 E-6
142.38	7.54	1.80	0.1501 E-5
143.87	9.36	1.80	0.1467 E-5
145.37	3.58	7.59	0.1055 E-5
146.81	8.17	8.97	0.1459 E-5
148.37	12.30	14.41	0.1075 E-5
150.69	5.30	8.20	0.1670 E-5
152.11	10.16	3.56	0.1565 E-5
153.61	12.11	5.64	0.1432 E-5
154.36	5.80	-18.86	0.1494 E-5
155.86	7.10	-6.06	0.1502 E-5
157.77	20.82	-12.47	0.1587 E-5
158.84	14.42	-13.32	0.1059 E-5

Appendix B. (Continued).

Sub-bottom depth (m)	Declination (°)	Inclination (°)	Intensity (G)
----------------------	-----------------	-----------------	---------------

Hole 573B

142.36	-3.48	16.36	0.7763 E-6
143.97	-27.05	33.28	0.6505 E-6
144.97	-2.55	19.79	0.5568 E-6
152.29	-13.15	-14.26	0.7916 E-6
155.27	12.83	-23.12	0.5982 E-6
158.74	-9.33	-13.35	0.1085 E-5
164.77	-7.16	-5.92	0.8191 E-6
176.03	-16.11	-7.67	0.9562 E-6
194.51	6.41	5.01	0.2402 E-5
195.49	-13.09	1.49	0.1063 E-5
195.83	-10.46	-16.54	0.9053 E-6
208.21	-5.61	-10.90	0.8185 E-6
211.58	-15.07	-13.18	0.1155 E-5
218.47	-9.28	-14.07	0.9271 E-6
222.52	-5.57	-12.21	0.8315 E-6
226.47	-9.48	2.97	0.8793 E-6
229.48	17.52	-15.09	0.1660 E-5
232.34	-7.49	-9.08	0.1147 E-5
235.39	-9.14	-4.67	0.1034 E-5
238.39	75.72	-41.19	0.6343 E-6
245.23	-0.67	5.27	0.9579 E-6
247.91	-13.44	-6.62	0.9069 E-6
254.47	-2.46	-8.96	0.8465 E-6
257.27	-43.96	-3.59	0.3488 E-6
262.71	126.90	-67.92	0.3921 E-5
263.18	152.60	1.97	0.8968 E-5
263.85	158.01	12.83	0.1067 E-4
264.34	10.55	10.97	0.3819 E-5
264.84	-92.07	-9.79	0.3357 E-5
265.83	12.11	4.09	0.1434 E-4
265.85	-113.28	-1.23	0.8724 E-5
266.34	-81.93	2.62	0.7963 E-6
266.79	-66.41	20.68	0.1091 E-4
267.39	22.03	-19.93	0.2294 E-5
267.92	-133.81	12.03	0.6803 E-5
268.19	-24.30	3.25	0.3354 E-5
268.86	31.36	-2.32	0.1702 E-5
269.33	-91.14	-35.33	0.1746 E-5
269.79	44.14	18.83	0.2735 E-5
270.30	38.93	5.04	0.8556 E-5
270.88	-93.38	-9.58	0.8369 E-5
271.31	-51.93	4.44	0.2675 E-5
271.75	-68.92	2.29	0.6279 E-5
272.47	73.34	-0.71	0.3252 E-5
272.65	29.95	54.79	0.1649 E-3
273.30	1.27	-14.26	0.2003 E-5
273.85	61.17	-21.78	0.1701 E-5
274.43	14.31	21.77	0.1156 E-5
274.84	109.63	1.37	0.2742 E-5
275.49	-158.77	17.87	0.9944 E-6
276.70	24.78	-0.03	0.2334 E-5
277.03	-134.29	-15.78	0.3077 E-5
277.77	169.35	-17.68	0.6023 E-5
278.65	36.79	-9.31	0.1965 E-5
279.69	-75.92	0.74	0.3634 E-5
281.06	-71.61	11.08	0.2286 E-5
281.73	103.88	-4.28	0.5347 E-5
282.21	35.24	-2.86	0.7671 E-5
282.82	-87.06	-5.26	0.5426 E-5
283.32	-40.73	-8.96	0.3548 E-5
283.92	36.47	-5.45	0.2603 E-5
284.54	-27.46	-5.29	0.1903 E-5
285.27	37.00	-27.47	0.9356 E-6
286.17	-54.40	34.91	0.1466 E-5
286.62	-114.84	-2.39	0.5767 E-5
287.13	175.08	-1.11	0.4377 E-5
287.57	172.02	4.80	0.9397 E-5
288.40	23.10	10.87	0.4489 E-5
290.63	-125.40	-36.20	0.1221 E-5
291.10	-34.57	-12.26	0.2990 E-5
291.67	37.29	-7.48	0.1681 E-5
292.09	-90.20	37.44	0.1097 E-5
292.89	159.39	16.11	0.2984 E-5
293.12	-9.91	1.68	0.4774 E-5

Appendix B. (Continued).

Sub-bottom depth (m)	Declination (°)	Inclination (°)	Intensity (G)
----------------------	-----------------	-----------------	---------------

Hole 573B (Cont.)

293.69	162.76	15.20	0.3546 E-5
296.11	-131.53	2.90	0.1730 E-5
300.35	-73.17	26.28	0.7788 E-6
301.70	169.34	1.56	0.2245 E-5
302.44	-110.61	-6.75	0.3257 E-5
303.05	1.45	-13.76	0.1619 E-5
303.62	-54.66	3.74	0.2483 E-5
304.06	-81.02	-4.04	0.2845 E-5
309.66	91.88	24.74	0.1601 E-5
310.13	85.09	41.56	0.2700 E-5
312.34	-25.76	-20.87	0.1287 E-5
312.65	-26.14	6.13	0.3160 E-5
319.31	72.29	-5.06	0.3639 E-5
319.75	-15.43	11.99	0.1200 E-4
320.21	-107.50	-20.09	0.3259 E-5
320.73	-154.99	14.37	0.1337 E-4
321.18	178.93	7.22	0.9509 E-5
321.67	-40.87	6.66	0.1291 E-5
322.28	-149.77	-4.70	0.1373 E-4
322.61	88.39	-10.42	0.6825 E-5
324.73	-110.58	-7.28	0.1464 E-4
325.19	147.45	-10.71	0.9675 E-5
325.93	-121.45	18.05	0.2280 E-5
326.76	159.89	24.15	0.1566 E-4
327.83	26.56	12.56	0.8943 E-4
328.10	-147.20	6.68	0.9576 E-5
328.62	14.25	4.48	0.1614 E-4
329.52	50.84	-3.84	0.2894 E-4
329.95	-61.68	2.59	0.2324 E-4
330.05	128.47	-3.28	0.5178 E-5
331.74	40.22	2.22	0.5733 E-5
332.64	-125.41	-29.77	0.1772 E-5
338.06	-70.58	-10.66	0.4178 E-5
338.58	-51.32	-11.75	0.8574 E-5
339.56	-134.77	-10.71	0.1148 E-4
340.58	-160.80	-9.96	0.6950 E-5
342.61	-101.35	3.46	0.1970 E-4
343.11	-98.33	-5.13	0.9847 E-5
348.75	104.53	1.69	0.6326 E-5
350.81	-146.67	-23.11	0.6124 E-5
352.54	-171.57	-38.14	0.2393 E-5
357.23	35.25	-55.40	0.3830 E-6
357.81	-133.69	-15.61	0.1155 E-4
358.86	-116.82	-29.49	0.5531 E-5
359.87	8.59	-68.75	0.1017 E-5
360.29	-145.86	-28.99	0.2135 E-5
360.64	-46.90	-1.57	0.7405 E-5
361.36	-53.66	-12.91	0.2598 E-5
361.54	74.01	-28.51	0.1542 E-5
366.69	-94.48	-17.81	0.2459 E-5
367.29	104.72	2.06	0.3896 E-5
367.65	6.12	-45.35	0.7391 E-6
377.66	-127.01	23.13	0.8867 E-6
378.06	-122.70	1.47	0.3539 E-5
378.55	-36.81	9.35	0.8119 E-5
379.12	2.85	-1.35	0.1317 E-5
379.88	-15.36	-14.50	0.9022 E-6
380.21	-171.80	19.88	0.7166 E-6
380.64	56.45	-17.48	0.5820 E-5
381.50	12.81	-43.76	0.2222 E-6
382.23	135.31	-15.02	0.4045 E-5
383.05	5.73	-23.06	0.8870 E-6
385.66	-98.72	-17.65	0.5337 E-6
386.25	-127.45	-20.58	0.6318 E-5
386.88	-7.57	-18.02	0.1104 E-5
387.53	129.43	9.31	0.4779 E-6
388.03	-6.74	-12.52	0.1541 E-5
388.57	-82.63	-24.86	0.9358 E-6
389.07	-20.34	-16.57	0.4100 E-6
389.77	22.88	-23.60	0.1440 E-5
390.47	-153.11	-15.11	0.5431 E-6
390.98	14.63	-2.53	0.1817 E-5

Appendix B. (Continued).

Sub-bottom depth (m)	Declination (°)	Inclination (°)	Intensity (G)
----------------------	-----------------	-----------------	---------------

Hole 573B (Cont.)

391.46	71.43	14.77	0.1064 E-5
391.92	-35.39	-3.71	0.7785 E-6
396.34	-26.35	-17.69	0.3195 E-5
396.99	0.36	-12.71	0.1076 E-5
398.75	-19.46	3.32	0.5444 E-6
399.24	12.90	18.20	0.2169 E-5
404.57	102.67	10.02	0.3522 E-5
404.98	-121.21	30.19	0.6779 E-6
405.73	105.01	-59.02	0.6213 E-6
406.29	8.36	-13.91	0.2309 E-5
406.86	13.34	2.93	0.1580 E-5
407.43	-108.95	13.77	0.6658 E-6
408.36	12.57	-10.04	0.6624 E-6
408.61	2.04	-6.00	0.3624 E-6
409.19	-20.50	-34.89	0.5770 E-6
410.01	-11.80	-5.94	0.5892 E-6
410.91	16.57	-21.89	0.6050 E-6
411.23	17.62	-14.97	0.7586 E-6
414.33	-14.49	-31.00	0.6793 E-6
415.25	4.45	-33.34	0.4999 E-6
418.28	-32.64	1.81	0.4464 E-6
418.79	11.05	-35.19	0.5381 E-6
424.07	175.16	23.15	0.1697 E-5
424.64	71.38	-37.83	0.3329 E-6
425.45	-146.19	-20.66	0.5830 E-6
433.25	-29.70	-32.21	0.5071 E-6
434.30	2.04	-49.06	0.4829 E-6
435.07	-21.80	-15.24	0.1427 E-5
435.48	-2.84	-13.51	0.9517 E-6
435.80	-23.32	-21.05	0.4468 E-6
436.06	5.14	-37.47	0.6220 E-6
436.57	13.63	-23.41	0.3267 E-6
442.74	52.58	-10.44	0.7661 E-6
447.69	-65.33	8.87	0.6548 E-6
452.15	24.65	-21.61	0.6318 E-6
452.55	66.18	-12.20	0.8267 E-6
453.36	39.78	13.17	0.2101 E-5
453.63	-29.45	12.52	0.1961 E-5
453.97	22.36	-12.31	0.2094 E-5
461.69	-32.23	-27.03	0.8095 E-6
462.51	-4.80	-2.12	0.4820 E-6
463.53	-29.01	-1.70	0.6072 E-6
464.96	-27.17	-61.94	0.8356 E-6
465.59	-3.83	-47.50	0.1450 E-5
466.12	-14.14	-48.15	0.9443 E-6
466.51	5.19	-39.94	0.1039 E-5
467.01	1.05	-36.00	0.6648 E-6
467.61	-18.21	-31.69	0.9446 E-6
468.43	-31.19	34.48	0.8813 E-6
471.27	-34.38	19.41	0.9195 E-6
471.70	-5.71	28.11	0.9408 E-6
472.30	-11.41	-36.00	0.1291 E-5
473.96	-19.03	-37.41	0.1375 E-5
474.03	-35.68	-39.57	0.1206 E-5
480.62	-23.28	1.75	0.4327 E-6
490.14	-161.24	7.57	0.1907 E-5
492.43	-28.98	4.98	0.7220 E-6
494.02	-21.97	-8.18	0.7251 E-6
499.77	-152.15	-15.96	0.5986 E-5
501.14	-108.37	-3.21	0.1513 E-5
502.02	-32.39	8.87	0.9539 E-5
502.85	-39.21	15.21	0.2282 E-5
503.37	-79.10	11.46	0.1810 E-4
503.58	-102.37	14.02	0.1488 E-4
510.24	61.41	14.09	0.2007 E-4
520.63	-110.70	1.02	0.1584 E-4
521.07	-112.64	2.11	0.1954 E-4
521.47	-112.67	-1.46	0.1341 E-4
521.91	-111.50	4.88	0.1761 E-4
522.37	-40.59	6.42	0.2150 E-4
523.65	-89.88	-0.25	0.8600 E-4
526.06	-114.01	-13.11	0.3485 E-3

Appendix B. (Continued).

Sub-bottom depth (m)	Declination (°)	Inclination (°)	Intensity (G)
----------------------	-----------------	-----------------	---------------

Hole 573B (Cont.)

526.35	-139.06	-47.52	0.6530 E-4
526.55	179.56	10.27	0.2383 E-4
527.00	-128.69	-1.69	0.1553 E-4

Hole 574

93.34	15.74	5.72	0.1262 E-5
96.39	16.33	10.50	0.1451 E-5
100.22	8.63	3.83	0.1533 E-5
101.74	6.54	-1.58	0.1547 E-5
103.79	10.15	-7.07	0.1410 E-5
110.69	11.50	4.71	0.1534 E-5
113.86	8.98	-13.74	0.8777 E-6
115.96	10.66	2.42	0.1459 E-5
117.16	11.24	1.57	0.1482 E-5
121.02	7.91	4.56	0.1419 E-5
127.71	12.05	11.96	0.1402 E-5
127.96	9.52	11.38	0.1352 E-5
128.26	-5.33	8.55	0.1327 E-5
128.48	9.91	-2.16	0.1145 E-5
128.91	11.32	0.52	0.1216 E-5
129.40	-12.44	6.81	0.1391 E-5
129.98	75.68	0.99	0.5927 E-6
130.40	51.12	-13.05	0.4902 E-6
130.90	10.50	1.62	0.1269 E-5
131.48	10.91	13.06	0.1313 E-5
131.90	43.68	-7.80	0.3600 E-6
133.54	52.54	-41.28	0.8282 E-6
135.04	20.80	6.69	0.1650 E-5
136.54	18.67	-16.38	0.1537 E-5
138.54	20.72	2.04	0.1580 E-5
140.04	28.60	-1.38	0.1246 E-5
141.54	21.22	-1.05	0.1569 E-5
145.01	26.74	-8.48	0.1283 E-6
146.34	30.94	-2.09	0.1590 E-5
148.91	21.38	-5.81	0.1716 E-5
150.41	21.95	-3.68	0.1374 E-5
151.91	33.03	7.32	0.1461 E-5
153.81	52.13	-6.86	0.1003 E-5
155.31	26.84	-8.26	0.1368 E-5
156.81	30.68	8.71	0.1570 E-5
158.81	54.74	-37.27	0.1014 E-5
160.31	55.51	-35.46	0.9009 E-6
161.81	61.59	-42.07	0.7480 E-6
163.81	50.98	-27.94	0.8071 E-6
165.31	78.09	-27.78	0.6284 E-6
166.66	60.62	-38.43	0.8329 E-6
166.81	69.09	-39.44	0.8563 E-6
168.81	59.61	-28.17	0.7275 E-6
170.31	66.36	-40.39	0.8703 E-6
171.81	79.49	-35.24	0.7439 E-6
173.35	47.42	-28.84	0.1023 E-5
175.16	65.70	-35.96	0.8586 E-6
179.88	44.65	-41.10	0.8922 E-6
183.24	48.12	-41.15	0.8318 E-6
183.77	49.38	-36.07	0.9404 E-6
184.63	-116.99	17.83	0.2612 E-5
185.66	-16.54	-2.83	0.9616 E-6
187.35	-43.85	-28.84	0.1156 E-5
188.85	-34.53	-23.40	0.8712 E-6
193.74	7.48	7.14	0.1429 E-5
196.83	15.04	-10.59	0.8767 E-6
197.02	119.67	-41.13	0.4188 E-6
199.64	-37.39	-13.28	0.2298 E-5
199.85	51.17	-8.44	0.2696 E-5
200.05	49.67	-8.47	0.2832 E-5
200.32	46.45	9.63	0.1254 E-5
200.50	87.35	-0.38	0.4257 E-4
200.86	38.04	7.48	0.1288 E-5
201.16	52.76	17.87	0.1883 E-5
201.36	-58.98	-13.46	0.3352 E-5
201.56	-97.02	-0.05	0.1598 E-4
201.77	-110.41	-3.22	0.2250 E-4
201.98	-71.31	19.98	0.1186 E-4

Appendix B. (Continued).

Sub-bottom depth (m)	Declination (°)	Inclination (°)	Intensity (G)
----------------------	-----------------	-----------------	---------------

Hole 574 (Cont.)

202.53	128.58	-24.90	0.6949 E-5
202.76	137.30	9.33	0.1053 E-4
203.06	122.50	-11.86	0.6840 E-5
203.36	117.13	10.45	0.5108 E-5
203.66	79.40	-11.10	0.3030 E-5
204.03	97.01	-15.92	0.1374 E-4
204.26	87.75	-7.32	0.9311 E-5
204.56	78.33	15.84	0.1846 E-4
205.16	41.16	9.38	0.2323 E-5
205.53	4.90	-14.65	0.1995 E-5
205.76	10.50	-41.27	0.2302 E-5
206.06	15.46	-53.03	0.2849 E-5
206.36	31.17	-55.06	0.6456 E-5
206.48	32.42	-53.28	0.4737 E-5

Hole 574A

96.26	57.22	19.11	0.1344 E-5
99.26	2.57	25.44	0.3752 E-6
102.96	11.36	15.44	0.2959 E-6
104.65	3.37	-13.70	0.3964 E-6
106.15	0.10	-14.01	0.1102 E-5
112.25	-27.76	16.08	0.8613 E-6
116.04	-13.75	18.23	0.1077 E-5
122.71	66.28	67.55	0.8800 E-6
125.44	5.50	16.16	0.8511 E-6
128.34	21.48	8.02	0.8496 E-6
132.03	34.39	9.02	0.1317 E-5
135.69	37.87	23.39	0.1267 E-5
140.15	31.75	21.00	0.1223 E-5
141.89	16.96	26.89	0.1232 E-5
144.02	64.65	0.00	0.1219 E-5
149.87	3.28	24.47	0.1346 E-5
150.27	16.27	8.68	0.1146 E-5
150.71	15.70	6.90	0.1248 E-5
150.98	21.93	17.60	0.1424 E-5
151.37	24.16	14.25	0.1682 E-5
151.77	45.03	-34.33	0.1335 E-5
163.27	59.35	-28.65	0.1173 E-5
164.77	-5.12	-19.41	0.8764 E-6
166.29	60.75	-30.69	0.1191 E-5
167.80	48.41	-28.92	0.1368 E-5
169.30	51.77	-25.34	0.1315 E-5
170.80	64.21	-33.14	0.1182 E-5
173.21	53.88	-18.97	0.8601 E-6
174.71	50.05	-34.16	0.1202 E-5
176.21	-89.00	-0.61	0.2962 E-4
177.71	45.59	1.14	0.1392 E-5
179.21	39.35	-15.31	0.1620 E-5
180.05	41.46	-4.99	0.1458 E-5

Hole 574B

186.21	43.34	-5.10	0.1609 E-5
187.76	41.93	13.73	0.1428 E-5
189.11	24.59	0.60	0.2102 E-5
190.59	40.12	3.67	0.1511 E-5
192.22	51.53	1.62	0.1694 E-5
193.71	41.94	10.06	0.1368 E-5

Hole 574C

195.18	60.55	-47.36	0.8097 E-6
196.48	60.42	-43.81	0.8281 E-6
197.06	59.90	-51.40	0.1160 E-5
197.84	55.94	-37.40	0.1028 E-5
198.12	49.85	-45.53	0.9664 E-6
198.43	53.28	-65.64	0.9683 E-6
198.83	113.16	-53.32	0.7672 E-6
199.21	117.42	-35.87	0.1927 E-5
199.61	-129.81	-46.78	0.1616 E-5
199.93	143.11	-60.74	0.5775 E-6
201.61	-100.36	-7.76	0.1163 E-4
201.91	-87.73	-19.54	0.1750 E-4

Appendix B. (Continued).

Sub-bottom depth (m)	Declination (°)	Inclination (°)	Intensity (G)
Hole 574C (Cont.)			
202.05	52.20	-11.79	0.1599 E-4
204.07	-66.66	-16.84	0.1311 E-4
204.80	127.55	-14.10	0.1285 E-4
205.89	66.55	19.15	0.1796 E-4
206.80	37.74	-8.74	0.2284 E-4
208.28	55.26	-47.60	0.9504 E-6
210.39	30.91	-85.21	0.1353 E-5
210.78	101.92	13.53	0.4225 E-5
210.98	97.06	6.03	0.1121 E-4
211.28	124.61	-8.36	0.1525 E-4
211.74	42.01	-7.62	0.1055 E-4
212.05	83.59	1.37	0.2425 E-4
212.40	79.06	10.21	0.3348 E-4
213.16	-137.98	-0.20	0.1528 E-4
216.70	-0.01	-52.32	0.1026 E-5
217.14	28.65	-37.64	0.1986 E-5
217.56	-0.72	-7.82	0.1356 E-4
217.76	-5.81	11.17	0.5048 E-6
218.31	13.34	-70.21	0.1746 E-5
218.61	-154.22	-19.59	0.3892 E-5
223.14	24.59	-0.34	0.1511 E-5
223.93	173.44	5.07	0.2008 E-5
224.31	-0.45	-1.56	0.2345 E-5
224.58	-77.21	-1.41	0.1626 E-5
224.91	114.23	-26.87	0.1224 E-5
225.14	155.20	-20.41	0.3134 E-5
225.43	-65.60	-30.80	0.2426 E-5
225.81	126.05	3.60	0.7823 E-5
226.14	-73.97	-31.49	0.2212 E-5
226.55	119.82	-3.79	0.2855 E-6
232.64	61.59	-23.97	0.3427 E-6
233.11	106.10	-26.34	0.8366 E-6
233.84	45.86	37.80	0.2831 E-6
234.31	-24.30	27.01	0.4259 E-6
234.61	100.40	-9.90	0.8560 E-6
234.90	29.76	39.02	0.5207 E-6
236.86	-93.76	-6.29	0.7998 E-6
237.11	-90.95	0.55	0.4208 E-4
252.29	53.06	-9.47	0.2306 E-6
258.23	70.21	-12.73	0.8032 E-6
261.29	48.24	-46.37	0.1080 E-5
263.12	59.15	-57.03	0.1080 E-5
264.04	48.41	-49.88	0.7906 E-6
271.74	171.81	-10.20	0.1638 E-6
273.35	26.71	-55.26	0.1007 E-5
274.37	51.37	-45.97	0.1076 E-5
280.21	-10.02	-43.03	0.9234 E-6
282.90	25.60	8.09	0.1345 E-5
282.93	3.35	-15.88	0.9385 E-6
284.02	41.75	-1.98	0.1350 E-5
285.67	43.39	7.14	0.1399 E-5
286.31	33.27	4.77	0.1507 E-5
287.29	32.28	-11.16	0.1435 E-5
287.68	29.46	11.76	0.1506 E-5
288.62	33.36	0.42	0.1413 E-5
290.71	18.58	25.87	0.5799 E-6
291.59	40.41	7.46	0.1562 E-5
292.80	42.25	1.37	0.1388 E-5
293.71	27.54	-15.39	0.1552 E-5
299.17	38.47	12.85	0.2522 E-5
300.26	29.53	-8.61	0.1313 E-5
301.62	23.97	-18.47	0.1662 E-5
302.52	30.20	-18.77	0.1320 E-5
303.41	27.77	-8.25	0.1290 E-5
303.83	23.93	-21.54	0.1417 E-5
304.63	20.74	-29.43	0.1502 E-5
305.12	35.76	1.54	0.1327 E-5
306.02	29.45	-25.87	0.1597 E-5
307.05	47.30	-14.14	0.1213 E-5
307.75	32.59	8.63	0.1254 E-5
309.06	47.90	14.66	0.1298 E-5
310.41	-5.62	-55.95	0.6842 E-6
311.09	26.45	-34.24	0.9832 E-6
312.04	-5.61	-23.51	0.6033 E-5

Appendix B. (Continued).

Sub-bottom depth (m)	Declination (°)	Inclination (°)	Intensity (G)
Hole 574C (Cont.)			
312.75	2.84	-41.94	0.8577 E-6
313.94	-2.14	-42.67	0.7843 E-6
318.11	-11.98	-45.66	0.8622 E-6
320.17	-19.52	-43.65	0.7608 E-6
320.90	-1.29	-32.89	0.9536 E-6
327.72	5.57	-54.42	0.6613 E-6
333.94	-9.42	-53.42	0.1048 E-5
336.78	-5.70	-34.58	0.7271 E-6
338.25	-164.93	-74.77	0.1213 E-5
339.39	-65.57	-21.21	0.3826 E-5
340.85	14.24	-9.68	0.1965 E-5
346.68	-33.25	-52.19	0.1028 E-5
350.52	46.30	-26.72	0.1337 E-5
351.65	-122.44	-24.31	0.2946 E-5
358.33	0.31	-7.65	0.4370 E-5
366.76	-64.51	-13.82	0.1579 E-5
375.17	153.65	-20.03	0.1403 E-4
375.63	52.62	3.28	0.1632 E-4
376.39	-22.44	24.18	0.4732 E-5
384.57	-1.62	11.65	0.1188 E-5
348.79	-43.67	-5.75	0.1897 E-6
385.01	-15.51	-1.26	0.5421 E-6
385.78	-63.01	-7.23	0.9591 E-6
394.15	-24.26	25.83	0.2262 E-5
395.68	103.04	-48.27	0.5252 E-6
396.23	87.75	-6.61	0.5772 E-5
396.68	-155.64	-22.51	0.2848 E-5
403.64	-38.37	22.28	0.7695 E-5
404.97	3.51	44.37	0.1415 E-5
406.34	-136.99	62.10	0.6916 E-6
408.46	-55.06	43.24	0.1312 E-5
409.92	1.83	13.98	0.1447 E-5
414.95	12.27	12.00	0.1541 E-5
416.52	-22.45	13.95	0.1383 E-5
418.36	-99.63	20.55	0.1317 E-5
422.76	18.26	17.62	0.1684 E-5
423.73	-147.43	-14.83	0.1827 E-5
432.24	-63.79	17.12	0.1981 E-5
432.90	-17.03	9.66	0.4725 E-5
433.27	-10.67	6.39	0.7738 E-5
434.41	-48.50	-3.76	0.2565 E-5
434.86	-62.87	4.55	0.3776 E-5
435.07	-91.93	-27.16	0.8642 E-6
435.78	-167.00	-16.53	0.3390 E-5
441.65	-86.57	3.77	0.1183 E-5
442.40	-61.07	30.56	0.5119 E-5
442.76	109.96	9.53	0.8783 E-5
443.14	7.92	58.99	0.3506 E-6
443.81	85.22	13.28	0.5486 E-5
444.46	71.22	22.28	0.1142 E-4
444.63	-140.18	26.24	0.3159 E-5
445.19	127.89	34.43	0.4085 E-5
445.84	30.72	16.50	0.3527 E-5
446.30	-2.81	-3.84	0.1814 E-5
451.29	-139.49	-16.81	0.3040 E-4
460.57	49.47	27.35	0.2052 E-4
461.24	-169.78	-2.94	0.1708 E-4
461.73	80.28	6.84	0.1323 E-4
462.11	127.51	13.31	0.8898 E-5
462.71	21.12	10.28	0.6760 E-5
463.29	-64.44	23.81	0.1332 E-4
463.68	178.52	22.96	0.2193 E-5
464.28	-24.65	31.18	0.1195 E-5
464.92	-20.61	16.86	0.1578 E-5
470.06	-52.13	7.79	0.8996 E-6
470.40	22.56	8.73	0.2109 E-5
470.77	-85.33	-10.21	0.1322 E-5
479.63	-75.18	-29.90	0.4698 E-6
480.03	98.18	-5.03	0.1753 E-5
480.28	-7.03	-14.33	0.5751 E-6
480.61	-10.33	15.17	0.1388 E-5
481.13	-6.61	10.35	0.1724 E-5
481.53	-13.12	-6.16	0.1059 E-5
481.86	-37.98	-21.11	0.6720 E-6

Appendix B. (Continued).

Sub-bottom depth (m)	Declination (°)	Inclination (°)	Intensity (G)
----------------------	-----------------	-----------------	---------------

Hole 574C (Cont.)

482.13	-18.59	8.83	0.8269 E-6
482.86	-22.85	3.41	0.2190 E-5
489.07	-5.24	-14.83	0.5807 E-6
490.17	-9.85	-10.53	0.1276 E-5
490.84	-5.15	16.89	0.1506 E-5
491.20	-6.34	-3.81	0.8450 E-6
491.41	-16.22	-7.91	0.1172 E-5
491.86	-51.99	-4.37	0.4625 E-6
492.64	-6.45	-0.41	0.2556 E-5
498.57	-32.06	22.74	0.8648 E-6
498.77	-2.99	-1.98	0.1185 E-5
499.05	-1.33	23.09	0.9921 E-6
499.54	-38.40	15.09	0.8277 E-6
499.97	-8.78	25.79	0.1269 E-5
500.23	-11.81	24.94	0.6042 E-6
500.60	-30.62	27.16	0.7612 E-6
500.99	-51.21	38.99	0.6702 E-6
501.37	13.20	-30.67	0.8634 E-6
501.70	-17.76	-0.08	0.1623 E-5
502.19	-28.28	1.53	0.5164 E-6
502.72	-90.72	6.35	0.1302 E-5
503.16	-76.54	19.96	0.1533 E-5
503.40	-0.47	10.48	0.2513 E-5
503.93	-14.59	15.38	0.4226 E-5
504.40	121.50	66.10	0.4311 E-4
504.77	-108.40	-13.90	0.7935 E-4
505.05	101.60	-65.70	0.4581 E-4
505.23	-133.10	-63.80	0.7238 E-4
505.92	-103.20	-22.40	0.5667 E-4
508.40	96.80	-07.00	0.7053 E-4
508.72	101.70	37.30	0.3732 E-4
509.05	-104.90	-04.60	0.1367 E-4
509.39	-92.80	-48.70	0.5195 E-4
509.76	98.00	24.30	0.1961 E-4
510.30	0.98	8.18	0.2011 E-4
510.61	-154.19	26.19	0.1264 E-4
517.57	78.00	63.20	0.8394 E-4
518.48	69.10	53.60	0.8369 E-4
518.77	93.50	55.70	0.7338 E-4
519.52	-077.20	-37.40	0.2965 E-5
520.00	-085.40	-21.60	0.4318 E-4

Hole 575

35.31	-132.23	-40.33	0.3275 E-5
35.91	30.01	1.64	0.7878 E-6
36.38	30.57	-33.43	0.2323 E-5
36.81	6.00	-13.37	0.4402 E-5
37.39	44.58	-72.20	0.5699 E-6
37.88	16.75	-18.17	0.2509 E-5
38.31	123.23	-75.13	0.7707 E-6
38.81	35.06	-16.40	0.4074 E-5
39.38	15.85	-17.24	0.5058 E-5
39.81	29.11	-4.70	0.5978 E-5
40.31	15.28	6.54	0.1040 E-4
41.31	-165.24	4.31	0.8456 E-5
41.81	-171.23	-1.21	0.6947 E-5
42.38	0.68	-5.84	0.5870 E-5
42.81	0.45	0.60	0.4508 E-5
43.31	5.14	-14.79	0.2149 E-5
43.88	168.28	-2.33	0.4982 E-5
44.31	-174.24	1.96	0.3889 E-5
44.81	65.25	-38.57	0.1766 E-5
45.31	68.29	-1.37	0.1177 E-5
45.88	145.21	-8.08	0.2724 E-5
46.31	90.55	-7.71	0.2369 E-5
46.81	82.22	-13.13	0.1981 E-5
47.38	68.71	-19.75	0.1242 E-5
47.81	-13.25	-28.74	0.8124 E-6
48.31	-1.18	-20.98	0.6653 E-6
48.88	-9.99	-33.96	0.7818 E-6
49.25	1.15	-32.17	0.8997 E-6
49.74	23.17	-39.85	0.4713 E-6
50.38	27.19	-59.34	0.1331 E-5

Appendix B. (Continued).

Sub-bottom depth (m)	Declination (°)	Inclination (°)	Intensity (G)
----------------------	-----------------	-----------------	---------------

Hole 575 (Cont.)

50.81		1.89	-23.08	0.4949 E-6	
51.31		19.28	-45.25	0.6055 E-6	
51.88		-14.80	-21.33	0.8629 E-6	
52.31		-8.19	-15.71	0.6173 E-6	
52.81		2.93	-52.25	0.4420 E-6	
53.38		21.92	-12.56	0.5383 E-6	
53.81		27.90	-31.70	0.5439 E-6	
54.31		23.53	-10.51	0.5020 E-6	
54.81		-12.35	-23.90	0.9652 E-6	
55.31		0.29	-39.52	0.9079 E-6	
55.81		-9.21	-36.53	0.9259 E-6	
56.31		-23.30	-22.30	0.1030 E-5	
57.31		-8.86	-20.84	0.7780 E-6	
57.81		-6.62	-12.77	0.8860 E-6	
58.31		-12.70	-31.21	0.6390 E-6	
58.81		-25.28	-8.84	0.5837 E-6	
59.31		-147.25	-68.27	0.3380 E-6	
59.81		-14.78	-25.54	0.5255 E-6	
60.31		15.64	10.33	0.6936 E-6	
60.81		-12.53	-16.07	0.6049 E-6	
61.31		-27.53	-35.50	0.4338 E-6	
61.81		-52.16	-40.55	0.3788 E-6	
62.31		-15.23	-2.99	0.6925 E-6	
62.81		-25.07	-18.11	0.9862 E-6	
63.31		-13.40	-33.70	0.7146 E-6	
63.81		-47.45	-11.13	0.1023 E-5	
64.31		-61.65	-6.77	0.5349 E-6	
64.81		-50.61	-17.31	0.8744 E-6	
65.31		-146.23	-8.01	0.3055 E-5	
65.81		30.21	-15.42	0.4612 E-6	
66.31		-13.40	-33.70	0.7146 E-6	
67.31		-167.56	12.88	0.1068 E-4	
67.81		55.09	7.18	0.3255 E-5	
68.31		58.85	1.60	0.2543 E-4	
68.81		52.10	-5.54	0.3630 E-5	
69.31		68.71	-0.51	0.4731 E-5	
69.81		-117.90	-35.53	0.7902 E-5	
70.31		171.22	-25.81	0.4558 E-5	
70.81		4.01	-11.51	0.9678 E-6	
71.31		-30.33	-41.84	0.3782 E-6	
71.81		-26.42	-34.29	0.5776 E-6	
72.31		86.51	-2.19	0.3996 E-6	
72.81		-19.90	-26.83	0.5451 E-6	
73.31		87.06	-18.76	0.5183 E-6	
73.81		87.49	-12.94		
74.31		94.13	-44.97	0.4593 E-5	
74.81		75.96	83.77	-22.12	0.4000 E-5
75.31		76.11	73.25	-2.26	0.3183 E-5
75.81		76.71	-93.09	-12.89	0.7775 E-5
76.31		77.06	-103.64	-5.71	0.6628 E-5
76.81		77.46	-75.88	-37.91	0.1364 E-5
77.31		78.01	55.09	7.18	0.3255 E-5
77.81		78.56	58.85	1.60	0.2543 E-4
78.31		78.96	52.10	-5.54	0.3630 E-5
78.81		79.30	68.71	-0.51	0.4731 E-5
79.31		79.93	-117.90	-35.53	0.7902 E-5
79.81		84.51	171.22	-25.81	0.4558 E-5
80.31		85.01	4.01	-11.51	0.9678 E-6
80.81		85.62	-30.33	-41.84	0.3782 E-6
81.31		85.99	-26.42	-34.29	0.5776 E-6
81.81		86.51	-26.55	-2.19	0.3996 E-6
82.31		87.06	-19.90	-26.83	0.5451 E-6
82.81		87.49	-12.94	-18.76	0.5183 E-6
83.31		94.09	46.91	-14.27	0.4029 E-5
83.81		94.49	50.13	-3.48	0.9490 E-5
84.31		95.09	56.08	2.89	0.6587 E-5
84.81		95.59	62.36	-5.36	0.8648 E-5
85.31		95.99	-97.36	-19.58	0.6722 E-5
85.81		96.59	-102.62	-3.36	0.6496 E-5
86.31		97.09	-86.56	35.92	0.7884 E-5
86.81		97.49	60.58	21.11	0.1183 E-4
87.31		98.09	71.76	1.55	0.3652 E-4
87.81		98.99	4.54	-3.42	0.1298 E-4
88.31		99.39	28.45	1.57	0.3044 E-5
88.81		99.99	-166.22	-20.38	0.9745 E-5

Appendix B. (Continued).

Sub-bottom depth (m)	Declination (°)	Inclination (°)	Intensity (G)
----------------------------	--------------------	--------------------	------------------

Hole 575A (Cont.)

100.49	-164.99	-3.88	0.1021 E-4
100.89	-163.03	-13.43	0.2448 E-4
101.49	-163.62	3.98	0.5921 E-5
101.99	5.40	16.31	0.2991 E-5
102.39	137.23	-25.54	0.2033 E-5
102.89	6.25	8.22	0.1458 E-4
103.29	7.11	-1.49	0.2232 E-4
103.89	3.44	3.39	0.1986 E-4
104.39	3.63	2.60	0.8409 E-5
104.79	-5.49	-3.87	0.6198 E-5
105.87	-25.75	-19.98	0.7246 E-5
106.49	-20.50	-3.84	0.6080 E-5
106.99	-30.44	2.43	0.1126 E-4
107.39	-21.15	-20.45	0.4619 E-5
107.99	-19.55	-33.84	0.4231 E-5
108.54	-24.50	-4.23	0.2497 E-4
108.89	-24.33	-0.43	0.8369 E-5
109.49	-18.87	-0.17	0.6972 E-5
110.79	-164.29	-3.49	0.1832 E-4
111.19	-154.46	-16.78	0.3999 E-5
111.79	-126.48	-18.25	0.2192 E-5
112.29	-169.33	14.68	0.5741 E-5
112.69	177.97	-2.64	0.2623 E-4
113.29	153.35	-69.57	0.4002 E-5
113.87	-26.07	-23.92	0.7485 E-5
114.39	142.97	-10.88	0.1279 E-4
114.79	-44.85	11.02	0.1783 E-4
115.39	-42.33	2.94	0.1678 E-4
115.89	-48.54	8.38	0.8713 E-5
116.29	-20.22	42.01	0.1532 E-4
116.89	-47.25	0.97	0.9641 E-5
117.39	-39.11	12.09	0.2598 E-5
117.79	-48.58	-9.06	0.5359 E-5
118.39	131.96	1.61	0.5687 E-5
118.89	119.40	-25.28	0.3092 E-5
119.17	133.43	-26.52	0.3820 E-5
119.69	136.97	0.21	0.9366 E-5
120.19	173.42	2.25	0.4720 E-5
120.59	147.86	3.93	0.1153 E-4
121.19	166.54	-12.30	0.1347 E-5
121.69	144.69	-6.23	0.5368 E-5
122.09	135.63	-28.00	0.1082 E-4
122.69	138.85	-0.81	0.1277 E-4
123.19	138.02	4.02	0.1580 E-4
123.39	-77.57	-34.25	0.6874 E-5
123.79	-70.72	-19.20	0.6944 E-5
124.39	-70.40	-18.80	0.2046 E-5
124.89	-84.47	-6.00	0.7238 E-5
125.29	-66.81	-36.58	0.3555 E-5
125.89	94.03	4.88	0.3131 E-5
126.59	-7.00	-62.15	0.5840 E-5
127.09	-34.14	-21.30	0.1440 E-5
127.49	-33.97	-3.81	0.1026 E-4
128.03	-31.33	-18.84	0.4055 E-5
128.21	-35.19	19.16	0.1060 E-4
128.66	122.84	-17.65	0.4536 E-6
129.11	132.28	-81.47	0.1043 E-5
129.54	140.63	6.25	0.2655 E-5
130.11	-92.24	0.52	0.4117 E-4
130.61	125.30	-32.15	0.5678 E-6
131.04	12.80	-31.12	0.4453 E-6
131.61	28.53	-60.73	0.4245 E-6
132.26	-14.25	-15.57	0.3794 E-6
132.76	-9.03	-29.52	0.9063 E-6
133.26	-17.55	-20.18	0.6959 E-6
133.76	-89.93	1.77	0.4232 E-4
134.76	-17.57	-28.50	0.6724 E-6
135.42	-22.97	-67.61	0.9312 E-6
135.80	8.91	-8.42	0.1559 E-5
136.41	87.80	-1.30	0.4177 E-4
136.73	-16.90	-31.54	0.6977 E-6
137.31	64.47	-54.39	0.1251 E-5
137.91	-90.20	0.37	0.4224 E-4
138.26	-18.09	-23.70	0.6456 E-6

Appendix B. (Continued).

Sub-bottom depth (m)	Declination (°)	Inclination (°)	Intensity (G)
----------------------------	--------------------	--------------------	------------------

Hole 575A (Cont.)

139.01	6.11	-45.89	0.6391 E-6
139.95	-46.26	-6.20	0.2427 E-5
140.46	-25.90	-28.55	0.8430 E-6
141.04	-30.42	-40.59	0.9949 E-6
141.44	-24.37	-33.18	0.6581 E-6
141.96	-14.63	-38.48	0.7713 E-6
142.71	-131.56	-5.92	0.5062 E-5
143.20	-15.68	-31.65	0.8875 E-6
143.71	-17.00	-13.29	0.8446 E-6
144.26	-30.83	-69.62	0.1275 E-5
144.86	-8.15	-18.29	0.6746 E-6
145.16	-16.56	-9.83	0.5855 E-6
145.61	-12.11	-16.73	0.6973 E-6
145.76	126.20	-31.37	0.2952 E-7
146.06	35.00	-5.66	0.1235 E-5
147.11	-7.89	-21.31	0.1222 E-5
147.66	-13.20	-17.08	0.6800 E-6
148.01	-10.93	-37.50	0.1335 E-5
149.81	-5.64	-37.66	0.4633 E-6
150.35	-25.56	-37.34	0.6518 E-6
150.96	0.99	15.91	0.9398 E-6
151.31	-19.04	-20.17	0.7237 E-6
151.71	-16.26	-22.43	0.8365 E-6
152.06	-15.51	-31.34	0.6051 E-6
152.46	-9.02	-33.64	0.6866 E-6
152.96	-11.91	-29.47	0.7326 E-6
153.16	-5.81	-25.20	0.7660 E-6
153.51	-12.97	-26.34	0.7771 E-6
153.96	-10.34	-39.50	0.8570 E-6
154.31	-30.10	-40.18	0.8498 E-6
154.86	-14.95	-18.39	0.9572 E-6
155.31	-4.72	-36.31	0.6784 E-6
155.66	-22.36	-34.28	0.5156 E-6
156.06	-22.98	-23.17	0.9095 E-6
156.46	-10.22	-42.70	0.7463 E-6
157.31	-21.97	-40.22	0.5130 E-6
157.71	-10.03	-4.24	0.3095 E-6
158.11	54.24	-35.22	0.1181 E-5
158.61	66.83	-48.62	0.1454 E-5
159.16	89.50	-64.41	0.1348 E-5
159.76	17.70	-74.18	0.1455 E-5
160.11	19.43	2.61	0.9537 E-6
160.51	-34.77	-72.29	0.1509 E-5
161.11	42.96	-16.53	0.1177 E-5
161.66	60.39	-70.93	0.1698 E-5
162.26	36.37	-11.38	0.1378 E-5
162.61	27.53	-14.02	0.1531 E-5
163.16	-31.42	-1.02	0.1044 E-5
163.76	-38.36	-12.32	0.4906 E-6
163.96	-9.71	-50.92	0.6072 E-6
164.51	-28.62	-62.75	0.7096 E-6
164.99	11.40	-27.43	0.8673 E-6
165.39	17.43	-34.06	0.6178 E-6
165.99	2.22	-21.21	0.7960 E-6
166.49	12.86	-21.48	0.1490 E-5
166.89	3.33	-30.88	0.1469 E-5
167.49	6.52	-27.04	0.1054 E-5
167.99	-6.19	-55.41	0.1181 E-5
168.39	14.47	-50.37	0.6947 E-6
168.79	-4.35	-44.73	0.5452 E-6
169.39	-8.16	-34.11	0.7868 E-6
169.89	-9.31	-29.47	0.4717 E-6
170.29	-12.21	-36.50	0.8016 E-6
170.89	81.88	-4.26	0.6930 E-5
171.39	-13.43	-41.40	0.6439 E-6
171.79	-12.51	-37.82	0.9849 E-6
172.39	-3.64	-52.40	0.7415 E-6
172.79	-5.10	-41.37	0.9638 E-6
173.39	-7.78	-45.22	0.6168 E-6
174.29	-19.21	-41.25	0.8716 E-6
175.49	-13.88	-70.59	0.5769 E-6
175.99	-39.15	-64.36	0.1071 E-5
176.39	-15.47	-39.26	0.9960 E-6
176.89	-2.89	-38.15	0.7263 E-6

Appendix B. (Continued).

Sub-bottom depth (m)	Declination (°)	Inclination (°)	Intensity (G)
----------------------	-----------------	-----------------	---------------

Hole 575A (Cont.)

177.49	28.18	-44.11	0.7518 E-6
177.89	-18.89	-38.70	0.6630 E-6
178.49	3.44	-49.64	0.6612 E-6
178.99	-1.42	-42.86	0.8350 E-6
179.99	-10.18	-42.37	0.8043 E-6
180.89	-5.95	-69.22	0.8150 E-6
181.49	16.59	-64.68	0.6790 E-6
182.19	-4.05	-59.13	0.8538 E-6
183.69	0.49	-14.23	0.4606 E-6
184.59	-2.61	-19.76	0.4839 E-6
186.19	10.47	-26.50	0.4911 E-6
187.69	6.90	-30.06	0.5668 E-6
188.99	11.86	-45.23	0.8030 E-6
189.99	-3.08	-41.56	0.1133 E-5
193.39	2.70	-41.90	0.7166 E-6
195.79	-9.15	-43.40	0.8092 E-6
198.31	-2.23	-42.84	0.8488 E-6
199.76	-2.90	-40.86	0.7369 E-6
201.52	11.96	-46.23	0.8036 E-6
202.41	-14.28	-49.89	0.8254 E-6
205.01	-3.00	-39.99	0.1015 E-5
205.41	-9.15	-49.72	0.9256 E-6
206.91	9.10	-40.05	0.5588 E-6

Hole 575B

39.51	-79.29	-21.35	0.2461 E-4
39.76	-68.60	-10.73	0.2979 E-4
40.01	-56.86	10.94	0.2714 E-4
40.24	-57.44	-5.41	0.2191 E-4
40.47	-57.02	1.06	0.2174 E-4
40.60	-60.05	-0.64	0.2301 E-4
40.86	-60.88	3.86	0.2307 E-4
41.09	-55.41	3.40	0.2023 E-4
41.36	-55.00	2.12	0.1724 E-4
41.61	-52.92	-5.51	0.1235 E-4
41.86	-75.09	-5.88	0.2153 E-4
42.10	-67.92	-7.98	0.2929 E-4
42.36	-65.75	1.24	0.3816 E-4
42.59	-43.03	-5.58	0.6883 E-5
42.86	-4.82	38.21	0.2249 E-5
43.11	-13.51	40.94	0.2964 E-5
43.36	-14.59	7.86	0.2973 E-5
43.60	112.07	-3.31	0.5084 E-5
43.86	-38.65	4.78	0.1060 E-4
44.09	-23.02	7.86	0.6013 E-5
44.36	-96.49	0.72	0.6921 E-5
44.61	-76.42	-8.74	0.1251 E-4
44.86	-74.93	-5.38	0.3289 E-5
45.10	-46.73	7.09	0.3172 E-5
45.36	-21.72	5.83	0.1885 E-5
45.59	-26.12	9.05	0.2234 E-5
45.86	-3.28	33.20	0.2271 E-5
46.11	106.79	1.05	0.1273 E-5
46.36	100.76	29.05	0.1186 E-5
46.60	69.03	6.34	0.5959 E-6
46.86	-121.47	22.26	0.2994 E-5
47.09	-94.56	18.45	0.3989 E-5
47.36	-73.05	17.69	0.2109 E-5
47.61	-49.99	47.70	0.3226 E-5
47.86	-26.67	23.84	0.1326 E-5
48.46	-24.59	-28.28	0.4139 E-5
48.75	-11.40	-4.03	0.2573 E-5
49.16	-23.53	-6.11	0.4615 E-5
49.46	-9.45	-44.96	0.4950 E-5
49.66	-41.85	-1.12	0.4654 E-5
49.96	-70.19	26.48	0.4693 E-5
50.28	-66.58	21.64	0.3239 E-5
50.56	-56.51	26.60	0.2572 E-5
50.86	53.54	29.52	0.2446 E-5
51.16	-39.21	17.79	0.2284 E-5
51.46	76.65	-17.21	0.1847 E-5
51.78	50.38	-32.39	0.1072 E-5
52.06	70.34	19.41	0.1518 E-5

Appendix B. (Continued).

Sub-bottom depth (m)	Declination (°)	Inclination (°)	Intensity (G)
----------------------	-----------------	-----------------	---------------

Hole 575B (Cont.)

52.36	54.27	37.69	0.2865 E-5
52.66	24.37	29.18	0.1860 E-5
52.96	138.50	36.09	0.3997 E-5
53.28	114.24	73.40	0.6093 E-5
53.56	81.35	20.54	0.4892 E-5
53.86	-52.34	6.56	0.9651 E-5
54.16	-54.80	4.65	0.1058 E-4
54.46	-46.47	28.63	0.1040 E-4
54.78	-4.19	10.10	0.1339 E-5
55.06	74.24	5.10	0.2921 E-5
55.66	4.06	13.41	0.2414 E-5
56.16	107.71	7.33	0.2675 E-5
56.46	-43.31	21.95	0.4141 E-5
56.76	-42.15	9.45	0.1069 E-4
57.16	-30.07	11.20	0.5584 E-5
57.46	-22.08	1.84	0.7635 E-5
57.76	-10.18	2.09	0.2852 E-5
58.06	-6.04	4.77	0.2567 E-5
58.36	2.29	19.29	0.1752 E-5
58.66	-7.70	38.37	0.1918 E-5
58.96	-19.97	5.44	0.2862 E-5
59.26	-0.11	-2.10	0.3586 E-5
59.56	9.13	16.12	0.3122 E-5
59.86	3.15	17.58	0.2341 E-5
60.16	-6.18	31.90	0.2400 E-5
60.46	9.23	20.67	0.2117 E-5
60.76	7.63	31.78	0.2346 E-5
61.06	1.84	-5.88	0.6080 E-6
61.36	-18.70	-2.21	0.6506 E-6
61.66	-1.68	11.85	0.1143 E-5
61.96	-16.55	6.49	0.9023 E-6
62.26	2.11	10.18	0.6143 E-6
62.56	-7.08	6.71	0.7528 E-6
62.86	-10.29	13.27	0.7168 E-6
63.16	-13.77	15.64	0.7226 E-6
63.46	-4.30	8.95	0.7998 E-6
63.76	-4.82	-12.58	0.1221 E-5
64.06	-31.03	-21.57	0.8960 E-6
64.36	0.99	26.70	0.1221 E-5
65.26	-19.54	-14.57	0.7907 E-6
65.56	-37.93	-28.08	0.1174 E-5
65.86	-0.68	-14.25	0.5836 E-6
66.16	-8.36	-12.74	0.1132 E-5
66.46	-2.24	-7.59	0.1100 E-5
66.76	-40.40	-16.08	0.5730 E-6
67.06	-46.99	-22.00	0.9893 E-6
67.36	-28.90	-22.63	0.6940 E-6
67.66	-40.34	-24.20	0.9952 E-6
67.96	-13.94	12.94	0.2398 E-5
68.26	4.68	-7.39	0.5811 E-5
68.56	12.81	-8.67	0.1207 E-4
68.86	-15.38	-31.82	0.5909 E-6
69.16	-36.63	-13.25	0.1825 E-5
69.46	-22.47	1.48	0.9839 E-6
69.76	10.50	-4.56	0.2184 E-5
70.06	7.62	-16.42	0.1160 E-5
70.36	-7.99	-21.01	0.8531 E-6
70.66	-7.14	-17.05	0.1001 E-5
70.96	-6.28	-15.04	0.1307 E-5
71.26	-38.94	-15.48	0.6867 E-6
71.56	-0.90	-0.11	0.7850 E-6
71.96	-9.45	-35.85	0.9126 E-6
72.16	-23.92	4.48	0.5764 E-6
72.46	24.06	12.24	0.4894 E-6
72.76	4.95	28.30	0.4658 E-6
73.06	-20.15	19.87	0.4327 E-6
73.36	-28.56	-30.04	0.8948 E-6
74.06	-90.43	0.17	0.4064 E-4
74.36	-13.37	-15.10	0.7696 E-6
74.66	-29.44	-12.55	0.1080 E-5
74.96	-0.76	0.85	0.1254 E-5
75.26	-13.18	-12.39	0.9283 E-6
75.86	-26.76	-14.11	0.1404 E-5
76.16	-16.21	-18.59	0.1106 E-5

Appendix B. (Continued).

Sub-bottom depth (m)	Declination (°)	Inclination (°)	Intensity (G)
----------------------------	--------------------	--------------------	------------------

Hole 575B (Cont.)

76.46	-10.90	-22.29	0.1367 E-5
76.76	-8.00	-12.59	0.1769 E-5
77.06	-6.46	-21.96	0.1377 E-5
77.36	-13.31	-9.59	0.6332 E-6
77.66	-25.10	-12.18	0.9532 E-6
77.96	-82.82	2.57	0.1424 E-5
78.26	-17.19	-14.61	0.1169 E-5
78.56	1.01	-3.93	0.1600 E-5
78.86	-59.17	-20.35	0.1300 E-5
79.16	-0.80	-7.88	0.1201 E-5
79.46	-21.53	-14.54	0.7287 E-6
79.76	-30.55	-10.79	0.7325 E-6
80.06	-66.67	6.52	0.1545 E-5
80.36	-34.79	-14.49	0.1739 E-5
80.66	-29.33	-0.65	0.1132 E-5
80.96	-10.81	11.35	0.1788 E-5
81.26	-11.71	-13.77	0.9595 E-6
81.56	-14.35	-14.06	0.8809 E-6
81.66	-18.93	-10.93	0.1317 E-5
81.96	-34.99	0.68	0.1219 E-5
82.26	-23.84	13.90	0.1250 E-5
83.16	19.77	-6.70	0.1522 E-5
83.42	-7.59	-10.74	0.8915 E-6
83.76	1.75	-5.61	0.1242 E-5
84.06	3.32	-9.99	0.1252 E-5
84.36	35.49	-0.32	0.1812 E-5
84.66	70.37	3.80	0.7487 E-5
84.96	57.09	4.27	0.2568 E-5
85.26	33.18	15.33	0.1448 E-5
85.56	58.77	2.78	0.2919 E-5
85.86	84.94	6.36	0.2389 E-4
86.16	89.82	1.76	0.3007 E-4
86.46	91.93	-7.88	0.1799 E-4
86.76	84.18	2.16	0.2245 E-4
87.06	-24.97	16.88	0.2725 E-5
87.36	-71.72	9.86	0.9756 E-5
87.66	-40.84	7.16	0.4260 E-5
87.96	83.85	-11.33	0.4756 E-5
88.26	-22.24	25.09	0.5686 E-5
88.56	102.97	57.54	0.3542 E-5
88.86	66.35	-11.05	0.3495 E-5
89.16	32.50	8.77	0.2541 E-5
89.46	-46.89	24.29	0.7547 E-5
89.76	-71.71	45.53	0.6058 E-5
90.06	18.51	19.75	0.1815 E-5
90.36	55.82	5.41	0.6397 E-5
90.66	29.97	2.82	0.5057 E-5
91.16	146.45	-7.14	0.8780 E-5
91.46	145.40	8.99	0.7528 E-5
91.76	76.89	-60.75	0.1491 E-5
92.06	127.81	-17.86	0.5163 E-5
92.36	133.17	-20.26	0.6041 E-5
92.66	157.33	-10.46	0.1373 E-4
92.96	157.63	-4.13	0.9955 E-5
93.26	157.81	-12.11	0.2681 E-5
93.56	155.85	-13.21	0.1977 E-5
93.86	-117.09	-45.19	0.4498 E-5
94.16	-19.78	7.09	0.7326 E-5
94.46	132.45	-6.88	0.5738 E-6
94.76	-9.05	22.01	0.2779 E-5
95.06	-6.60	-64.02	0.1746 E-5
95.36	144.25	19.96	0.2065 E-5
95.66	-0.46	5.15	0.2929 E-5
95.96	-0.74	13.59	0.3015 E-5
96.26	-10.14	11.93	0.1482 E-4
96.56	-6.51	3.07	0.2065 E-4
96.86	-60.01	-55.05	0.6704 E-5

Appendix B. (Continued).

Sub-bottom depth (m)	Declination (°)	Inclination (°)	Intensity (G)
----------------------------	--------------------	--------------------	------------------

Hole 575B (Cont.)

97.16	-176.90	-1.03	0.6099 E-5
97.46	178.33	-10.71	0.9730 E-5
97.76	179.56	-1.30	0.6344 E-5
98.06	86.70	5.50	0.4404 E-6
98.36	-125.74	-52.16	0.5685 E-5
98.96	173.29	39.86	0.8889 E-6
99.26	151.86	32.10	0.1766 E-5
99.86	-17.13	-22.42	0.1027 E-4
100.16	-86.85	-53.50	0.9060 E-6
100.46	-9.43	-7.56	0.1923 E-5
100.76	-40.98	-7.20	0.1272 E-4
101.06	2.43	-17.90	0.1723 E-5
101.36	-52.32	-40.93	0.8013 E-5
101.66	-109.80	-17.03	0.1783 E-5
101.96	-35.92	-3.36	0.1620 E-5
102.26	2.00	4.02	0.8173 E-6
102.56	-1.35	-1.32	0.2005 E-5
102.86	-6.37	-19.62	0.1964 E-5
103.46	-56.46	1.46	0.1908 E-5
103.76	-101.92	-3.87	0.1656 E-5
104.06	-72.82	-15.17	0.2156 E-5
104.36	-1.31	-14.98	0.6102 E-6
104.66	-2.15	-0.92	0.7449 E-6
104.96	-50.93	-13.78	0.1806 E-5
105.26	-4.52	-12.01	0.1153 E-5
105.56	-63.75	-30.20	0.1696 E-5
105.86	-2.15	-18.88	0.1801 E-5
106.16	-28.52	-20.47	0.4574 E-5
106.46	43.37	-11.14	0.8331 E-5
106.76	25.25	-14.07	0.4791 E-5
107.06	-53.15	-28.19	0.3274 E-5
107.36	-5.72	-18.47	0.9945 E-6
107.66	-9.07	6.60	0.1371 E-5
108.26	-17.97	-19.47	0.1213 E-4
108.86	-42.15	19.83	0.3178 E-4
109.46	-80.07	2.60	0.3019 E-4
109.76	-76.33	-18.74	0.2381 E-4
110.06	-57.28	13.37	0.6019 E-5
110.36	-91.20	-19.19	0.9835 E-5
110.66	-98.53	-10.65	0.6354 E-5
110.96	-45.36	-19.66	0.4839 E-5
111.26	-82.87	-24.12	0.4936 E-5
111.56	-92.97	-1.40	0.3689 E-4
111.86	67.74	49.61	0.2473 E-5
112.46	179.73	11.33	0.1053 E-4
112.76	37.84	8.25	0.2326 E-5
113.06	46.41	7.98	0.9392 E-5
113.36	69.82	12.65	0.2791 E-4
113.66	46.45	18.48	0.7660 E-5
113.96	71.69	-0.52	0.3150 E-5
114.42	92.58	-30.47	0.7197 E-5
114.66	124.66	-8.40	0.4473 E-5
114.96	159.35	34.72	0.1882 E-4
115.26	135.74	16.43	0.1159 E-4
115.56	-48.30	3.83	0.5576 E-4
115.86	-31.86	10.05	0.1060 E-4
116.16	-35.28	28.83	0.1309 E-4
116.46	-44.92	22.00	0.4554 E-5
116.76	-37.86	7.38	0.6037 E-5
117.06	139.31	-2.87	0.1220 E-4
117.36	150.60	7.96	0.1796 E-4
117.66	115.59	-11.01	0.1223 E-5
117.96	84.11	15.25	0.3027 E-5
118.26	-29.03	4.87	0.4357 E-4
118.56	-80.39	1.25	0.9431 E-4
118.86	-43.96	0.99	0.1959 E-4